A priori and a posteriori error analyses of an augmented HDG method for a class of quasi-Newtonian Stokes flows*

Gabriel N. Gatica† Filánder A. Sequeira‡

Abstract

In a recent work we developed a new hybridizable discontinuous Galerkin (HDG) method for a class of nonlinear Stokes models arising in quasi-Newtonian fluids. The approach there uses the incompressibility condition to eliminate the pressure, sets the gradient of the velocity as an auxiliary unknown, and enriches the original formulation with convenient redundant equations, thus giving rise to an augmented scheme. However, the corresponding analysis, which makes use of a fixed point strategy that depends on a suitably chosen parameter, yields optimal rates of convergence for only two of the six resulting unknowns, whereas the reported numerical results, showing higher orders than predicted, support the conjecture that the *a priori* error estimates are not sharp. In the present paper, the main features of the aforementioned augmented formulation are maintained, but after introducing slight modifications of the finite element subspaces for the pseudostress and velocity, we are able to significantly improve our previous analyses and results. More precisely, on one hand we omit the utilization of any fixed-point argument and related parameters to establish the well-posedness of the discrete scheme, and on the other hand we now prove optimally convergent approximations for all the unknowns. Furthermore, we develop a reliable and efficient residual-based *a posteriori* error estimator, and propose the associated adaptive algorithm for our HDG approximation of the nonlinear model problem. Finally, several numerical results illustrating the performance of the method, confirming the theoretical properties of the estimator, and showing the expected behaviour of the adaptive refinements, even for an example not fully covered by the theory, are presented.

Key words: nonlinear Stokes model, hybridized discontinuous Galerkin method, augmented formulation, a posteriori error estimate

1 Introduction

The study of new and more efficient numerical methods for linear and nonlinear Stokes flows and related problems, has become a very active research area lately (see, e.g., [15, 20, 21, 27, 10], and the references therein). In particular, *a priori* and *a posteriori* error analyses of non-augmented and augmented mixed finite element methods for a quasi-Newtonian Stokes flow are developed in [21], whereas discontinuous Galerkin schemes are considered in [5] and more recently in [22]. More precisely, the application of the local discontinuous Galerkin (LDG) method to the aforementioned nonlinear

*This work was partially supported by CONICYT-Chile through BASAL project CMM, Universidad de Chile, project Anillo ACT1118 (ANANUM), and the Becas-Chile Programme for foreign students; and by Centro de Investigación en Ingeniería Matemática (CI^{2}MA), Universidad de Concepción.

†CI^{2}MA and Departamento de Ingeniería Matemática, Universidad de Concepción, Casilla 160-C, Concepción, Chile, email: ggatica@ci2ma.udec.cl.

‡Escuela de Matemática, Universidad Nacional de Costa Rica, Heredia, Costa Rica, email: filander.sequeira@una.cr. Present address: CI^{2}MA and Departamento de Ingeniería Matemática, Universidad de Concepción, Casilla 160-C, Concepción, Chile, email: fsequeira@ci2ma.udec.cl.

problem was studied in [5] by using a pseudostress-based formulation in which the velocity, its gradient, and the pressure complete the set of unknowns. On the other hand, a hybridizable discontinuous Galerkin (HDG) method for the same model and approach from [5] is introduced and analyzed in [22]. This HDG formulation is enriched with two suitable redundant equations, thanks to which the well-posedness, that is the unique solvability, stability, and Céa's estimate of the proposed discrete scheme, can be easily established. Indeed, the resulting augmented HDG scheme is reformulated as a fixed point problem, which, under the assumption that certain stabilization parameter is small enough, allows to apply a nonlinear version of the Babuška-Brezzi theory and the classical Banach fixed-point theorem. However, according to the numerical experiments reported in [22, Section 6], some of the unknowns show higher orders of convergence than predicted by the theoretical results, which suggests that the corresponding *a priori* error analysis is not sharp. In addition, those examples also showed that for large values of the stabilization parameter the method does not break down, thus insinuating that the restriction on the choice of this parameter could very well be just a technical assumption for the analysis. These drawbacks of the approach in [22] constitute the main motivation for the present contribution.

In the present paper, we reconsider the nonlinear model and the associated augmented HDG formulation from [22], and provide a significant improvement of the corresponding analyses and results. In fact, after suitable redefinitions of the finite element subspaces approximating the pseudostress and velocity, and without resorting to any fixed-point strategy, but only applying a nonlinear version of the well known Babuška-Brezzi theory, we are able to prove in a cleaner way the well-posedness of the discrete scheme and to establish optimal orders of convergence for all the unknowns. Furthermore, a second contribution of this work consists of the derivation of a reliable and efficient residual-based *a posteriori* error estimator for our problem. Regarding this issue, it is important to remark here that the development of *a posteriori* error estimates for discontinuous Galerkin schemes is not as exhaustive as for conforming methods, which is confirmed by the scarce literature on the subject. One of the first results in this direction goes back to [6], where a new residual-based reliable *a posteriori* error estimator for the local discontinuous Galerkin approximations of linear and nonlinear diffusion problems in polygonal regions of R^2 is derived. The analysis in [6], which applies to convex and non-convex domains, is based on Helmholtz decompositions of the error and a suitable auxiliary polynomial function interpolating the Dirichlet datum. In turn, the first *a posteriori* error analysis of the HDG method for second-order elliptic problems was presented in [13]. A postprocessing variable was used there in order to prove reliability and efficiency of the proposed local *a posteriori* error indicator. More recently, an *a posteriori* error estimator for the HDG method applied to convection-diffusion equations with dominant convection was introduced in [7]. No postprocessed solution was employed in that approach. Other works dealing with the development of *a posteriori* error estimates for discontinuous Galerkin schemes include [5, 14] and the references therein. However, in spite of the aforementioned papers, there is still no contribution available in the literature on the *a posteriori* error analysis of HDG methods for nonlinear models in fluid mechanics. According to the above discussion, and as a first attempt in this regard, in this paper we also develop a reliable and efficient residual-based *a posteriori* error estimator, and propose the associated adaptive algorithm, for the HDG approximation of the quasi-Newtonian Stokes flow from [22].

The rest of this work is organized as follows. In Section 2 we recall the augmented hybridizable discontinuous Galerkin formulation from [22], which involves the velocity, the pseudostress, the gradient of the velocity, and the trace of the velocity, as main unknowns. In Section 3 we show the unique solvability of this augmented HDG scheme by considering first an equivalent formulation, and then by applying a nonlinear version of the Babuška-Brezzi theory. The corresponding optimal *a priori* error estimates are then established in Section 4. Next, in Section 5 we derive a reliable and efficient residual-based *a posteriori* error estimator for arbitrary 2D polygonal domains and for convex polyhedral domains in 3D. Similarly as in [13], we use an element-by-element postprocessing formula for the

pseudostress, which allows us to prove reliability and efficiency of the *a posteriori* estimator. Finally, several numerical results showing the good performance of the method, confirming the reliability and efficiency of the estimator, and illustrating the behaviour of the associated adaptive algorithm, even for a 3D example with a non-convex domain, are reported in Section 6.

We end this section with some notations to be used below. Given $n \in \{2,3\}$, the space of square matrices of order n with real entries is denoted by $R^{n\times n}$. In addition, $\mathbb{I} := (\delta_{ij})$ is the identity matrix of $R^{n\times n}$, and for any $\boldsymbol{\tau} := (\tau_{ij})$, $\boldsymbol{\zeta} := (\zeta_{ij}) \in R^{n\times n}$, we write as usual

$$\boldsymbol{\tau}^{\mathtt{t}} := (\tau_{ji}), \quad \mathrm{tr}\,(\boldsymbol{\tau}) := \sum_{i=1}^{n} \tau_{ii}, \quad \boldsymbol{\tau}^{\mathtt{d}} := \boldsymbol{\tau} - \frac{1}{n}\,\mathrm{tr}\,(\boldsymbol{\tau})\,\mathbb{I}, \quad \text{and} \quad \boldsymbol{\tau} : \boldsymbol{\zeta} := \sum_{i,j=1}^{n} \tau_{ij}\zeta_{ij}\,.$$

Also, in what follows we utilize standard simplified terminology for Sobolev spaces and norms. In particular, if $\mathcal{O} \subset R^n$ is a domain, $\mathcal{S} \subset R^n$ is an open or closed Lipschitz curve if $n = 2$ (resp. surface if $n = 3$), and $r \in R$, we define

$$\mathbf{H}^r(\mathcal{O}) := [H^r(\mathcal{O})]^n, \quad \mathbb{H}^r(\mathcal{O}) := [H^r(\mathcal{O})]^{n\times n}, \quad \text{and} \quad \mathbf{H}^r(\mathcal{S}) := [H^r(\mathcal{S})]^n\,.$$

However, when $r = 0$ we usually write $\mathbf{L}^2(\mathcal{O})$, $\mathbb{L}^2(\mathcal{O})$, and $\mathbf{L}^2(\mathcal{S})$ instead of $\mathbf{H}^0(\mathcal{O})$, $\mathbb{H}^0(\mathcal{O})$, and $\mathbf{H}^0(\mathcal{S})$, respectively. The corresponding norms are denoted by $\|\cdot\|_{r,\mathcal{O}}$ and $\|\cdot\|_{r,\mathcal{S}}$. In general, given any Hilbert space H, we use $\mathbf{H}$ and $\mathbb{H}$ to denote H^n and $H^{n\times n}$, respectively. In addition, with div denoting the usual divergence operator, the Hilbert space

$$\mathbf{H}(\mathrm{div};\mathcal{O}) := \left\{\mathbf{w} \in \mathbf{L}^2(\mathcal{O}) \,:\, \mathrm{div}(\mathbf{w}) \in L^2(\mathcal{O})\right\},$$

is standard in the realm of mixed problems (see, e.g. [3, 23, 16]). The space of matrix-valued functions whose rows belong to $\mathbf{H}(\mathrm{div};\mathcal{O})$ will be denoted $\mathbb{H}(\mathbf{div};\mathcal{O})$, where **div** stands for the action of div along each row of a tensor. The Hilbert norms of $\mathbf{H}(\mathrm{div};\mathcal{O})$ and $\mathbb{H}(\mathbf{div};\mathcal{O})$ are denoted by $\|\cdot\|_{\mathrm{div},\mathcal{O}}$ and $\|\cdot\|_{\mathbf{div},\mathcal{O}}$, respectively. Finally, we employ $\mathbf{0}$ to denote a generic null vector, null tensor or null operator, and use C or c, with or without subscripts, bars, tildes or hats, to denote generic constants independent of the discretization parameters, which may take different values at different places.

2 The augmented HDG method

2.1 The model problem

In order to define the boundary value problem of interest, we now let Ω be a bounded and simply connected polygonal domain in R^n with boundary Γ. As in [21], our goal is to determine the velocity $\mathbf{u}$, the pseudostress tensor $\boldsymbol{\sigma}$, and the pressure p of a steady flow occupying the region Ω, under the action of external forces. More precisely, given a volume force $\mathbf{f} \in \mathbf{L}^2(\Omega)$ and $\mathbf{g} \in \mathbf{H}^{1/2}(\Gamma)$, we seek a tensor field $\boldsymbol{\sigma}$, a vector field $\mathbf{u}$, and a scalar field p such that

$$\begin{aligned} &\boldsymbol{\sigma} = \mu(|\nabla\mathbf{u}|)\,\nabla\mathbf{u} - p\,\mathbb{I} \quad \text{in} \quad \Omega, \qquad \mathbf{div}(\boldsymbol{\sigma}) = -\mathbf{f} \quad \text{in} \quad \Omega, \\ &\mathrm{div}(\mathbf{u}) = 0 \quad \text{in} \quad \Omega, \qquad \mathbf{u} = \mathbf{g} \quad \text{on} \quad \Gamma, \qquad \int_\Omega p = 0, \end{aligned} \tag{2.1}$$

where $\mu : R^+ \to R^+$ is the nonlinear kinematic viscosity function of the fluid, $\nabla\mathbf{u}$ is the tensor gradient of $\mathbf{u}$, and $|\cdot|$ is the Euclidean norm of $R^{n\times n}$. As required by the incompressibility condition, we assume from now on that the datum $\mathbf{g}$ satisfies the compatibility condition $\int_\Gamma \mathbf{g}\cdot\boldsymbol{\nu} = 0$, where $\boldsymbol{\nu}$ stands for the unit outward normal at Γ. The kind of nonlinear Stokes problem given by (2.1) appears in the modeling of a large class of non-Newtonian fluids (see, e.g. [2, 25, 26, 29]). In particular, the

Ladyzhenskaya law is given by $\mu(t) := \mu_0 + \mu_1 t^{\beta-2} \ \forall\, t \in R^+$, with $\mu_0 \geq 0$, $\mu_1 > 0$, and $\beta > 1$, and the Carreau law for viscoplastic flows (see, e.g. [26, 29]) reads $\mu(t) := \mu_0 + \mu_1(1+t^2)^{(\beta-2)/2} \ \forall\, t \in R^+$, with $\mu_0 \geq 0$, $\mu_1 > 0$, and $\beta \geq 1$.

We now let $\psi_{ij} : R^{n\times n} \to R$ be the mapping given by $\psi_{ij}(\mathbf{r}) := \mu(|\mathbf{r}|) r_{ij}$ for all $\mathbf{r} := (r_{ij}) \in R^{n\times n}$, for all $i, j \in \{1, \ldots, n\}$. Then, throughout this paper we assume that μ is of class C^1 and that there exist $\gamma_0, \alpha_0 > 0$ such that for all $\mathbf{r} := (r_{ij})$, $\mathbf{s} := (s_{ij}) \in R^{n\times n}$, there holds

$$|\psi_{ij}(\mathbf{r})| \ \leq \ \gamma_0 \, \|\mathbf{r}\|_{R^{n\times n}} , \qquad \left| \frac{\partial}{\partial r_{kl}} \psi_{ij}(\mathbf{r}) \right| \ \leq \ \gamma_0 , \quad \forall\, i, j, k, l \in \{1, \ldots, n\} , \tag{2.2}$$

and

$$\sum_{i,j,k,l=1}^{n} \frac{\partial}{\partial r_{kl}} \psi_{ij}(\mathbf{r}) s_{ij} s_{kl} \quad \geq \quad \alpha_0 \, \|\mathbf{s}\|^2_{R^{n\times n}} . \tag{2.3}$$

It is easy to check that the Carreau law satisfies (2.2) and (2.3) for all $\mu_0 > 0$, and for all $\beta \in [1, 2]$. In particular, with $\beta = 2$ we recover the usual linear Stokes model.

On the other hand, we know from [21, Section 2.1] that the pair given by the first and third equations in (2.1) is equivalent to

$$\boldsymbol{\sigma} \ = \ \boldsymbol{\psi}(\nabla \mathbf{u}) - p\,\mathbb{I} \quad \text{in} \quad \Omega \qquad \text{and} \qquad p \ = \ -\frac{1}{n} \operatorname{tr}(\boldsymbol{\sigma}) \quad \text{in} \quad \Omega , \tag{2.4}$$

where $\boldsymbol{\psi} : R^{n\times n} \to R^{n\times n}$ is given by $\boldsymbol{\psi}(\mathbf{r}) := (\psi_{ij}(\mathbf{r}))$ for all $\mathbf{r} \in R^{n\times n}$. Hence, replacing p by $-\frac{1}{n}\operatorname{tr}(\boldsymbol{\sigma})$ in the first equation of (2.1), and introducing the gradient $\mathbf{t} := \nabla \mathbf{u}$ in Ω as an auxiliary unknown, we arrive at the system

$$\begin{aligned} \boldsymbol{\psi}(\mathbf{t}) - \boldsymbol{\sigma}^{\mathtt{d}} \ = \ \mathbf{0} \quad \text{in} \quad \Omega , \qquad & \mathbf{t} - \nabla \mathbf{u} \ = \ \mathbf{0} \quad \text{in} \quad \Omega , \\ -\mathbf{div}(\boldsymbol{\sigma}) \ = \ \mathbf{f} \quad \text{in} \quad \Omega , \qquad & \operatorname{tr}(\mathbf{t}) \ = \ 0 \quad \text{in} \quad \Omega , \\ \mathbf{u} \ = \ \mathbf{g} \quad \text{on} \quad \Gamma , \qquad & \int_\Omega \operatorname{tr}(\boldsymbol{\sigma}) \ = \ 0 . \end{aligned} \tag{2.5}$$

Next, we let $X_1 := \{\mathbf{s} \in \mathbb{L}^2(\Omega) \ : \ \operatorname{tr}(\mathbf{s}) = 0\}$ and $\mathbb{H}_0(\mathbf{div}; \Omega) := \big\{\boldsymbol{\tau} \in \mathbb{H}(\mathbf{div}; \Omega) \ : \ \int_\Omega \operatorname{tr}(\boldsymbol{\tau}) = 0\big\}$, and recall that the continuous formulation of (2.5), whose well-posedness has been established in [21, Section 2], reads: Find $(\mathbf{t}, \boldsymbol{\sigma}, \mathbf{u}) \in X_1 \times \mathbb{H}_0(\mathbf{div}; \Omega) \times \mathbf{L}^2(\Omega)$ such that

$$\begin{aligned} \int_\Omega \boldsymbol{\psi}(\mathbf{t}) : \mathbf{s} - \int_\Omega \boldsymbol{\sigma}^{\mathtt{d}} : \mathbf{s} \quad &= \quad 0 \quad \forall\, \mathbf{s} \in X_1 , \\ -\int_\Omega \mathbf{t} : \boldsymbol{\tau}^{\mathtt{d}} - \int_\Omega \mathbf{u} \cdot \mathbf{div}(\boldsymbol{\tau}) \quad &= \quad -\langle \boldsymbol{\tau}\boldsymbol{\nu}, \mathbf{g} \rangle_\Gamma \quad \forall\, \boldsymbol{\tau} \in \mathbb{H}_0(\mathbf{div}; \Omega) , \\ -\int_\Omega \mathbf{v} \cdot \mathbf{div}(\boldsymbol{\sigma}) \quad &= \quad \int_\Omega \mathbf{f} \cdot \mathbf{v} \quad \forall\, \mathbf{v} \in \mathbf{L}^2(\Omega) , \end{aligned} \tag{2.6}$$

The *a priori* error analysis given below in Section 4 makes use of (2.6).

2.2 The hybridizable discontinuous Galerkin method

We begin by introducing some preliminary notations. Let $\mathcal{T}_h$ be a shape-regular triangulation of $\bar{\Omega}$ without the presence of hanging nodes, and let $\mathcal{E}_h$ be the set of faces F of $\mathcal{T}_h$. In addition, we let $\mathcal{E}_h^i$ and $\mathcal{E}_h^\partial$ be the set of interior and boundary faces, respectively, of $\mathcal{E}_h$, and set $\partial\mathcal{T}_h := \cup\{\partial T \ : \ T \in \mathcal{T}_h\}$.

Next, given a domain $U \subseteq R^n$ and a surface $G \subseteq R^{n-1}$, we let $(\cdot,\cdot)_U$ (resp. $\langle\cdot,\cdot\rangle_G$) be the usual L^2, $\mathbf{L}^2$ and $\mathbb{L}^2$ (resp. L^2 and $\mathbf{L}^2$) inner products over U (resp. G). Then, we introduce the inner products:

$$(\cdot,\cdot)_{\mathcal{T}_h} := \sum_{T\in\mathcal{T}_h}(\cdot,\cdot)_T\,, \quad \langle\cdot,\cdot\rangle_{\partial\mathcal{T}_h} := \sum_{T\in\mathcal{T}_h}\langle\cdot,\cdot\rangle_{\partial T}\,, \quad \text{and} \quad \langle\cdot,\cdot\rangle_{\partial\mathcal{T}_h\setminus\Gamma} := \sum_{T\in\mathcal{T}_h}\sum_{F\in\partial T\setminus\Gamma}\langle\cdot,\cdot\rangle_F\,.$$

On the other hand, given second-order tensorial and vectorial functions $\boldsymbol{\tau}$ and $\mathbf{v}$, respectively, and denoting by $\boldsymbol{\nu}^+$ and $\boldsymbol{\nu}^-$ the outward unit normal vectors on the boundaries of two neighboring elements T^+ and T^-, we let $(\boldsymbol{\tau}^\pm,\mathbf{v}^\pm)$ be the trace of $(\boldsymbol{\tau},\mathbf{v})$ on $F := \partial T^+\cap\partial T^-$ from the interior of $T^\pm$. Then, we define the means $\{\!\{\cdot\}\!\}$ and jumps $[\![\cdot]\!]$ for $F\in\mathcal{E}_h^i$, as follows

$$\begin{aligned}\{\!\{\boldsymbol{\tau}\}\!\} &:= \frac{1}{2}\left(\boldsymbol{\tau}^+ + \boldsymbol{\tau}^-\right), \qquad \{\!\{\mathbf{v}\}\!\} := \frac{1}{2}\left(\mathbf{v}^+ + \mathbf{v}^-\right),\\ [\![\boldsymbol{\tau}]\!] &:= \boldsymbol{\tau}^+\boldsymbol{\nu}^+ + \boldsymbol{\tau}^-\boldsymbol{\nu}^-, \qquad [\![\mathbf{v}]\!] := \mathbf{v}^+\otimes\boldsymbol{\nu}^+ + \mathbf{v}^-\otimes\boldsymbol{\nu}^-,\end{aligned}$$

where $\otimes$ denotes the usual dyadic or tensor product.

Now we are ready to describe below the HDG method for the boundary value problem (2.5). To this end, given an integer $k\geq 0$ and a domain U, we let $P_k(U)$ be the space of polynomials of total degree at most k defined on U. Then, the finite dimensional discontinuous subspaces are given by

$$\begin{aligned}S_h &:= \left\{\mathbf{s}\in\mathbb{L}^2(\Omega) \,:\, \mathbf{s}|_T\in\mathbb{P}_k(T) \quad \forall\, T\in\mathcal{T}_h\right\},\\ \Sigma_h &:= \left\{\boldsymbol{\tau}\in\mathbb{L}^2(\Omega) \,:\, \boldsymbol{\tau}|_T\in\mathbb{RT}_k(T) \quad \forall\, T\in\mathcal{T}_h, \quad \text{and} \quad \int_\Omega \mathrm{tr}\,(\boldsymbol{\tau}) = 0\right\},\\ V_h &:= \left\{\mathbf{v}\in\mathbf{L}^2(\Omega) \,:\, \mathbf{v}|_T\in\mathbf{P}_k(T) \quad \forall\, T\in\mathcal{T}_h\right\},\\ M_h &:= \left\{\boldsymbol{\mu}\in\mathbf{L}^2(\mathcal{E}_h^i) \,:\, \boldsymbol{\mu}|_F\in\mathbf{P}_k(F) \quad \forall\, F\in\mathcal{E}_h^i\right\},\end{aligned}$$

where $\mathbb{RT}_k(T) := \left\{\boldsymbol{\tau}\in\mathbb{L}^2(T) \,:\, (\tau_{i1},\ldots,\tau_{in})^{\mathtt{t}}|_T\in\mathbf{RT}_k(T) \quad \forall\, i\in\{1,\ldots,n\}\right\}$, $\mathbf{RT}_k(T)$ is the local Raviart-Thomas space of order k (see, e.g. [3, 28]), that is

$$\mathbf{RT}_k(T) := \mathbf{P}_k(T) \,\oplus\, P_k(T)\,\mathbf{x}\,,$$

$\mathbf{x} = \begin{pmatrix} x_1\\ \vdots\\ x_n\end{pmatrix}$ is a generic vector of R^n, and, according to the notation introduced at the end of Section 1, $\mathbf{P}_k(T)$ denotes $[P_k(T)]^n$. At this point we remark that, differently from [22] where the lowest polynomial degree that can be employed is $k=1$, the present definitions of the subspaces S_h and M_h allow the utilization of $k=0$. This fact and the foregoing definition of Σ_h will be useful in the new *a priori* error analysis to be developed below in Section 4.

Then, proceeding exactly as in [10, 22], the HDG formulation of the nonlinear model (2.5) reduces to: Find $(\mathbf{t}_h,\boldsymbol{\sigma}_h,\mathbf{u}_h,\boldsymbol{\lambda}_h)\in S_h\times\Sigma_h\times V_h\times M_h$, such that

$$\begin{aligned}(\boldsymbol{\psi}(\mathbf{t}_h),\mathbf{s}_h)_{\mathcal{T}_h} - (\mathbf{s}_h,\boldsymbol{\sigma}_h^{\mathtt{d}})_{\mathcal{T}_h} &= 0 \quad \forall\,\mathbf{s}_h\in S_h\,,\\ (\mathbf{t}_h,\boldsymbol{\tau}_h^{\mathtt{d}})_{\mathcal{T}_h} + (\mathbf{u}_h,\mathbf{div}_h(\boldsymbol{\tau}_h))_{\mathcal{T}_h} - \langle\boldsymbol{\tau}_h\boldsymbol{\nu},\widehat{\mathbf{u}}_h\rangle_{\partial\mathcal{T}_h} &= 0 \quad \forall\,\boldsymbol{\tau}_h\in\Sigma_h\,,\\ (\boldsymbol{\sigma}_h,\nabla_h\mathbf{v}_h)_{\mathcal{T}_h} - \langle\widehat{\boldsymbol{\sigma}_h\boldsymbol{\nu}},\mathbf{v}_h\rangle_{\partial\mathcal{T}_h} &= (\mathbf{f},\mathbf{v}_h)_{\mathcal{T}_h} \quad \forall\,\mathbf{v}_h\in V_h\,,\\ \langle\widehat{\boldsymbol{\sigma}_h\boldsymbol{\nu}},\boldsymbol{\mu}_h\rangle_{\partial\mathcal{T}_h\setminus\Gamma} &= 0 \quad \forall\,\boldsymbol{\mu}_h\in M_h\,,\end{aligned} \tag{2.7}$$

where, letting Π_Γ be the $\mathbf{L}^2(\Gamma)$ projection onto the space of piecewise polynomials of degree $\leq k$ on $\mathcal{E}_h^\partial$, we define the numerical fluxes $\widehat{\mathbf{u}}_h$ and $\widehat{\boldsymbol{\sigma}_h\boldsymbol{\nu}}$ as

$$\widehat{\mathbf{u}}_h := \begin{cases}\Pi_\Gamma(\mathbf{g}) & \text{on } \mathcal{E}_h^\partial\,,\\ \boldsymbol{\lambda}_h & \text{on } \mathcal{E}_h^i\,,\end{cases} \qquad \text{and} \qquad \widehat{\boldsymbol{\sigma}_h\boldsymbol{\nu}} := \boldsymbol{\sigma}_h\boldsymbol{\nu} - \mathbf{S}(\mathbf{u}_h-\widehat{\mathbf{u}}_h) \ \text{ on } \partial\mathcal{T}_h\,,$$

where $\mathbf{S}$ is a stabilization operator to be defined below. Note that the condition $\widehat{\mathbf{u}}_h = \Pi_\Gamma(\mathbf{g})$ on $\mathcal{E}_h^\partial$ is usually imposed in the equivalent way $\langle \widehat{\mathbf{u}}_h, \boldsymbol{\mu}_h\rangle_\Gamma = \langle \mathbf{g}, \boldsymbol{\mu}_h\rangle_\Gamma \ \forall\ \boldsymbol{\mu}_h \in \mathbf{P}_k(\mathcal{E}_h)$, which is employed to perform the solvability analysis of (2.7). In addition, as in [22], we consider the special case in which $\mathbf{S}^+ = \mathbf{S}^-$ in each $F \in \mathcal{E}_h^i$, that is, $\mathbf{S}$ has only one value on each $F \in \mathcal{E}_h$. More precisely, given $F \in \mathcal{E}_h$, we assume that $\mathbf{S}|_F$ is a symmetric and positive definite constant tensor. Furthermore, observe that $\mathbf{S}^{-1}$ is well defined and symmetric and positive definite as well on each $F \in \mathcal{E}_h$. In (3.1) below, we select a particular choice for tensor $\mathbf{S}$ in order to establish the well-posedness of (2.8).

2.3 The augmented HDG formulation

In order to establish the unique solvability of the nonlinear problem (2.7), we now enrich the HDG formulation with two redundant equations arising from the constitutive and equilibrium equations, that is

$$\kappa_1(\boldsymbol{\sigma}_h^{\mathtt{d}} - \boldsymbol{\psi}(\mathbf{t}_h),\, \boldsymbol{\tau}_h^{\mathtt{d}})_{\mathcal{T}_h} \;=\; 0 \quad \forall\ \boldsymbol{\tau}_h \in \Sigma_h\,,$$

and

$$\kappa_2(\mathbf{div}_h(\boldsymbol{\sigma}_h),\, \mathbf{div}_h(\boldsymbol{\tau}_h))_{\mathcal{T}_h} \;=\; -\kappa_2(\mathbf{f},\, \mathbf{div}_h(\boldsymbol{\tau}_h))_{\mathcal{T}_h} \quad \forall\ \boldsymbol{\tau}_h \in \Sigma_h\,,$$

where $\kappa_1, \kappa_2 > 0$ are parameters to be determined later on. In this way, our augmented formulation becomes: Find $(\mathbf{t}_h, \boldsymbol{\sigma}_h, \mathbf{u}_h, \boldsymbol{\lambda}_h) \in S_h \times \Sigma_h \times V_h \times M_h$ such that

$$\begin{aligned}
(\boldsymbol{\psi}(\mathbf{t}_h), \mathbf{s}_h)_{\mathcal{T}_h} - (\mathbf{s}_h, \boldsymbol{\sigma}_h^{\mathtt{d}})_{\mathcal{T}_h} &= 0\,,\\
(\mathbf{t}_h, \boldsymbol{\tau}_h^{\mathtt{d}})_{\mathcal{T}_h} + (\mathbf{u}_h, \mathbf{div}_h(\boldsymbol{\tau}_h))_{\mathcal{T}_h} - \langle \boldsymbol{\tau}_h\boldsymbol{\nu}, \boldsymbol{\lambda}_h\rangle_{\partial\mathcal{T}_h\setminus\Gamma} &= \langle \boldsymbol{\tau}_h\boldsymbol{\nu}, \mathbf{g}\rangle_\Gamma\,,\\
-(\mathbf{v}_h, \mathbf{div}_h(\boldsymbol{\sigma}_h))_{\mathcal{T}_h} + \langle \mathbf{S}(\mathbf{u}_h - \boldsymbol{\lambda}_h), \mathbf{v}_h\rangle_{\partial\mathcal{T}_h\setminus\Gamma} + \langle \mathbf{S}\mathbf{u}_h, \mathbf{v}_h\rangle_\Gamma &= (\mathbf{f}, \mathbf{v}_h)_{\mathcal{T}_h} + \langle \mathbf{S}\mathbf{g}, \mathbf{v}_h\rangle_\Gamma\,,\\
\langle \boldsymbol{\sigma}_h\boldsymbol{\nu}, \boldsymbol{\mu}_h\rangle_{\partial\mathcal{T}_h\setminus\Gamma} - \langle \mathbf{S}(\mathbf{u}_h - \boldsymbol{\lambda}_h), \boldsymbol{\mu}_h\rangle_{\partial\mathcal{T}_h\setminus\Gamma} &= 0\,,\\
\kappa_1(\boldsymbol{\sigma}_h^{\mathtt{d}} - \boldsymbol{\psi}(\mathbf{t}_h), \boldsymbol{\tau}_h^{\mathtt{d}})_{\mathcal{T}_h} &= 0\,,\\
\kappa_2(\mathbf{div}_h(\boldsymbol{\sigma}_h), \mathbf{div}_h(\boldsymbol{\tau}_h))_{\mathcal{T}_h} &= -\kappa_2(\mathbf{f}, \mathbf{div}_h(\boldsymbol{\tau}_h))_{\mathcal{T}_h}\,,
\end{aligned} \tag{2.8}$$

for all $(\mathbf{s}_h, \boldsymbol{\tau}_h, \mathbf{v}_h, \boldsymbol{\mu}_h) \in S_h \times \Sigma_h \times V_h \times M_h$. Hence, in what follows we proceed as in [22] and derive an equivalent formulation to (2.8) (see (2.10) below), for which we prove its unique solvability. In addition, the *a priori* error estimates for (2.8) will also be based on the analysis of (2.10). We emphasize, however, that the introduction of this equivalent formulation is just for theoretical purposes and by no means for the explicit computation of the solution of (2.8), which is solved directly as we explain in [22, Section 5].

It follows, proceeding as in [22, Section 2.2], that from the fourth equation in (2.8), we obtain

$$\boldsymbol{\lambda}_h \;=\; \{\!\{\mathbf{u}_h\}\!\} \;-\; \frac{1}{2}\,\mathbf{S}^{-1}\,[\![\boldsymbol{\sigma}_h]\!] \quad \text{on} \quad \mathcal{E}_h^i\,, \tag{2.9}$$

which, allows us to rewrite (2.8) as: Find $((\mathbf{t}_h, \boldsymbol{\sigma}_h), \mathbf{u}_h) \in H_h \times V_h$ such that

$$\begin{aligned}
[\mathcal{A}_h(\mathbf{t}_h, \boldsymbol{\sigma}_h), (\mathbf{s}_h, \boldsymbol{\tau}_h)] \;+\; [\mathcal{B}_h(\mathbf{s}_h, \boldsymbol{\tau}_h), \mathbf{u}_h] &= [\mathcal{F}_h, (\mathbf{s}_h, \boldsymbol{\tau}_h)] \quad \forall\ (\mathbf{s}_h, \boldsymbol{\tau}_h) \in H_h\,,\\
[\mathcal{B}_h(\mathbf{t}_h, \boldsymbol{\sigma}_h), \mathbf{v}_h] \;-\; [\mathcal{S}_h(\mathbf{u}_h), \mathbf{v}_h] &= [\mathcal{G}_h, \mathbf{v}_h] \quad \forall\ \mathbf{v}_h \in V_h\,,
\end{aligned} \tag{2.10}$$

where $H_h := S_h \times \Sigma_h$, and the operators $\mathcal{A}_h : H_h \to H_h'$, $\mathcal{B}_h : H_h \to V_h'$ and $\mathcal{S}_h : V_h \to V_h'$, and the functionals $\mathcal{F}_h : H_h \to R$ and $\mathcal{G}_h : V_h \to R$, are defined by

$$\begin{aligned}
[\mathcal{A}_h(\mathbf{t}_h,\boldsymbol{\sigma}_h),(\mathbf{s}_h,\boldsymbol{\tau}_h)] &:= (\boldsymbol{\psi}(\mathbf{t}_h),\mathbf{s}_h)_{\mathcal{T}_h} - (\mathbf{s}_h,\boldsymbol{\sigma}_h^{\mathtt{d}})_{\mathcal{T}_h} + (\mathbf{t}_h,\boldsymbol{\tau}_h^{\mathtt{d}})_{\mathcal{T}_h} + \frac{1}{2}\int_{\mathcal{E}_h^i} \mathbf{S}^{-1}[\![\boldsymbol{\sigma}_h]\!]\cdot[\![\boldsymbol{\tau}_h]\!] \\
&\quad + \kappa_1(\boldsymbol{\sigma}_h^{\mathtt{d}} - \boldsymbol{\psi}(\mathbf{t}_h),\boldsymbol{\tau}_h^{\mathtt{d}})_{\mathcal{T}_h} + \kappa_2(\mathbf{div}_h(\boldsymbol{\sigma}_h),\mathbf{div}_h(\boldsymbol{\tau}_h))_{\mathcal{T}_h}\,, \qquad (2.11)\\
[\mathcal{B}_h(\mathbf{s}_h,\boldsymbol{\tau}_h),\mathbf{v}_h] &:= (\mathbf{v}_h,\mathbf{div}_h(\boldsymbol{\tau}_h))_{\mathcal{T}_h} - \int_{\mathcal{E}_h^i} \{\!\{\mathbf{v}_h\}\!\}\cdot[\![\boldsymbol{\tau}_h]\!]\,, \qquad (2.12)\\
[\mathcal{S}_h(\mathbf{u}_h),\mathbf{v}_h] &:= \langle \mathbf{S}\mathbf{u}_h,\mathbf{v}_h\rangle_{\partial\mathcal{T}_h} - 2\int_{\mathcal{E}_h^i} \mathbf{S}\{\!\{\mathbf{u}_h\}\!\}\cdot\{\!\{\mathbf{v}_h\}\!\}\,, \qquad (2.13)\\
[\mathcal{F}_h,(\mathbf{s}_h,\boldsymbol{\tau}_h)] &:= \langle \boldsymbol{\tau}_h\boldsymbol{\nu},\mathbf{g}\rangle_\Gamma - \kappa_2(\mathbf{f},\mathbf{div}_h(\boldsymbol{\tau}_h))_{\mathcal{T}_h}\,,\\
[\mathcal{G}_h,\mathbf{v}_h] &:= -(\mathbf{f},\mathbf{v}_h)_{\mathcal{T}_h} - \langle \mathbf{S}\mathbf{g},\mathbf{v}_h\rangle_\Gamma\,,
\end{aligned}$$

where $[\cdot,\cdot]$ stands in each case for the duality pairing induced by the corresponding operators and functionals. We remark in advance that we do not plan to use any fixed point strategy to derive the well-posedness of (2.10) (as we did in [22]), which, as announced in Section 1, constitutes another advantage of the present approach. In addition, while the above operators and functionals are defined on discrete spaces, it is not difficult to see that they can act on continuous spaces as well. For example, $\mathcal{A}_h$ can actually be defined on $(S_h + \mathbb{L}^2(\Omega)) \times (\Sigma_h + \mathbb{H}(\mathbf{div};\Omega))$ and similarly for the other ones. In particular, this fact will be employed at the beginning of Section 4.

3 Solvability analysis

In this section, we establish the unique solvability of the nonlinear problem (2.10). To this end, and following [4, 5], we let $\mathtt{h} \in L^\infty(\mathcal{E}_h)$ be the function related to the local meshsizes, that is

$$\mathtt{h}(x) := \begin{cases} \min\{h_{T_1}, h_{T_2}\} & \text{if } x \in \mathrm{int}(\partial T_1 \cap \partial T_2)\,, \\ h_T & \text{if } x \in \mathrm{int}(\partial T \cap \Gamma)\,. \end{cases}$$

The main idea of our analysis consists of proving the conditions of the following abstract theorem.

Theorem 3.1. *Let X, M be Hilbert spaces and assume that:*

i) the operator $\mathcal{A} : X \to X'$ is Lipschitz continuous and strongly monotone, that is, there exist γ, $\alpha > 0$ such that

$$\|\mathcal{A}(\mathbf{s}_1) - \mathcal{A}(\mathbf{s}_2)\|_{X'} \;\le\; \gamma\,\|\mathbf{s}_1 - \mathbf{s}_2\|_X \quad \forall\, \mathbf{s}_1,\mathbf{s}_2 \in X$$

and

$$[\mathcal{A}(\mathbf{s}_1) - \mathcal{A}(\mathbf{s}_2),\mathbf{s}_1 - \mathbf{s}_2] \;\ge\; \alpha\,\|\mathbf{s}_1 - \mathbf{s}_2\|_X^2 \quad \forall\, \mathbf{s}_1,\mathbf{s}_2 \in X;$$

ii) the linear operator $\mathcal{S}$ is positive semidefinite on M, that is

$$[\mathcal{S}(\boldsymbol{\tau}),\boldsymbol{\tau}] \;\ge\; 0 \quad \forall\, \boldsymbol{\tau} \in M;$$

iii) the linear operator $\mathcal{B}$ satisfies an inf-sup condition on $X \times M$, that is, there exists $\beta > 0$ such that

$$\sup_{\substack{\mathbf{s}\in X\\ \mathbf{s}\neq\mathbf{0}}} \frac{[\mathcal{B}(\mathbf{s}),\boldsymbol{\tau}]}{\|\mathbf{s}\|_X} \;\ge\; \beta\,\|\boldsymbol{\tau}\|_M \quad \forall\, \boldsymbol{\tau} \in M.$$

Then, given $\mathcal{F} \in X'$ and $\mathcal{G} \in M'$, there exists a unique solution $(\mathbf{t}, \boldsymbol{\sigma}) \in X \times M$ of the problem

$$\begin{aligned} [\mathcal{A}(\mathbf{t}), \mathbf{s}] \ + \ [\mathcal{B}^*(\boldsymbol{\sigma}), \mathbf{s}] \ &= \ [\mathcal{F}, \mathbf{s}] \quad \forall\, \mathbf{s} \in X, \\ [\mathcal{B}(\mathbf{t}), \boldsymbol{\tau}] \ - \ [\mathcal{S}(\boldsymbol{\sigma}), \boldsymbol{\tau}] \ &= \ [\mathcal{G}, \boldsymbol{\tau}] \quad \forall\, \boldsymbol{\tau} \in M. \end{aligned}$$

In addition, there exists $C > 0$, depending only on γ, α, β and $\|\mathcal{B}\|$, such that

$$\|(\mathbf{t}, \boldsymbol{\sigma})\|_{X \times M} \ \leq \ C \Big\{ \|\mathcal{F}\|_{X'} \ + \ \|\mathcal{G}\|_{M'} \ + \ \|\mathcal{A}(\mathbf{0})\|_{X'} \Big\}.$$

Proof. See [19, Lemma 2.1]. □

In order to apply Theorem 3.1 to the augmented formulation (2.10), we now recall the following technical result from [22].

Lemma 3.1. *There exists a constant $c_1 > 0$, independent of h, such that*

$$\|\boldsymbol{\tau}_h\|^2_{0,\Omega} \ \leq \ c_1 \Big\{ \|\boldsymbol{\tau}_h^{\mathtt{d}}\|^2_{0,\Omega} \ + \ \|\mathbf{div}_h(\boldsymbol{\tau}_h)\|^2_{0,\Omega} \ + \ \|\mathtt{h}^{-1/2} [\![\boldsymbol{\tau}_h]\!]\|^2_{0,\mathcal{E}_h^i} \Big\} \quad \forall\, \boldsymbol{\tau}_h \in \Sigma_h \, .$$

Proof. See [22, Lemma 3.3]. □

Now, similarly as in [22] (but with the stabilization parameter employed there given by $\tau = 1$), we set the tensor $\mathbf{S}$ as follows

$$\mathbf{S}|_F \ := \ \mathtt{h}\, \mathbb{I} \qquad \forall\, F \in \mathcal{E}_h \, , \tag{3.1}$$

which certainly yields

$$\mathbf{S}^{-1}|_F \ := \ \mathtt{h}^{-1}\, \mathbb{I} \qquad \forall\, F \in \mathcal{E}_h \, . \tag{3.2}$$

In addition, we consider the following definition of a norm onto Σ_h

$$\|\boldsymbol{\tau}_h\|^2_{\Sigma_h} \ := \ \|\boldsymbol{\tau}_h^{\mathtt{d}}\|^2_{0,\Omega} \ + \ \|\mathbf{div}_h(\boldsymbol{\tau}_h)\|^2_{0,\Omega} \ + \ \|\mathtt{h}^{-1/2} [\![\boldsymbol{\tau}_h]\!]\|^2_{0,\mathcal{E}_h^i} \quad \forall\, \boldsymbol{\tau}_h \in \Sigma_h$$

which, according to Lemma 3.1, satisfies

$$\|\boldsymbol{\tau}_h\|_{0,\Omega} \ \leq \ c_2 \|\boldsymbol{\tau}_h\|_{\Sigma_h} \quad \forall\, \boldsymbol{\tau}_h \in \Sigma_h \, , \tag{3.3}$$

with $c_2 := c_1^{1/2} > 0$. Note that the above suggests the following norm on $H_h := S_h \times \Sigma_h$

$$\|(\mathbf{s}_h, \boldsymbol{\tau}_h)\|_{H_h} \ := \ \Big\{ \|\mathbf{s}_h\|^2_{0,\Omega} \ + \ \|\boldsymbol{\tau}_h\|^2_{\Sigma_h} \Big\}^{1/2} \quad \forall\, (\mathbf{s}_h, \boldsymbol{\tau}_h) \in H_h \, .$$

On the other hand, we define the nonlinear operator $\mathbb{A} : \mathbb{L}^2(\Omega) \to [\mathbb{L}^2(\Omega)]'$ by

$$[\mathbb{A}(\mathbf{r}),\, \mathbf{s}] \ := \ \int_\Omega \boldsymbol{\psi}(\mathbf{r}) : \mathbf{s} \qquad \forall\, \mathbf{r},\, \mathbf{s} \in \mathbb{L}^2(\Omega) \, . \tag{3.4}$$

The following result shows that $\mathbb{A}$ is Lipschitz-continuous and strongly monotone.

Lemma 3.2. *Let γ_0 and α_0 be the constants from* (2.2) *and* (2.3)*, respectively. Then, for all $\mathbf{r}, \mathbf{s} \in \mathbb{L}^2(\Omega)$ there hold*

$$\|\mathbb{A}(\mathbf{r}) - \mathbb{A}(\mathbf{s})\|_{[\mathbb{L}^2(\Omega)]'} \ \leq \ \gamma_0 \|\mathbf{r} - \mathbf{s}\|_{0,\Omega}, \quad \textit{and} \quad [\mathbb{A}(\mathbf{r}) - \mathbb{A}(\mathbf{s}), \mathbf{r} - \mathbf{s}] \ \geq \ \alpha_0 \|\mathbf{r} - \mathbf{s}\|^2_{0,\Omega} \, .$$

Proof. It suffices to observe that for each $\widetilde{\mathbf{r}} \in \mathbb{L}^2(\Omega)$ the Gâteuax derivative $\mathcal{D}\mathbb{A}(\widetilde{\mathbf{r}})$ is a bilinear form on $\mathbb{L}^2(\Omega) \times \mathbb{L}^2(\Omega)$, which is uniformly bounded and uniformly $\mathbb{L}^2(\Omega)$-elliptic (see [21, Lemma 2.1] or [5, Section 3] for details). □

The following two lemmas, which establish that the nonlinear operator $\mathcal{A}_h$ defining the problem (2.10) shares the same properties of $\mathbb{A}$, were provided in [22].

Lemma 3.3. *Let $\mathcal{A}_h$ be the nonlinear operator defined by* (2.11)*. Then, there exists a constant $C_{\rm LC} > 0$, independent of h, such that*

$$\|\mathcal{A}_h(\mathbf{t}_h, \boldsymbol{\sigma}_h) - \mathcal{A}_h(\mathbf{s}_h, \boldsymbol{\tau}_h)\|_{H_h'} \;\leq\; C_{\rm LC}\, \|(\mathbf{t}_h, \boldsymbol{\sigma}_h) - (\mathbf{s}_h, \boldsymbol{\tau}_h)\|_{H_h} \quad \forall\; (\mathbf{t}_h, \boldsymbol{\sigma}_h), (\mathbf{s}_h, \boldsymbol{\tau}_h) \in H_h\,.$$

Proof. See [22, Lemma 3.5] □

Lemma 3.4. *Let $\mathcal{A}_h$ be the nonlinear operator defined by* (2.11)*, and assume that, given $\delta \in \left(0, \frac{2}{\gamma_0}\right)$, the parameter κ_1 lies in $\left(0, \frac{2\alpha_0\delta}{\gamma_0}\right)$, where α_0 and γ_0 are the positive constants from* (2.2) *and* (2.3)*. Then, there exists a constant $C_{\rm SM} > 0$, independent of h, such that*

$$[\mathcal{A}_h(\mathbf{t}_h, \boldsymbol{\sigma}_h) - \mathcal{A}_h(\mathbf{s}_h, \boldsymbol{\tau}_h), (\mathbf{t}_h, \boldsymbol{\sigma}_h) - (\mathbf{s}_h, \boldsymbol{\tau}_h)] \;\geq\; C_{\rm SM}\, \|(\mathbf{t}_h, \boldsymbol{\sigma}_h) - (\mathbf{s}_h, \boldsymbol{\tau}_h)\|^2_{H_h}\,,$$

for all $(\mathbf{t}_h, \boldsymbol{\sigma}_h), (\mathbf{s}_h, \boldsymbol{\tau}_h) \in H_h$.

Proof. See [22, Lemma 3.6] □

We remark here that the optimal choice of the stabilization parameter κ_1, that is the one yielding the largest value of the strong monotonicity constant $C_{\rm SM}$, arises by taking $\delta = \frac{1}{\gamma_0}$ and $\kappa_1 = \frac{\alpha_0}{\gamma_0^2}$. This will be used in Section 6. Our next goal is to show the discrete inf-sup condition for the linear operator $\mathcal{B}_h$. More precisely, we have the following result.

Lemma 3.5. *There exists a constant $C_{\rm inf} > 0$, independent of h, such that*

$$\sup_{\substack{(\mathbf{s}_h, \boldsymbol{\tau}_h) \in H_h \\ (\mathbf{s}_h, \boldsymbol{\tau}_h) \neq \mathbf{0}}} \frac{[\mathcal{B}_h(\mathbf{s}_h, \boldsymbol{\tau}_h), \mathbf{v}_h]}{\|(\mathbf{s}_h, \boldsymbol{\tau}_h)\|_{H_h}} \;\geq\; C_{\rm inf}\, \|\mathbf{v}_h\|_{0,\Omega} \quad \forall\; \mathbf{v}_h \in V_h\,.$$

Proof. We adapt the proof of [22, Lemma 3.7]. Indeed, we begin by recalling from (2.12) that $\mathcal{B}_h$ does not depend on $\mathbf{s}_h$, and hence it suffices to show the existence of $C_{\rm inf} > 0$ such that

$$\sup_{\substack{\boldsymbol{\tau}_h \in \Sigma_h \\ \boldsymbol{\tau}_h \neq \mathbf{0}}} \frac{\displaystyle\int_\Omega \mathbf{v}_h \cdot \mathbf{div}_h(\boldsymbol{\tau}_h) - \int_{\mathcal{E}_h^i} \{\!\!\{\mathbf{v}_h\}\!\!\} \cdot [\![\boldsymbol{\tau}_h]\!]}{\|\boldsymbol{\tau}_h\|_{\Sigma_h}} \;\geq\; C_{\rm inf}\, \|\mathbf{v}_h\|_{0,\Omega} \quad \forall\; \mathbf{v}_h \in V_h\,.$$

To this end we let $\mathbb{RT}_k(\mathcal{T}_h)$ be the global Raviart-Thomas space of degree k, which is clearly contained in Σ_h, and note that

$$\sup_{\substack{\boldsymbol{\tau}_h \in \Sigma_h \\ \boldsymbol{\tau}_h \neq \mathbf{0}}} \frac{\displaystyle\int_\Omega \mathbf{v}_h \cdot \mathbf{div}_h(\boldsymbol{\tau}_h) - \int_{\mathcal{E}_h^i} \{\!\!\{\mathbf{v}_h\}\!\!\} \cdot [\![\boldsymbol{\tau}_h]\!]}{\|\boldsymbol{\tau}_h\|_{\Sigma_h}} \;\geq\; \sup_{\substack{\boldsymbol{\tau}_h \in \mathbb{RT}_k(\mathcal{T}_h) \setminus \{\mathbf{0}\} \\ \int_\Omega \mathrm{tr}(\boldsymbol{\tau}_h) = 0}} \frac{\displaystyle\int_\Omega \mathbf{v}_h \cdot \mathbf{div}(\boldsymbol{\tau}_h)}{\|\boldsymbol{\tau}_h\|_{\Sigma_h}}\,.$$

In this way, and observing that $\|\boldsymbol{\tau}_h\|_{\Sigma_h}$ is equivalent to $\|\boldsymbol{\tau}_h\|_{\mathbf{div},\Omega}$ $\forall\; \boldsymbol{\tau}_h \in \mathbb{RT}_k(\mathcal{T}_h)$ such that $\int_\Omega \mathrm{tr}\,(\boldsymbol{\tau}_h) = 0$, with constants independent of h, the rest of the proof follows from classical results from mixed finite element methods (see, e.g. [16, Section 4.2 and Lemma 2.6]). □

The following lemma establishes the positive semidefiniteness of $\mathcal{S}_h$.

Lemma 3.6. *The operator $\mathcal{S}_h : V_h \to V_h'$ (cf. (2.13)) is positive semidefinite, that is,*

$$[\mathcal{S}_h(\mathbf{v}_h), \mathbf{v}_h] \;\geq\; 0 \quad \forall\, \mathbf{v}_h \in V_h\,.$$

Proof. It is clear from (2.13) and the symmetry of $\mathbf{S}$ that

$$\begin{aligned}
[\mathcal{S}_h(\mathbf{v}_h), \mathbf{v}_h] \;&=\; \sum_{T\in\mathcal{T}_h}\sum_{F\in\partial T}\int_F \mathbf{S}\mathbf{v}_h\cdot\mathbf{v}_h - 2\int_{\mathcal{E}_h^i}\mathbf{S}\{\!\{\mathbf{v}_h\}\!\}\cdot\{\!\{\mathbf{v}_h\}\!\}\\
&=\; \int_{\mathcal{E}_h^i}\left(\mathbf{S}\mathbf{v}_h^+\cdot\mathbf{v}_h^+ + \mathbf{S}\mathbf{v}_h^-\cdot\mathbf{v}_h^-\right) - \frac{1}{2}\int_{\mathcal{E}_h^i}\left(\mathbf{S}\mathbf{v}_h^+\cdot\mathbf{v}_h^+ + 2\,\mathbf{S}\mathbf{v}_h^+\cdot\mathbf{v}_h^- + \mathbf{S}\mathbf{v}_h^-\cdot\mathbf{v}_h^-\right) + \int_{\mathcal{E}_h^\partial}\mathbf{S}\mathbf{v}_h\cdot\mathbf{v}_h\\
&=\; \frac{1}{2}\int_{\mathcal{E}_h^i}\left(\mathbf{S}\mathbf{v}_h^+\cdot\mathbf{v}_h^+ - 2\,\mathbf{S}\mathbf{v}_h^+\cdot\mathbf{v}_h^- + \mathbf{S}\mathbf{v}_h^-\cdot\mathbf{v}_h^-\right) \;+\; \int_{\mathcal{E}_h^\partial}\mathbf{S}\mathbf{v}_h\cdot\mathbf{v}_h\\
&=\; \frac{1}{2}\int_{\mathcal{E}_h^i}\mathbf{S}\left(\mathbf{v}_h^+ - \mathbf{v}_h^-\right)\cdot\left(\mathbf{v}_h^+ - \mathbf{v}_h^-\right) \;+\; \int_{\mathcal{E}_h^\partial}\mathbf{S}\mathbf{v}_h\cdot\mathbf{v}_h\,,
\end{aligned}$$

which, thanks to the fact that $\mathbf{S}$ is a positive definite tensor on $\mathcal{E}_h$, completes the proof. □

Now we are ready to establish the main result of this section.

Theorem 3.2. *Assume that $\mathbf{f}\in\mathbf{L}^2(\Omega)$, $\mathbf{g}\in\mathbf{H}^{1/2}(\Gamma)$, and that, given $\delta\in\left(0,\frac{2}{\gamma_0}\right)$, the parameter κ_1 lies in $\left(0,\frac{2\alpha_0\delta}{\gamma_0}\right)$, where α_0 and γ_0 are the positive constants from (2.2) and (2.3). Then, there exists a unique $((\mathbf{t}_h,\boldsymbol{\sigma}_h),\mathbf{u}_h)\in H_h\times V_h$ solution of (2.10). Moreover, there holds*

$$\|(\mathbf{t}_h,\boldsymbol{\sigma}_h)\|_{H_h} \;+\; \|\mathbf{u}_h\|_{0,\Omega} \;\leq\; C\left\{\|\mathbf{f}\|_{0,\Omega} \;+\; \|\mathtt{h}^{-1/2}\mathbf{g}\|_{0,\mathcal{E}_h^\partial}\right\}.$$

Proof. Thanks to Lemmas 3.3, 3.4, 3.5, and 3.6, the proof is a direct application of Theorem 3.1. □

4 A priori error analysis

We now aim to derive the *a priori* error estimates for the augmented HDG scheme (2.10). We begin by remarking that the proof from [22, Section 4] is suitably adapted. Thus, since $\mathbf{u}\in\mathbf{L}^2(\Omega)$ and $\nabla\mathbf{u}=\mathbf{t}\in\mathbb{L}^2(\Omega)$ (cf. (2.5)), we observe that actually $\mathbf{u}\in\mathbf{H}^1(\Omega)$, which guarantees that the jump $[\![\mathbf{u}]\!]$ vanishes on any interior face of $\mathcal{T}_h$ and there holds $\{\!\{\mathbf{u}\}\!\}=\mathbf{u}$. In addition, since $\boldsymbol{\sigma}=\boldsymbol{\psi}(\nabla\mathbf{u})-p\,\mathbb{I}\in\mathbb{L}^2(\Omega)$ and $\mathbf{div}(\boldsymbol{\sigma})=-\mathbf{f}$ in Ω, with $\mathbf{f}\in\mathbf{L}^2(\Omega)$, we conclude that $\boldsymbol{\sigma}\in\mathbb{H}(\mathbf{div};\Omega)$, whence $[\![\boldsymbol{\sigma}]\!]=\mathbf{0}$ on each $F\in\mathcal{E}_h^i$. Then, it is easy to check that $(\mathbf{t},\boldsymbol{\sigma},\mathbf{u})$ satisfies the equations of (2.10), and then there holds

$$\begin{aligned}
[\mathcal{A}_h(\mathbf{t},\boldsymbol{\sigma})-\mathcal{A}_h(\mathbf{t}_h,\boldsymbol{\sigma}_h),(\mathbf{s}_h,\boldsymbol{\tau}_h)] \;+\; [\mathcal{B}_h(\mathbf{s}_h,\boldsymbol{\tau}_h),\mathbf{u}-\mathbf{u}_h] \;&=\; 0 \quad \forall\,(\mathbf{s}_h,\boldsymbol{\tau}_h)\in H_h\,,\\
[\mathcal{B}_h((\mathbf{t},\boldsymbol{\sigma})-(\mathbf{t}_h,\boldsymbol{\sigma}_h)),\mathbf{v}_h] \;-\; [\mathcal{S}_h(\mathbf{u}-\mathbf{u}_h),\mathbf{v}_h] \;&=\; 0 \quad \forall\,\mathbf{v}_h\in V_h\,.
\end{aligned} \tag{4.1}$$

The following result establishes the Céa estimate for (2.6) and (2.10).

Lemma 4.1. *Let $(\mathbf{t},\boldsymbol{\sigma},\mathbf{u})\in\mathbb{L}^2(\Omega)\times\mathbb{H}(\mathbf{div};\Omega)\times\mathbf{L}^2(\Omega)$ and $((\mathbf{t}_h,\boldsymbol{\sigma}_h),\mathbf{u}_h)\in H_h\times V_h$ be the unique solutions of (2.6) and (2.10), respectively. Then, there exists $C>0$, independent of h, such that*

$$\begin{aligned}
&\|(\mathbf{t},\boldsymbol{\sigma})-(\mathbf{t}_h,\boldsymbol{\sigma}_h)\|_{H_h} \;+\; \|\mathbf{u}-\mathbf{u}_h\|_{0,\Omega}\\
&\quad\leq\; C\left\{\inf_{(\mathbf{s}_h,\boldsymbol{\tau}_h)\in H_h}\|(\mathbf{t},\boldsymbol{\sigma})-(\mathbf{s}_h,\boldsymbol{\tau}_h)\|_{H_h} \;+\; \inf_{\mathbf{v}_h\in V_h}\|\mathbf{u}-\mathbf{v}_h\|_{0,\Omega}\right\}.
\end{aligned}$$

Proof. It is not difficult to see that $\mathcal{A}_h$ has a uniformly bounded and uniformly H_h-elliptic Gâteuax derivative, and hence the proof is a straightforward adaptation of the arguments from [19, Theorem 3.3], together with simple applications of the triangle inequality and (4.1). □

Next, in order to provide the rate of convergence of the discontinuous Galerkin scheme (2.10), we need the approximation properties of the finite element subspaces involved. For this purpose, given $T \in \mathcal{T}_h$, we let $\boldsymbol{\mathcal{P}}_T^k : \mathbb{L}^2(T) \to \mathbb{P}_k(T)$ and $\mathcal{P}_T^k : \mathbf{L}^2(T) \to \mathbf{P}_k(T)$ be the $\mathbb{L}^2(T)$ and $\mathbf{L}^2(T)$ − orthogonal projectors, respectively, which satisfy (see, e.g. [8, 16])

$$\|\mathbf{s} - \boldsymbol{\mathcal{P}}_T^k(\mathbf{s})\|_{0,T} \leq C\, h_T^{\min\{\ell,k+1\}} |\mathbf{s}|_{\ell,T} \quad \forall\, \mathbf{s} \in \mathbb{H}^\ell(T)\,, \quad \forall\, T \in \mathcal{T}_h\,, \tag{4.2}$$

and

$$\|\mathbf{v} - \mathcal{P}_T^k(\mathbf{v})\|_{0,T} \leq C\, h_T^{\min\{\ell,k+1\}} |\mathbf{v}|_{\ell,T} \quad \forall\, \mathbf{v} \in \mathbf{H}^\ell(T)\,, \quad \forall\, T \in \mathcal{T}_h\,. \tag{4.3}$$

Furthermore, let $\Pi_T^k : \mathbb{H}^1(T) \to \mathbb{RT}_k(T)$ be the Raviart-Thomas interpolation operator (see [3, 16, 28]), which, given $\boldsymbol{\tau} \in \mathbb{H}^1(\Omega)$, is characterized by the following identities:

$$\int_F \Pi_T^k(\boldsymbol{\tau})\boldsymbol{\nu} \cdot \boldsymbol{\mu} \;=\; \int_F \boldsymbol{\tau}\boldsymbol{\nu} \cdot \boldsymbol{\mu} \qquad \forall\, \boldsymbol{\mu} \in \mathbf{P}_k(F)\,, \quad \forall\, F \in \partial T\,, \quad \text{when } k \geq 0\,, \tag{4.4}$$

and

$$\int_T \Pi_T^k(\boldsymbol{\tau}) : \boldsymbol{\rho} \;=\; \int_T \boldsymbol{\tau} : \boldsymbol{\rho} \qquad \forall\, \boldsymbol{\rho} \in \mathbb{P}_{k-1}(T)\,, \quad \text{when } k \geq 1\,. \tag{4.5}$$

It is well-known that Π_T^k satisfies the approximation property

$$\|\boldsymbol{\tau} - \Pi_T^k(\boldsymbol{\tau})\|_{\mathbf{div},T} \;\leq\; C h_T^{\min\{\ell,k+1\}} \Big\{ |\boldsymbol{\tau}|_{\ell,T} \;+\; |\mathbf{div}(\boldsymbol{\tau})|_{\ell,T} \Big\} \quad \forall\, T \in \mathcal{T}_h\,, \tag{4.6}$$

for each $\boldsymbol{\tau} \in \mathbb{H}^\ell(T)$ such that $\mathbf{div}(\boldsymbol{\tau}) \in \mathbf{H}^\ell(T)$, with $\ell \geq 1$. Moreover, the interpolation operator Π_T^k can also be defined as a bounded linear operator from the larger space $\mathbb{H}^\ell(T) \cap \mathbb{H}(\mathbf{div};T)$ into $\mathbb{RT}_k(T)$ for all $\ell \in (0,1]$ (see, e.g. [24, Theorem 3.16]). In this case there holds (see [16, Lemma 3.19])

$$\|\boldsymbol{\tau} - \Pi_T^k(\boldsymbol{\tau})\|_{0,T} \;\leq\; C h_T^{\ell} \Big\{ |\boldsymbol{\tau}|_{\ell,T} \;+\; \|\mathbf{div}(\boldsymbol{\tau})\|_{0,T} \Big\} \quad \forall\, T \in \mathcal{T}_h\,,$$

which, thanks to (4.6) and interpolation estimates, implies for $\ell > 0$ that

$$\|\boldsymbol{\tau} - \Pi_T^k(\boldsymbol{\tau})\|_{\mathbf{div},T} \;\leq\; C h_T^{\min\{\ell,k+1\}} \Big\{ |\boldsymbol{\tau}|_{\ell,T} \;+\; \|\mathbf{div}(\boldsymbol{\tau})\|_{\ell,T} \Big\} \quad \forall\, T \in \mathcal{T}_h\,. \tag{4.7}$$

Next, observe that, given $Z := \{\boldsymbol{\tau} \in \mathbb{L}^2(\Omega) \;:\; \boldsymbol{\tau}|_T \in \mathbb{H}^\ell(T) \quad \forall\, T \in \mathcal{T}_h\}$, we can define $\Pi_{\Sigma_h} : \mathbb{H}(\mathbf{div};\Omega) \cap Z \to \Sigma_h$ by

$$\Pi_{\Sigma_h}(\boldsymbol{\tau})|_T \;:=\; \Pi_T^k(\boldsymbol{\tau}|_T) \;+\; d\,\mathbb{I} \quad \forall\, T \in \mathcal{T}_h\,,$$

with $d := -\frac{1}{n|\Omega|} \sum\limits_{T \in \mathcal{T}_h} \int_T \mathrm{tr}\,\big(\Pi_T^k(\boldsymbol{\tau}|_T)\big) \in R$. Then, it is easy to prove that

$$\|\boldsymbol{\tau} - \Pi_{\Sigma_h}(\boldsymbol{\tau})\|_{\Sigma_h}^2 \;\leq\; \sum_{T \in \mathcal{T}_h} \|\boldsymbol{\tau} - \Pi_T^k(\boldsymbol{\tau})\|_{\mathbf{div},T}^2 \quad \forall\, \boldsymbol{\tau} \in \mathbb{H}(\mathbf{div};\Omega) \cap Z\,,$$

and hence, employing the estimate (4.7), we arrive at

$$\|\boldsymbol{\tau} - \Pi_{\Sigma_h}(\boldsymbol{\tau})\|_{\Sigma_h} \;\leq\; C \sum_{T \in \mathcal{T}_h} h_T^{\min\{\ell,k+1\}} \Big\{ |\boldsymbol{\tau}|_{\ell,T} \;+\; \|\mathbf{div}(\boldsymbol{\tau})\|_{\ell,T} \Big\}\,. \tag{4.8}$$

In this way, as a consequence of (4.2), (4.3), (4.8), and the usual interpolation estimates, we find that S_h, Σ_h and V_h satisfy the following approximation properties:

($\mathbf{AP}_h^{\mathbf{t}}$) For each $\ell \geq 0$ and for each $\mathbf{s} \in \mathbb{H}^\ell(\Omega)$ there exists $\mathbf{s}_h \in S_h$ such that

$$\|\mathbf{s} - \mathbf{s}_h\|_{0,\Omega} \ \leq \ C \sum_{T \in \mathcal{T}_h} h_T^{\min\{\ell, k+1\}} |\mathbf{s}|_{\ell,T} \, .$$

($\mathbf{AP}_h^{\boldsymbol{\sigma}}$) For each $\ell > 0$ and for each $\boldsymbol{\tau} \in \mathbb{H}^\ell(\Omega)$ with $\mathbf{div}(\boldsymbol{\tau}) \in \mathbf{H}^\ell(\Omega)$ there exists $\boldsymbol{\tau}_h \in \Sigma_h$ such that

$$\|\boldsymbol{\tau} - \boldsymbol{\tau}_h\|_{\Sigma_h} \ \leq \ C \sum_{T \in \mathcal{T}_h} h_T^{\min\{\ell, k+1\}} \Big\{ |\boldsymbol{\tau}|_{\ell,T} \ + \ \|\mathbf{div}(\boldsymbol{\tau})\|_{\ell,T} \Big\} \, .$$

($\mathbf{AP}_h^{\mathbf{u}}$) For each $\ell \geq 0$ and for each $\mathbf{v} \in \mathbf{H}^\ell(\Omega)$ there exists $\mathbf{v}_h \in V_h$ such that

$$\|\mathbf{v} - \mathbf{v}_h\|_{0,\Omega} \ \leq \ C \sum_{T \in \mathcal{T}_h} h_T^{\min\{\ell, k+1\}} |\mathbf{v}|_{\ell,T} \, .$$

The following theorem establishes the theoretical rates of convergence of the discrete scheme (2.10), under suitable regularity assumptions on the exact solution.

Theorem 4.1. *Let $(\mathbf{t}, \boldsymbol{\sigma}, \mathbf{u}) \in \mathbb{L}^2(\Omega) \times \mathbb{H}(\mathbf{div}; \Omega) \times \mathbf{L}^2(\Omega)$ and $((\mathbf{t}_h, \boldsymbol{\sigma}_h), \mathbf{u}_h) \in H_h \times V_h$ be the unique solutions of* (2.6) *and* (2.10)*, respectively. In addition, suppose that there exists an integer $\ell > 0$ such that $\mathbf{t}|_T \in \mathbb{H}^\ell(T)$, $\boldsymbol{\sigma}|_T \in \mathbb{H}^\ell(T)$, $\mathbf{div}(\boldsymbol{\sigma}|_T) \in \mathbf{H}^\ell(T)$ and $\mathbf{u}|_T \in \mathbf{H}^\ell(T)$, for all $T \in \mathcal{T}_h$. Then, there exists $C > 0$, independent of h and the polynomial approximation degree k, such that*

$$\begin{aligned} &\|\mathbf{t} - \mathbf{t}_h\|_{0,\Omega} \ + \ \|\boldsymbol{\sigma} - \boldsymbol{\sigma}_h\|_{\Sigma_h} \ + \ \|\mathbf{u} - \mathbf{u}_h\|_{0,\Omega} \\ &\leq \ C \sum_{T \in \mathcal{T}_h} h_T^{\min\{\ell, k+1\}} \Big\{ |\mathbf{t}|_{\ell,T} \ + \ |\boldsymbol{\sigma}|_{\ell,T} \ + \ \|\mathbf{div}(\boldsymbol{\sigma})\|_{\ell,T} \ + \ |\mathbf{u}|_{\ell,T} \Big\} \, . \end{aligned}$$

Proof. It follows from the Céa estimate (cf. Lemma 4.1) and the approximation properties ($\mathbf{AP}_h^{\mathbf{t}}$), ($\mathbf{AP}_h^{\boldsymbol{\sigma}}$) and ($\mathbf{AP}_h^{\mathbf{u}}$). □

Note from the previous theorem and (3.3) that we can also conclude that

$$\|\boldsymbol{\sigma} - \boldsymbol{\sigma}_h\|_{0,\Omega} \ \leq \ C \sum_{T \in \mathcal{T}_h} h_T^{\min\{\ell, k+1\}} \Big\{ |\mathbf{t}|_{\ell,T} + |\boldsymbol{\sigma}|_{\ell,T} + \|\mathbf{div}(\boldsymbol{\sigma})\|_{\ell,T} + |\mathbf{u}|_{\ell,T} \Big\} \, . \tag{4.9}$$

On the other hand, we know from (2.4) that $p = -\frac{1}{n}\mathrm{tr}\,(\boldsymbol{\sigma})$, which suggests to define the following postprocessed approximation of the pressure:

$$p_h \ := \ -\frac{1}{n}\,\mathrm{tr}\,(\boldsymbol{\sigma}_h) \quad \text{in} \quad \Omega \, . \tag{4.10}$$

It follows that

$$\|p - p_h\|_{0,\Omega} \ = \ \frac{1}{n}\,\|\mathrm{tr}\,(\boldsymbol{\sigma} - \boldsymbol{\sigma}_h)\,\|_{0,\Omega} \ \leq \ \frac{1}{\sqrt{n}}\,\|\boldsymbol{\sigma} - \boldsymbol{\sigma}_h\|_{0,\Omega} \, , \tag{4.11}$$

which, thanks to (4.9), gives the *a priori* error estimate for the pressure.

Finally, in order to measure the error for the trace variable, namely $\widehat{\mathbf{u}}_h$ or $\boldsymbol{\lambda}_h$, we define the error:

$$\|\mathbf{u} - \widehat{\mathbf{u}}_h\|_h \ := \ \left\{ \sum_{F \in \mathcal{E}_h^i} \Big\| \mathtt{h}^{1/2} \big(\{\!\!\{ \mathcal{P}_h^k(\mathbf{u}) \}\!\!\} - \boldsymbol{\lambda}_h \big) \Big\|_{0,F}^2 \right\}^{1/2} , \tag{4.12}$$

where $\mathcal{P}_h^k|_T := \mathcal{P}_T^k$, for each $T \in \mathcal{T}_h$. The corresponding *a priori* error estimate is established next.

Theorem 4.2. *Assume the same hypotheses of Theorem* 4.1. *Then, there exists $C > 0$, independent of h and the polynomial approximation degree k, such that*

$$\|\mathbf{u} - \widehat{\mathbf{u}}_h\|_h \;\leq\; C \sum_{T \in \mathcal{T}_h} h_T^{\min\{\ell, k+1\}} \Big\{ |\mathbf{t}|_{\ell,T} + |\boldsymbol{\sigma}|_{\ell,T} + \|\mathbf{div}(\boldsymbol{\sigma})\|_{\ell,T} + |\mathbf{u}|_{\ell,T} \Big\} .$$

Proof. From (2.9), (3.2) and the fact that $[\![\boldsymbol{\sigma}]\!] = \mathbf{0}$ on $\mathcal{E}_h^i$, we obtain that

$$\begin{aligned}
\|\mathbf{u} - \widehat{\mathbf{u}}_h\|_h^2 &= \sum_{F \in \mathcal{E}_h^i} \left\| \mathtt{h}^{1/2} \left(\{\!\{ \mathcal{P}_h^k(\mathbf{u}) \}\!\} - \{\!\{ \mathbf{u}_h \}\!\} + \frac{1}{2} \mathtt{h}^{-1} [\![\boldsymbol{\sigma}_h]\!] \right) \right\|_{0,F}^2 \\
&\leq 2 \sum_{F \in \mathcal{E}_h^i} \left\{ \|\mathtt{h}^{1/2} \{\!\{ \mathcal{P}_h^k(\mathbf{u}) - \mathbf{u}_h \}\!\}\|_{0,F}^2 + \frac{1}{4} \|\mathtt{h}^{-1/2} [\![\boldsymbol{\sigma} - \boldsymbol{\sigma}_h]\!]\|_{0,F}^2 \right\} \\
&\leq C \Big\{ \|\mathtt{h}^{1/2} \{\!\{ \mathcal{P}_h^k(\mathbf{u}) - \mathbf{u}_h \}\!\}\|_{0,\mathcal{E}_h^i}^2 \;+\; \|\boldsymbol{\sigma} - \boldsymbol{\sigma}_h\|_{\Sigma_h}^2 \Big\} . \qquad (4.13)
\end{aligned}$$

Next, using the analogue of [22, Lemma 3.10, part i)], we deduce that

$$\|\mathtt{h}^{1/2} \{\!\{ \mathcal{P}_h^k(\mathbf{u}) - \mathbf{u}_h \}\!\}\|_{0,\mathcal{E}_h^i} \leq \widetilde{C} \, \|\mathcal{P}_h^k(\mathbf{u}) - \mathbf{u}_h\|_{0,\Omega} ,$$

with $\widetilde{C}$ independent of h. Therefore, we conclude from (4.13) that

$$\begin{aligned}
\|\mathbf{u} - \widehat{\mathbf{u}}_h\|_h &\leq C \Big\{ \|\mathcal{P}_h^k(\mathbf{u}) - \mathbf{u}_h\|_{0,\Omega} \;+\; \|\boldsymbol{\sigma} - \boldsymbol{\sigma}_h\|_{\Sigma_h} \Big\} \\
&\leq C \Big\{ \|\mathbf{u} - \mathcal{P}_h^k(\mathbf{u})\|_{0,\Omega} \;+\; \|\mathbf{u} - \mathbf{u}_h\|_{0,\Omega} \;+\; \|\boldsymbol{\sigma} - \boldsymbol{\sigma}_h\|_{\Sigma_h} \Big\} ,
\end{aligned}$$

which, together with (4.3) and Theorem 4.1, complete the proof. □

5 A residual-based a posteriori error estimator

In this section we develop a residual-based *a posteriori* error analysis for the augmented HDG scheme (2.8). We begin by recalling that the equivalent formulation (2.10) was introduced in order to perform the solvability analysis and derive the *a priori* error estimates provided in Sections 3 and 4, respectively. In what follows we restrict ourselves to an arbitrary polygonal domain Ω in 2D, but keep in mind that the extension to convex polyhedral domains in 3D is quite straightforward (see, e.g. [18, Section 4] for a related approach in this regard).

First we introduce some notations. Given $T \in \mathcal{T}_h$, we let

$$\|\boldsymbol{\tau}_h\|_{\Sigma_h(T)}^2 \;:=\; \|\boldsymbol{\tau}_h^{\mathtt{d}}\|_{0,T}^2 \;+\; \|\mathbf{div}(\boldsymbol{\tau}_h)\|_{0,T}^2 \;+\; \frac{1}{2} \sum_{F \in \partial T \cap \mathcal{E}_h^i} \|\mathtt{h}^{-1/2} [\![\boldsymbol{\tau}_h]\!]\|_{0,F}^2 ,$$

be the local contribution of the norm $\|\cdot\|_{\Sigma_h}$, that is,

$$\|\boldsymbol{\tau}_h\|_{\Sigma_h} \;=\; \left\{ \sum_{T \in \mathcal{T}_h} \|\boldsymbol{\tau}_h\|_{\Sigma_h(T)}^2 \right\}^{1/2} . \qquad (5.1)$$

Also, for each edge $F \in \mathcal{E}_h$ we fix a unit normal vector $\boldsymbol{\nu}_F := (\nu_1, \nu_2)^{\mathtt{t}}$, and let $\boldsymbol{s}_F := (-\nu_2, \nu_1)^{\mathtt{t}}$ be the corresponding fixed unit tangential vector along F. Then, given $F \in \mathcal{E}_h^i$ such that $F = \partial T^+ \cap \partial T^-$, we let $[\![\boldsymbol{\tau} \boldsymbol{s}_F]\!]$ be the corresponding tangential jump across F, that is $[\![\boldsymbol{\tau} \boldsymbol{s}_F]\!] := (\boldsymbol{\tau}^+ - \boldsymbol{\tau}^-) \boldsymbol{s}_F$. From now

on, when no confusion arises, we simply write $\boldsymbol{s}$ and $\boldsymbol{\nu}$ instead of $\boldsymbol{s}_F$ and $\boldsymbol{\nu}_F$, respectively. Finally, given scalar, vector and tensor valued fields v, $\boldsymbol{\varphi} := (\varphi_1, \varphi_2)$ and $\boldsymbol{\tau} := (\tau_{ij})$, respectively, we let

$$\mathbf{curl}(v) := \begin{pmatrix} \frac{\partial v}{\partial x_2} \\ -\frac{\partial v}{\partial x_1} \end{pmatrix}, \quad \underline{\mathbf{curl}}(\boldsymbol{\varphi}) := \begin{pmatrix} \mathbf{curl}(\varphi_1)^{\mathrm{t}} \\ \mathbf{curl}(\varphi_2)^{\mathrm{t}} \end{pmatrix}, \quad \text{and} \quad \mathrm{curl}(\boldsymbol{\tau}) := \begin{pmatrix} \frac{\partial \tau_{12}}{\partial x_1} - \frac{\partial \tau_{11}}{\partial x_2} \\ \frac{\partial \tau_{22}}{\partial x_1} - \frac{\partial \tau_{21}}{\partial x_2} \end{pmatrix}.$$

5.1 Flux postprocessing

We now follow [11, Section 5.1] (see also [12]) and introduce a postprocessed flux $\boldsymbol{\sigma}_h^\star$ for the variable $\boldsymbol{\sigma}_h$, that is, we let $\boldsymbol{\sigma}_h^\star$ be the unique element in $\mathbb{RT}_k(\mathcal{T}_h)$ such that

$$\int_T \boldsymbol{\sigma}_h^\star : \boldsymbol{\tau}_h = \int_T \boldsymbol{\sigma}_h : \boldsymbol{\tau}_h \quad \forall\, \boldsymbol{\tau}_h \in \mathbb{P}_{k-1}(T)\,, \quad \forall\, T \in \mathcal{T}_h\,, \tag{5.2}$$

$$\int_F \boldsymbol{\sigma}_h^\star \boldsymbol{\nu} \cdot \boldsymbol{\mu}_h = \int_F \widehat{\boldsymbol{\sigma}_h \boldsymbol{\nu}} \cdot \boldsymbol{\mu}_h \quad \forall\, \boldsymbol{\mu}_h \in \mathbf{P}_k(F)\,, \quad \forall\, F \in \partial T\,, \quad \forall\, T \in \mathcal{T}_h\,, \tag{5.3}$$

where $\mathbb{RT}_k(\mathcal{T}_h)$ is the global Raviart-Thomas subspace of degree k. It is important to observe here, thanks to the fourth equation of (2.7), that $\boldsymbol{\sigma}_h^\star \in \mathbb{H}(\mathbf{div};\Omega)$. In addition, from the third equation in (2.7) and the foregoing definition of $\boldsymbol{\sigma}_h^\star$, we have that

$$(\mathbf{f}, \mathbf{v}_h)_{\mathcal{T}_h} = (\boldsymbol{\sigma}_h, \nabla \mathbf{v}_h)_{\mathcal{T}_h} - \langle \widehat{\boldsymbol{\sigma}_h \boldsymbol{\nu}}, \mathbf{v}_h \rangle_{\partial \mathcal{T}_h} = (\boldsymbol{\sigma}_h^\star, \nabla \mathbf{v}_h)_{\mathcal{T}_h} - \langle \boldsymbol{\sigma}_h^\star \boldsymbol{\nu}, \mathbf{v}_h \rangle_{\partial \mathcal{T}_h} = -(\mathbf{div}(\boldsymbol{\sigma}_h^\star), \mathbf{v}_h)_{\mathcal{T}_h}$$

for all $\mathbf{v}_h \in V_h$. The above identity and the fact that $\mathbf{div}(\boldsymbol{\sigma}_h^\star)|_T \in \mathbf{P}_k(T)$ for each $T \in \mathcal{T}_h$ imply that

$$\mathbf{div}(\boldsymbol{\sigma}_h^\star) = -\mathcal{P}_h^k(\mathbf{f}) \quad \text{in} \quad \Omega\,,$$

where $\mathcal{P}_h^k : \mathbf{L}^2(\Omega) \to V_h$ is the $\mathbf{L}^2(\Omega)$-orthogonal projector. More precisely, $\mathcal{P}_h^k|_T := \mathcal{P}_T^k$ for each $T \in \mathcal{T}_h$.

Now, recalling that $\mathbb{H}(\mathbf{div};\Omega) = \mathbb{H}_0(\mathbf{div};\Omega) \oplus R\,\mathbb{I}$, we denote by $\boldsymbol{\sigma}_{h,0}^\star$ the $\mathbb{H}_0(\mathbf{div};\Omega)$-component of $\boldsymbol{\sigma}_h^\star$. Equivalently, we write $\boldsymbol{\sigma}_h^\star = \boldsymbol{\sigma}_{h,0}^\star + d\,\mathbb{I}$, where $\boldsymbol{\sigma}_{h,0}^\star \in \mathbb{H}_0(\mathbf{div};\Omega)$ and $d := \frac{1}{n|\Omega|}\int_\Omega \mathrm{tr}\,(\boldsymbol{\sigma}_h^\star) \in R$. Notice from (5.2) and the fact that $\int_\Omega \mathrm{tr}\,(\boldsymbol{\sigma}_h) = 0$, that $\boldsymbol{\sigma}_h^\star = \boldsymbol{\sigma}_{h,0}^\star$ when $k \geq 1$.

We end this section by remarking in advance that the *a posteriori* error estimator to be introduced below (cf. (5.6)) will depend on $\boldsymbol{\sigma}_{h,0}^\star$.

5.2 The a posteriori error estimator

We now recall from [21] that the augmented continuous formulation associated with (2.6) reads: Find $((\mathbf{t}, \boldsymbol{\sigma}), \mathbf{u}) \in H \times V$ such that

$$\begin{aligned} [\mathcal{A}(\mathbf{t}, \boldsymbol{\sigma}), (\mathbf{s}, \boldsymbol{\tau})] + [\mathcal{B}(\mathbf{s}, \boldsymbol{\tau}), \mathbf{u}] &= [\mathcal{F}, (\mathbf{s}, \boldsymbol{\tau})] \quad \forall\, (\mathbf{s}, \boldsymbol{\tau}) \in H\,, \\ [\mathcal{B}(\mathbf{t}, \boldsymbol{\sigma}), \mathbf{v}] &= [\mathcal{G}, \mathbf{v}] \qquad \forall\, \mathbf{v} \in V\,, \end{aligned} \tag{5.4}$$

where $H := \mathbb{L}^2(\Omega) \times \mathbb{H}_0(\mathbf{div};\Omega)$, $V := \mathbf{L}^2(\Omega)$ and the nonlinear operator $\mathcal{A} : H \to H'$, the linear operator $\mathcal{B} : H \to V'$, and the functionals $\mathcal{F} \in H'$ and $\mathcal{G} \in V'$, are defined by:

$$[\mathcal{A}(\mathbf{t}, \boldsymbol{\sigma}), (\mathbf{s}, \boldsymbol{\tau})] := \int_\Omega \boldsymbol{\psi}(\mathbf{t}) : \mathbf{s} - \int_\Omega \mathbf{s} : \boldsymbol{\sigma}^{\mathtt{d}} + \int_\Omega \mathbf{t} : \boldsymbol{\tau}^{\mathtt{d}} + \kappa_1 \int_\Omega (\boldsymbol{\sigma}^{\mathtt{d}} - \boldsymbol{\psi}(\mathbf{t})) : \boldsymbol{\tau}^{\mathtt{d}} + \kappa_2 \int_\Omega \mathbf{div}(\boldsymbol{\sigma}) \cdot \mathbf{div}(\boldsymbol{\tau}),$$

$$[\mathcal{B}(\mathbf{s}, \boldsymbol{\tau}), \mathbf{v}] := \int_\Omega \mathbf{v} \cdot \mathbf{div}(\boldsymbol{\tau}), \quad [\mathcal{F}, (\mathbf{s}, \boldsymbol{\tau})] := \langle \boldsymbol{\tau}\boldsymbol{\nu}, \mathbf{g} \rangle_\Gamma - \kappa_2 \int_\Omega \mathbf{f} \cdot \mathbf{div}(\boldsymbol{\tau}), \quad \text{and} \quad [\mathcal{G}, \mathbf{v}] := -\int_\Omega \mathbf{f} \cdot \mathbf{v}.$$

We know from the analysis developed in [21, Section 3.1] that the problem (5.4) is well-posed, for $\kappa_1 \in \left(0, \frac{2\alpha_0\delta}{\gamma_0}\right)$, with $\delta \in \left(0, \frac{2}{\gamma_0}\right)$, and $\kappa_2 > 0$. Certainly, the same is valid for the linear operator $\mathcal{M}$ obtained by adding the two equations on the left hand side of (5.4), after replacing $\mathbb{A}$ (cf. (3.4)) within $\mathcal{A}$ by the Gâteaux derivative $\mathcal{D}\mathbb{A}(\widetilde{\mathbf{r}})$ at any $\widetilde{\mathbf{r}} \in \mathbb{L}^2(\Omega)$, that is

$$[\,\mathcal{M}((\mathbf{s},\boldsymbol{\tau}),\mathbf{v}),\,((\mathbf{r},\boldsymbol{\rho}),\mathbf{w})\,] := \mathcal{D}\mathbb{A}(\widetilde{\mathbf{r}})(\mathbf{r},\mathbf{s}-\kappa_1\boldsymbol{\tau}^{\mathtt{d}}) - \int_\Omega \mathbf{s}:\boldsymbol{\rho}^{\mathtt{d}} + \int_\Omega \mathbf{r}:\boldsymbol{\tau}^{\mathtt{d}} + \kappa_1\int_\Omega \boldsymbol{\rho}^{\mathtt{d}}:\boldsymbol{\tau}^{\mathtt{d}} + \kappa_2\int_\Omega \mathbf{div}(\boldsymbol{\rho})\cdot\mathbf{div}(\boldsymbol{\tau}) \;+\; [\mathcal{B}(\mathbf{s},\boldsymbol{\tau}),\mathbf{w}] \;+\; [\mathcal{B}(\mathbf{r},\boldsymbol{\rho}),\mathbf{v}]\,.$$

Then, applying the respective continuous dependence result to $\mathcal{M}$, we obtain a global inf-sup condition, which means that there exists a constant $\widetilde{C} > 0$ such that

$$\widetilde{C}\,\|((\mathbf{r},\boldsymbol{\rho}),\mathbf{w})\|_{H\times V} \;\leq\; \sup_{\substack{((\mathbf{s},\boldsymbol{\tau}),\mathbf{v})\in H\times V\\ ((\mathbf{s},\boldsymbol{\tau}),\mathbf{v})\neq\mathbf{0}}} \frac{[\,\mathcal{M}((\mathbf{s},\boldsymbol{\tau}),\mathbf{v}),\,((\mathbf{r},\boldsymbol{\rho}),\mathbf{w})\,]}{\|((\mathbf{s},\boldsymbol{\tau}),\mathbf{v})\|_{H\times V}} \tag{5.5}$$

for all $(\widetilde{\mathbf{r}},((\mathbf{r},\boldsymbol{\rho}),\mathbf{w})) \in \mathbb{L}^2(\Omega)\times(H\times V)$. This estimate will be employed below in Section 5.3 for the reliability of our *a posteriori* error estimator.

On the other hand, letting $((\mathbf{t},\boldsymbol{\sigma}),\mathbf{u}) \in H\times V$ and $((\mathbf{t}_h,\boldsymbol{\sigma}_h),\mathbf{u}_h) \in H_h\times V_h$ be the unique solutions of the continuous and discrete formulations (5.4) and (2.8), respectively, we define for each $T\in\mathcal{T}_h$ a local error indicator θ_T as follows:

$$\begin{aligned}
\theta_T^2 \;:=\; & \|(\boldsymbol{\sigma}^\star_{h,0}-\boldsymbol{\sigma}_h)^{\mathtt{d}}\|^2_{0,T} \;+\; \|\mathbf{div}(\boldsymbol{\sigma}^\star_{h,0}-\boldsymbol{\sigma}_h)\|^2_{0,T} \;+\; \|\mathbf{f}+\mathbf{div}(\boldsymbol{\sigma}_h)\|^2_{0,T} \;+\; \|\boldsymbol{\sigma}_h^{\mathtt{d}}-\boldsymbol{\psi}(\mathbf{t}_h)^{\mathtt{d}}\|^2_{0,T}\\
& +\; h_T^2\|\nabla\mathbf{u}_h-\mathbf{t}_h^{\mathtt{d}}\|^2_{0,T} \;+\; h_T^2\|\mathrm{curl}(\mathbf{t}_h^{\mathtt{d}})\|^2_{0,T} \;+\; h_T^2\|\mathrm{curl}(\boldsymbol{\sigma}_h^{\mathtt{d}}-\boldsymbol{\psi}(\mathbf{t}_h)^{\mathtt{d}})\|^2_{0,T}\\
& +\sum_{F\in\partial T\cap\mathcal{E}_h^i}\left\{h_F\|[\![\mathbf{t}_h^{\mathtt{d}}\boldsymbol{s}]\!]\|^2_{0,F} \;+\; \|\mathtt{h}^{-1/2}[\![\boldsymbol{\sigma}_h]\!]\|^2_{0,F} \;+\; h_F\left\|[\![\left(\boldsymbol{\sigma}_h^{\mathtt{d}}-\boldsymbol{\psi}(\mathbf{t}_h)^{\mathtt{d}}\right)\boldsymbol{s}]\!]\right\|^2_{0,F}\right\}\\
& +\sum_{F\in\partial T\cap\mathcal{E}_h^\partial} h_F\left\{\left\|\frac{d\mathbf{g}}{d\boldsymbol{s}}-\mathbf{t}_h^{\mathtt{d}}\boldsymbol{s}\right\|^2_{0,F} \;+\; \|\mathbf{g}-\mathbf{u}_h\|^2_{0,F} \;+\; \left\|\left(\boldsymbol{\sigma}_h^{\mathtt{d}}-\boldsymbol{\psi}(\mathbf{t}_h)^{\mathtt{d}}\right)\boldsymbol{s}\right\|^2_{0,F}\right\}.
\end{aligned} \tag{5.6}$$

The residual character of each term on the right hand side of (5.6) is quite clear. As usual the expression $\boldsymbol{\theta} := \left\{\sum_{T\in\mathcal{T}_h}\theta_T^2\right\}^{1/2}$ is employed as the global residual error estimator.

The following theorem constitutes the main result of this section.

Theorem 5.1. *Assume that Ω is an arbitrary polygonal domain in* 2D *or a convex polyhedral domain in* 3D*. Let $((\mathbf{t},\boldsymbol{\sigma}),\mathbf{u}) \in H\times V$ and $((\mathbf{t}_h,\boldsymbol{\sigma}_h),\mathbf{u}_h) \in H_h\times V_h$ be the unique solutions of* (5.4) *and* (2.8)*, respectively, and suppose that $\mathbf{g}\in\mathbf{H}^1(\Gamma)$. Also, let $\boldsymbol{\sigma}_h^\star \in \mathbb{H}(\mathbf{div};\Omega)$ be the postprocessed flux given by* (5.2) *and* (5.3)*. Then, there exist positive constants $C_{\mathtt{eff}}$ and $C_{\mathtt{rel}}$, independent of h, such that*

$$C_{\mathtt{eff}}\,\boldsymbol{\theta} \;+\; h.o.t. \;\leq\; \|(\mathbf{t}-\mathbf{t}_h,\boldsymbol{\sigma}-\boldsymbol{\sigma}_h)\|_{H_h} \;+\; \|\mathbf{u}-\mathbf{u}_h\|_{0,\Omega} \;+\; \|\boldsymbol{\sigma}-\boldsymbol{\sigma}^\star_{h,0}\|_{\mathbf{div},\Omega} \;\leq\; C_{\mathtt{rel}}\,\boldsymbol{\theta}\,, \tag{5.7}$$

where h.o.t. stands for one or several terms of higher order.

The proof of Theorem 5.1 is separated into the parts given by the next subsections. Firstly, we prove the reliability (upper bound in (5.7)) of the global error estimator, and then in Section 5.4 we derive the efficiency of the global error estimator (lower bound in (5.7)). We remark in advance that the convexity assumption for polyhedral domains Ω in 3D is required only for the reliability of $\boldsymbol{\theta}$, and more specifically, for the stability of a Helmholtz decomposition to be utilized below (cf. (5.12) - (5.13)).

5.3 Reliability

We begin with the following preliminary estimate.

Lemma 5.1. *Let* $((\mathbf{t},\boldsymbol{\sigma}),\mathbf{u}) \in H \times V$ *and* $((\mathbf{t}_h,\boldsymbol{\sigma}_h),\mathbf{u}_h) \in H_h \times V_h$ *be the unique solutions of* (5.4) *and* (2.8)*, respectively. Also, let* $\boldsymbol{\sigma}_h^\star \in \mathbb{H}(\mathbf{div};\Omega)$ *be the postprocessed flux defined by* (5.2) *and* (5.3)*. Then, there exists* $C > 0$*, independent of* h*, such that*

$$\begin{aligned} &\|(\mathbf{t}-\mathbf{t}_h,\boldsymbol{\sigma}-\boldsymbol{\sigma}_h)\|_{H_h} + \|\mathbf{u}-\mathbf{u}_h\|_{0,\Omega} + \|\boldsymbol{\sigma}-\boldsymbol{\sigma}_{h,0}^\star\|_{\mathbf{div},\Omega} \\ &\quad \leq C\left\{\|\boldsymbol{\sigma}_h^{\mathtt{d}} - \boldsymbol{\psi}(\mathbf{t}_h)^{\mathtt{d}}\|_{0,\Omega} + \|\mathbf{f}+\mathbf{div}(\boldsymbol{\sigma}_h)\|_{0,\Omega} + \|\boldsymbol{\sigma}_{h,0}^\star - \boldsymbol{\sigma}_h\|_{\Sigma_h} + \|R\|_{\mathbb{H}_0(\mathbf{div};\Omega)'}\right\}, \end{aligned} \tag{5.8}$$

where $R \in \mathbb{H}_0(\mathbf{div};\Omega)'$ *is defined by*

$$\begin{aligned} R(\boldsymbol{\tau}) := \int_\Omega \mathbf{t}_h^{\mathtt{d}} : \boldsymbol{\tau} + \int_\Omega \mathbf{u}_h \cdot \mathbf{div}(\boldsymbol{\tau}) - \langle \boldsymbol{\tau}\boldsymbol{\nu}, \mathbf{g}\rangle_\Gamma + \kappa_1 \int_\Omega \left(\boldsymbol{\sigma}_h^{\mathtt{d}} - \boldsymbol{\psi}(\mathbf{t}_h)^{\mathtt{d}}\right) : \boldsymbol{\tau} \\ + \kappa_2 \int_\Omega (\mathbf{f}+\mathbf{div}(\boldsymbol{\sigma}_h)) \cdot \mathbf{div}(\boldsymbol{\tau}) \qquad \forall\, \boldsymbol{\tau} \in \mathbb{H}_0(\mathbf{div};\Omega), \end{aligned} \tag{5.9}$$

and $R(\boldsymbol{\tau}_h) = 0$ *for all* $\boldsymbol{\tau}_h \in \mathbb{RT}(\mathcal{T}_h) \cap \mathbb{H}_0(\mathbf{div};\Omega)$*.*

Proof. We begin by observing that

$$\|\boldsymbol{\sigma}-\boldsymbol{\sigma}_h\|_{\Sigma_h} \leq \|\boldsymbol{\sigma}-\boldsymbol{\sigma}_{h,0}^\star\|_{\Sigma_h} + \|\boldsymbol{\sigma}_{h,0}^\star - \boldsymbol{\sigma}_h\|_{\Sigma_h} \leq \|\boldsymbol{\sigma}-\boldsymbol{\sigma}_{h,0}^\star\|_{\mathbf{div},\Omega} + \|\boldsymbol{\sigma}_{h,0}^\star - \boldsymbol{\sigma}_h\|_{\Sigma_h},$$

from which we readily deduce that

$$\begin{aligned} &\|(\mathbf{t}-\mathbf{t}_h,\boldsymbol{\sigma}-\boldsymbol{\sigma}_h)\|_{H_h} + \|\mathbf{u}-\mathbf{u}_h\|_{0,\Omega} + \|\boldsymbol{\sigma}-\boldsymbol{\sigma}_{h,0}^\star\|_{\mathbf{div},\Omega} \\ &\quad \leq C\left\{\|((\mathbf{t}-\mathbf{t}_h,\boldsymbol{\sigma}-\boldsymbol{\sigma}_{h,0}^\star),\mathbf{u}-\mathbf{u}_h)\|_{H\times V} + \|\boldsymbol{\sigma}_{h,0}^\star - \boldsymbol{\sigma}_h\|_{\Sigma_h}\right\}. \end{aligned} \tag{5.10}$$

Next, thanks to the mean value theorem, we know that there exists a convex combination of $\mathbf{t}$ and $\mathbf{t}_h$, say $\widetilde{\mathbf{r}}_h \in \mathbb{L}^2(\Omega)$, such that

$$\mathcal{D}\mathbb{A}(\widetilde{\mathbf{r}}_h)(\mathbf{t}-\mathbf{t}_h,\,\mathbf{s}) = [\mathbb{A}(\mathbf{t}),\,\mathbf{s}] - [\mathbb{A}(\mathbf{t}_h),\,\mathbf{s}] \quad \forall\, \mathbf{s} \in \mathbb{L}^2(\Omega). \tag{5.11}$$

Hence, applying (5.5) to $\widetilde{\mathbf{r}} := \widetilde{\mathbf{r}}_h$ and the error $((\mathbf{r},\boldsymbol{\rho}),\mathbf{w}) := ((\mathbf{t}-\mathbf{t}_h,\boldsymbol{\sigma}-\boldsymbol{\sigma}_{h,0}^\star),\mathbf{u}-\mathbf{u}_h) \in H\times V$, and then using the identity (5.11) together with the definition of $\mathbb{A}$ (cf. (3.4)), we find that

$$\begin{aligned} &\widetilde{C}\,\|((\mathbf{t}-\mathbf{t}_h,\boldsymbol{\sigma}-\boldsymbol{\sigma}_{h,0}^\star),\mathbf{u}-\mathbf{u}_h)\|_{H\times V} \\ &\leq \sup_{\substack{((\mathbf{s},\boldsymbol{\tau}),\mathbf{v})\in H\times V \\ ((\mathbf{s},\boldsymbol{\tau}),\mathbf{v})\neq \mathbf{0}}} \left\{ \frac{[\mathcal{A}(\mathbf{t},\boldsymbol{\sigma}),(\mathbf{s},\boldsymbol{\tau})] + [\mathcal{B}(\mathbf{s},\boldsymbol{\tau}),\mathbf{u}] + [\mathcal{B}(\mathbf{t},\boldsymbol{\sigma}),\mathbf{v}] + \displaystyle\int_\Omega [(\boldsymbol{\sigma}_{h,0}^\star)^{\mathtt{d}} - \boldsymbol{\psi}(\mathbf{t}_h)^{\mathtt{d}}] : \mathbf{s} - \int_\Omega \mathbf{t}_h^{\mathtt{d}} : \boldsymbol{\tau}}{\|((\mathbf{s},\boldsymbol{\tau}),\mathbf{v})\|_{H\times V}} \right. \\ &\quad \left. - \frac{\kappa_1 \displaystyle\int_\Omega [(\boldsymbol{\sigma}_{h,0}^\star)^{\mathtt{d}} - \boldsymbol{\psi}(\mathbf{t}_h)^{\mathtt{d}}] : \boldsymbol{\tau} + \kappa_2 \int_\Omega \mathbf{div}(\boldsymbol{\sigma}_{h,0}^\star)\cdot\mathbf{div}(\boldsymbol{\tau}) + \displaystyle\int_\Omega \mathbf{u}_h\cdot\mathbf{div}(\boldsymbol{\tau}) + \int_\Omega \mathbf{v}\cdot\mathbf{div}(\boldsymbol{\sigma}_{h,0}^\star)}{\|((\mathbf{s},\boldsymbol{\tau}),\mathbf{v})\|_{H\times V}} \right\}, \end{aligned}$$

which, utilizing (5.4) and defining

$$\widetilde{R}(\boldsymbol{\tau}) := R(\boldsymbol{\tau}) + \kappa_1 \int_\Omega (\boldsymbol{\sigma}_{h,0}^\star - \boldsymbol{\sigma}_h)^{\mathtt{d}} : \boldsymbol{\tau} + \kappa_2 \int_\Omega \mathbf{div}(\boldsymbol{\sigma}_{h,0}^\star - \boldsymbol{\sigma}_h)\cdot\mathbf{div}(\boldsymbol{\tau}) \qquad \forall\, \boldsymbol{\tau} \in \mathbb{H}_0(\mathbf{div};\Omega),$$

gives

$$\widetilde{C}\|((\mathbf{t}-\mathbf{t}_h,\boldsymbol{\sigma}-\boldsymbol{\sigma}^\star_{h,0}),\mathbf{u}-\mathbf{u}_h)\|_{H\times V}$$

$$\leq \sup_{\substack{((\mathbf{s},\boldsymbol{\tau}),\mathbf{v})\in H\times V\\((\mathbf{s},\boldsymbol{\tau}),\mathbf{v})\neq\mathbf{0}}} \frac{\displaystyle\int_\Omega[(\boldsymbol{\sigma}^\star_{h,0})^{\mathtt{d}}-\boldsymbol{\psi}(\mathbf{t}_h)^{\mathtt{d}}]:\mathbf{s}-\int_\Omega[\mathbf{f}+\mathbf{div}(\boldsymbol{\sigma}^\star_{h,0})]\cdot\mathbf{v}-\widetilde{R}(\boldsymbol{\tau})}{\|((\mathbf{s},\boldsymbol{\tau}),\mathbf{v})\|_{H\times V}}\,.$$

Then, applying the Cauchy-Schwarz inequality it follows that

$$\widetilde{C}\|((\mathbf{t}-\mathbf{t}_h,\boldsymbol{\sigma}-\boldsymbol{\sigma}^\star_{h,0}),\mathbf{u}-\mathbf{u}_h)\|_{H\times V}\ \leq\ \|(\boldsymbol{\sigma}^\star_{h,0})^{\mathtt{d}}-\boldsymbol{\psi}(\mathbf{t}_h)^{\mathtt{d}}\|_{0,\Omega}\ +\ \|\mathbf{f}+\mathbf{div}(\boldsymbol{\sigma}^\star_{h,0})\|_{0,\Omega}$$
$$+\ \|\boldsymbol{\sigma}^\star_{h,0}-\boldsymbol{\sigma}_h\|_{0,\Omega}\ +\ \|\mathbf{div}_h(\boldsymbol{\sigma}^\star_{h,0}-\boldsymbol{\sigma}_h)\|_{0,\Omega}\ +\|R\|_{\mathbb{H}_0(\mathbf{div};\Omega)'}\,,$$

which, together with (5.10) and the straightforward estimates

$$\|(\boldsymbol{\sigma}^\star_{h,0})^{\mathtt{d}}-\boldsymbol{\psi}(\mathbf{t}_h)^{\mathtt{d}}\|_{0,\Omega}\ \leq\ \|\boldsymbol{\sigma}^{\mathtt{d}}_h-\boldsymbol{\psi}(\mathbf{t}_h)^{\mathtt{d}}\|_{0,\Omega}+\|(\boldsymbol{\sigma}^\star_{h,0}-\boldsymbol{\sigma}_h)^{\mathtt{d}}\|_{0,\Omega}\,,$$

$$\|(\boldsymbol{\sigma}^\star_{h,0}-\boldsymbol{\sigma}_h)^{\mathtt{d}}\|_{0,\Omega}\ +\ \|\mathbf{div}_h(\boldsymbol{\sigma}^\star_{h,0}-\boldsymbol{\sigma}_h)\|_{0,\Omega}\ \leq\ \|\boldsymbol{\sigma}^\star_{h,0}-\boldsymbol{\sigma}_h\|_{\Sigma_h}\,,$$

and

$$\|\mathbf{f}+\mathbf{div}(\boldsymbol{\sigma}^\star_{h,0})\|_{0,\Omega}\leq\|\mathbf{f}+\mathbf{div}_h(\boldsymbol{\sigma}_h)\|_{0,\Omega}\ +\ \|\mathbf{div}_h(\boldsymbol{\sigma}^\star_{h,0}-\boldsymbol{\sigma}_h)\|_{0,\Omega}\,,$$

imply (5.8). Finally, from the second, fifth and sixth equations in (2.8), we know that

$$\int_\Omega\mathbf{t}^{\mathtt{d}}_h:\boldsymbol{\tau}_h\ +\ \int_\Omega\mathbf{u}_h\cdot\mathbf{div}_h(\boldsymbol{\tau}_h)\ -\ \int_{\mathcal{E}^i_h}[\![\boldsymbol{\tau}_h]\!]\cdot\boldsymbol{\lambda}_h\ +\ \kappa_1\int_\Omega[\boldsymbol{\sigma}^{\mathtt{d}}_h-\boldsymbol{\psi}(\mathbf{t}_h)^{\mathtt{d}}]:\boldsymbol{\tau}_h$$
$$+\ \kappa_2\int_\Omega\mathbf{div}_h(\boldsymbol{\sigma}_h)\cdot\mathbf{div}_h(\boldsymbol{\tau}_h)\ =\ \langle\boldsymbol{\tau}_h\boldsymbol{\nu},\mathbf{g}\rangle_\Gamma\ -\ \kappa_2\int_\Omega\mathbf{f}\cdot\mathbf{div}_h(\boldsymbol{\tau}_h)$$

for all $\boldsymbol{\tau}_h\in\Sigma_h$, which yields, in particular, $R(\boldsymbol{\tau}_h)\ =\ 0\quad$ for all $\boldsymbol{\tau}_h\in\mathbb{RT}(\mathcal{T}_h)\cap\mathbb{H}_0(\mathbf{div};\Omega)$, thus completing the proof. □

We now aim to bound $\|R\|_{\mathbb{H}_0(\mathbf{div};\Omega)'}:=\sup\limits_{\substack{\boldsymbol{\tau}\in\mathbb{H}_0(\mathbf{div};\Omega)\\\boldsymbol{\tau}\neq\mathbf{0}}}\dfrac{R(\boldsymbol{\tau})}{\|\boldsymbol{\tau}\|_{\mathbf{div},\Omega}}$ on the right-hand side of (5.8). For this purpose, and because of the vanishing property of R established by Lemma 5.1, we replace $R(\boldsymbol{\tau})$ in the above supremum by $R(\boldsymbol{\tau}-\boldsymbol{\tau}_h)$ with a suitable choice of $\boldsymbol{\tau}_h\in\mathbb{RT}_k(\mathcal{T}_h)\cap\mathbb{H}_0(\mathbf{div};\Omega)$. More precisely, proceeding exactly as in [17, Section 4.2], we now set $X_h\ :=\ \big\{v\in C(\bar\Omega)\ :\ v|_T\in P_1(T)\quad\forall\,T\in\mathcal{T}_h\big\}$ and introduce the Clément interpolation operator $\mathcal{I}_h:H^1(\Omega)\to X_h$ (cf. [9]). A vectorial version of $\mathcal{I}_h$, say $\boldsymbol{\mathcal{I}}_h:\mathbf{H}^1(\Omega)\to\mathbf{X}_h$, which is defined componentwise by $\mathcal{I}_h$, is also required. The following lemma establishes the local approximation properties of $\mathcal{I}_h$.

Lemma 5.2. *There exist constants $c_1,c_2>0$, independent of h, such that for all $v\in H^1(\Omega)$ there holds*

$$\|v-\mathcal{I}_h(v)\|_{0,T}\ \leq\ c_1h_T\|v\|_{1,\Delta(T)}\quad\forall\,T\in\mathcal{T}_h\,,$$

and

$$\|v-\mathcal{I}_h(v)\|_{0,F}\ \leq\ c_2h_F^{1/2}\|v\|_{1,\Delta(F)}\quad\forall\,F\in\mathcal{E}_h\,,$$

where $\Delta(T)$ and $\Delta(F)$ are the union of all elements intersecting with T and F, respectively.

Proof. See [9]. □

Next, for each $\boldsymbol{\tau} \in \mathbb{H}_0(\mathbf{div};\Omega)$ we consider its Helmholtz decomposition (see, e.g. [17, Section 4.2] for details)

$$\boldsymbol{\tau} \;=\; \nabla \mathbf{z} \;+\; \underline{\mathbf{curl}}(\boldsymbol{\chi})\,, \tag{5.12}$$

where $\mathbf{z} \in \mathbf{H}^2(\Omega)$ and $\boldsymbol{\chi} \in \mathbf{H}^1(\Omega)$ satisfy $\Delta \mathbf{z} = \mathbf{div}(\boldsymbol{\tau})$ in Ω, $\int_\Omega \boldsymbol{\chi} = \mathbf{0}$, and the stability estimate

$$\|\mathbf{z}\|_{2,\Omega} \;+\; \|\boldsymbol{\chi}\|_{1,\Omega} \;\leq\; C\,\|\boldsymbol{\tau}\|_{\mathbf{div},\Omega}\,. \tag{5.13}$$

We remark here that, while (5.12) also holds in 3D, the upper bound $\|\boldsymbol{\chi}\|_{1,\Omega} \leq C\,\|\boldsymbol{\tau}\|_{\mathbf{div},\Omega}$, and hence the respective estimate (5.13), is only known to be valid for convex polyhedral domains Ω (see [1, Theorems 2.17 and 3.12] for details). Note, however, that this is the only place of the present *a posteriori* error analysis where the convexity of the domain Ω is employed in the 3D case. Furthermore, we provide below in Section 6 extensive numerical evidences allowing us to conjecture that this might very well be just a technical assumption for the reliability of $\boldsymbol{\theta}$.

Next, we let $\boldsymbol{\zeta} := \nabla \mathbf{z} \in \mathbb{H}^1(\Omega)$, $\boldsymbol{\chi}_h := \boldsymbol{\mathcal{I}}_h(\boldsymbol{\chi})$, and define

$$\boldsymbol{\tau}_h \;:=\; \Pi_h^k(\boldsymbol{\zeta}) \;+\; \underline{\mathbf{curl}}(\boldsymbol{\chi}_{\boldsymbol{h}}) \;+\; c\,\mathbb{I} \;\in\; \mathbb{RT}_k(\mathcal{T}_h) \cap \mathbb{H}_0(\mathbf{div};\Omega)\,, \tag{5.14}$$

where Π_h^k is the global Raviart-Thomas interpolation operator introduced before (cf. (4.4) and (4.5)). Here, the constant c is chosen so that $\boldsymbol{\tau}_h$, which is already in $\mathbb{RT}_k(\mathcal{T}_h)$, belongs to $\mathbb{H}_0(\mathbf{div};\Omega)$. Equivalently, $\boldsymbol{\tau}_h$ is the $\mathbb{H}_0(\mathbf{div};\Omega)$-component of $\Pi_h^k(\boldsymbol{\zeta}) + \underline{\mathbf{curl}}(\boldsymbol{\chi}_{\boldsymbol{h}})$. We refer to (5.14) as a discrete Helmholtz decomposition of $\boldsymbol{\tau}_h$. Therefore, we can write

$$\boldsymbol{\tau} - \boldsymbol{\tau}_h \;=\; \boldsymbol{\tau} - \Pi_h^k(\boldsymbol{\zeta}) - \underline{\mathbf{curl}}(\boldsymbol{\chi}_{\boldsymbol{h}}) - c\,\mathbb{I} \;=\; \boldsymbol{\zeta} - \Pi_h^k(\boldsymbol{\zeta}) \;+\; \underline{\mathbf{curl}}(\boldsymbol{\chi} - \boldsymbol{\chi}_{\boldsymbol{h}}) \;-\; c\,\mathbb{I}\,, \tag{5.15}$$

which, using that $\mathbf{div}(\Pi_h^k(\boldsymbol{\tau})) = \mathcal{P}_h^k(\mathbf{div}(\boldsymbol{\tau}))$ and that $\mathbf{div}(\boldsymbol{\zeta}) = \Delta \mathbf{z} = \mathbf{div}(\boldsymbol{\tau})$ in Ω, and denoting by $\mathbf{I}$ a generic identity operator, yields

$$\mathbf{div}(\boldsymbol{\tau} - \boldsymbol{\tau}_h) \;=\; \mathbf{div}(\boldsymbol{\zeta} - \Pi_h^k(\boldsymbol{\zeta})) \;=\; (\mathbf{I} - \mathcal{P}_h^k)(\mathbf{div}(\boldsymbol{\zeta})) \;=\; (\mathbf{I} - \mathcal{P}_h^k)(\mathbf{div}(\boldsymbol{\tau}))\,.$$

Then, replacing each $\boldsymbol{\tau} \in \mathbb{H}_0(\mathbf{div};\Omega)$ by its Helmholtz decomposition (5.12), employing the associated discrete element $\boldsymbol{\tau}_h$ given by (5.14), recalling from Lemma 5.1 that $R(\boldsymbol{\tau}_h) = 0$, and observing that R vanishes $c\,\mathbb{I}$ as well, we deduce from (5.9) and (5.15) that $R(\boldsymbol{\tau}) = R(\boldsymbol{\tau} - \boldsymbol{\tau}_h)$ is decomposed as

$$R(\boldsymbol{\tau}) \;=\; R_1(\boldsymbol{\zeta} - \Pi_h^k(\boldsymbol{\zeta})) \;+\; R_2(\boldsymbol{\chi} - \boldsymbol{\chi}_h)\,, \tag{5.16}$$

where

$$\begin{aligned} R_1(\boldsymbol{\zeta} - \Pi_h^k(\boldsymbol{\zeta})) \;:=\; & \int_\Omega \mathbf{t}_h^{\mathtt{d}} : (\boldsymbol{\zeta} - \Pi_h^k(\boldsymbol{\zeta})) \;+\; \int_\Omega \mathbf{u}_h \cdot \mathbf{div}(\boldsymbol{\zeta} - \Pi_h^k(\boldsymbol{\zeta})) \;-\; \langle (\boldsymbol{\zeta} - \Pi_h^k(\boldsymbol{\zeta}))\boldsymbol{\nu}, \mathbf{g}\rangle_\Gamma \\ & + \kappa_1 \int_\Omega \big(\boldsymbol{\sigma}_h^{\mathtt{d}} - (\boldsymbol{\psi}(\mathbf{t}_h))^{\mathtt{d}}\big) : (\boldsymbol{\zeta} - \Pi_h^k(\boldsymbol{\zeta})) \;+\; \kappa_2 \int_\Omega (\mathbf{f} + \mathbf{div}_h(\boldsymbol{\sigma}_h)) \cdot \mathbf{div}(\boldsymbol{\zeta} - \Pi_h^k(\boldsymbol{\zeta})) \end{aligned}$$

and

$$\begin{aligned} R_2(\boldsymbol{\chi} - \boldsymbol{\chi}_h) \;:=\; & \int_\Omega \mathbf{t}_h^{\mathtt{d}} : \underline{\mathbf{curl}}(\boldsymbol{\chi} - \boldsymbol{\chi}_h) \;-\; \langle \underline{\mathbf{curl}}(\boldsymbol{\chi} - \boldsymbol{\chi}_h)\boldsymbol{\nu}, \mathbf{g}\rangle_\Gamma \\ & + \kappa_1 \int_\Omega \big(\boldsymbol{\sigma}_h^{\mathtt{d}} - (\boldsymbol{\psi}(\mathbf{t}_h))^{\mathtt{d}}\big) : \underline{\mathbf{curl}}(\boldsymbol{\chi} - \boldsymbol{\chi}_h)\,. \end{aligned}$$

The following two lemmas provide suitable upper bounds for $|R_1(\boldsymbol{\zeta} - \Pi_h^k(\boldsymbol{\zeta}))|$ and $|R_2(\boldsymbol{\chi} - \boldsymbol{\chi}_h)|$, which will yield the required estimate for $\|R\|_{\mathbb{H}_0(\mathbf{div};\Omega)'}$.

Lemma 5.3. *There exists $C_1 > 0$, independent of h, such that*

$$|R_1(\boldsymbol{\zeta} - \Pi_h^k(\boldsymbol{\zeta}))| \ \leq \ C_1 \left\{ \sum_{T \in \mathcal{T}_h} \theta_{1,T}^2 \right\}^{1/2} \|\boldsymbol{\tau}\|_{\mathbf{div},\Omega} \,,$$

where

$$\begin{aligned} \theta_{1,T}^2 \ := \ & h_T^2 \, \|\nabla \mathbf{u}_h - \mathbf{t}_h^{\mathtt{d}}\|_{0,T}^2 \, + \, h_T^2 \, \|\boldsymbol{\sigma}_h^{\mathtt{d}} - \boldsymbol{\psi}(\mathbf{t}_h)^{\mathtt{d}}\|_{0,T}^2 \\ & + \, \|\mathbf{f} + \mathbf{div}(\boldsymbol{\sigma}_h)\|_{0,T}^2 \, + \, \sum_{F \in \partial T \cap \mathcal{E}_h^{\partial}} h_F \, \|\mathbf{g} - \mathbf{u}_h\|_{0,F}^2 \,. \end{aligned}$$

Lemma 5.4. *Assume that $\mathbf{g} \in \mathbf{H}^1(\Gamma)$. Then there exists $C_2 > 0$, independent of h, such that*

$$|R_2(\boldsymbol{\chi} - \boldsymbol{\chi}_h)| \ \leq \ C_2 \left\{ \sum_{T \in \mathcal{T}_h} \theta_{2,T}^2 \right\}^{1/2} \|\boldsymbol{\tau}\|_{\mathbf{div},\Omega} \,,$$

where

$$\begin{aligned} \theta_{2,T}^2 \ := \ & h_T^2 \, \|\mathrm{curl}(\mathbf{t}_h^{\mathtt{d}})\|_{0,T}^2 \, + \, h_T^2 \, \|\mathrm{curl}\left(\boldsymbol{\sigma}_h^{\mathtt{d}} - \boldsymbol{\psi}(\mathbf{t}_h)^{\mathtt{d}}\right)\|_{0,T}^2 \\ & + \, \sum_{F \in \partial T \cap \mathcal{E}_h^i} h_F \left\{ \|[\![\mathbf{t}_h^{\mathtt{d}} \boldsymbol{\mathcal{S}}]\!]\|_{0,F}^2 \, + \, \|[\![(\boldsymbol{\sigma}_h^{\mathtt{d}} - \boldsymbol{\psi}(\mathbf{t}_h)^{\mathtt{d}}) \boldsymbol{\mathcal{S}}]\!]\|_{0,F}^2 \right\} \\ & + \, \sum_{F \in \partial T \cap \mathcal{E}_h^{\partial}} h_F \left\{ \left\| \frac{d\mathbf{g}}{d\boldsymbol{\mathcal{S}}} - \mathbf{t}_h^{\mathtt{d}} \boldsymbol{\mathcal{S}} \right\|_{0,F}^2 \, + \, \|(\boldsymbol{\sigma}_h^{\mathtt{d}} - \boldsymbol{\psi}(\mathbf{t}_h)^{\mathtt{d}}) \boldsymbol{\mathcal{S}}\|_{0,F}^2 \right\} . \end{aligned}$$

The proofs of Lemmas 5.3 and 5.4 follow by using exactly the same arguments from [20, Lemmas 4.3 and 4.4] (see, also [21, Lemmas 4.3 and 4.4]). Indeed, the main tools employed are integration by parts, the Cauchy-Schwarz inequality, the approximation properties provided by Lemma 5.2, the identities (4.4) and (4.5) characterizing Π_h^k, the approximation properties of Π_h^k, the fact that the number of triangles in $\Delta(T)$ and $\Delta(F)$ are bounded, and the stability estimate (5.13). We omit further details here and refer to the aforementioned works.

Finally, it readily follows from (5.16) and Lemmas 5.3 and 5.4 that

$$\|R\|_{\mathbb{H}_0(\mathbf{div};\Omega)'} \ \leq \ C \left\{ \sum_{T \in \mathcal{T}_h} \left(\theta_{1,T}^2 + \theta_{2,T}^2 \right) \right\}^{1/2} . \tag{5.17}$$

In this way, and having in mind that the term $h_T^2 \|\boldsymbol{\sigma}_h^{\mathtt{d}} - \boldsymbol{\psi}(\mathbf{t}_h)^{\mathtt{d}}\|_{0,T}^2$ is dominated by $\|\boldsymbol{\sigma}_h^{\mathtt{d}} - \boldsymbol{\psi}(\mathbf{t}_h)^{\mathtt{d}}\|_{0,T}^2$, we conclude from (5.1), Lemma 5.1, and (5.17), the reliability of the *a posteriori* error estimator $\boldsymbol{\theta}$ (upper bound in (5.7)).

5.4 Efficiency

In this section we establish the efficiency of our *a posteriori* error estimator $\boldsymbol{\theta}$ (lower bound in (5.7)). In other words, we provide suitable upper bounds for the thirteen terms defining the local error indicator θ_T^2 (cf. (5.6)). We first notice that the converse of the derivation of (5.4) from (2.5) holds true. Indeed, it is easy to show, applying integration by parts backwardly and using appropriate test functions, that the unique solution $((\mathbf{t}, \boldsymbol{\sigma}), \mathbf{u}) \in H \times V$ of (5.4) solves the original problem (2.5). Then, using that $\mathbf{f} = -\mathbf{div}(\boldsymbol{\sigma})$ in Ω, it follows that

$$\|\mathbf{f} + \mathbf{div}(\boldsymbol{\sigma}_h)\|_{0,T}^2 \ = \ \|\mathbf{div}(\boldsymbol{\sigma} - \boldsymbol{\sigma}_h)\|_{0,T}^2 \,. \tag{5.18}$$

Also, after adding and subtracting $\boldsymbol{\sigma}$, we have

$$\begin{aligned}\|(\boldsymbol{\sigma}^\star_{h,0}-\boldsymbol{\sigma}_h)^{\mathtt{d}}\|^2_{0,T} \;+\; \|\mathbf{div}(\boldsymbol{\sigma}^\star_{h,0}-\boldsymbol{\sigma}_h)\|^2_{0,T} \;+\; \sum_{F\in\partial T\cap\mathcal{E}_h^i}\|\mathtt{h}^{-1/2}[\![\boldsymbol{\sigma}_h]\!]\|^2_{0,F}\\ \leq\; 2\left\{\|\boldsymbol{\sigma}-\boldsymbol{\sigma}_h\|^2_{\Sigma_h(T)} \;+\; \|\boldsymbol{\sigma}-\boldsymbol{\sigma}^\star_{h,0}\|^2_{\mathbf{div},T}\right\}.\end{aligned} \tag{5.19}$$

Next, using that $\boldsymbol{\sigma}^{\mathtt{d}}=\boldsymbol{\psi}(\mathbf{t})=\boldsymbol{\psi}(\mathbf{t})^{\mathtt{d}}$ in Ω and applying the Lipschitz-continuity of $\mathbb{A}$ (cf. Lemma 3.2), but restricted to the triangle $T\in\mathcal{T}_h$ instead of Ω, we deduce that

$$\begin{aligned}\|\boldsymbol{\sigma}^{\mathtt{d}}_h-\boldsymbol{\psi}(\mathbf{t}_h)^{\mathtt{d}}\|^2_{0,T} &\leq 2\,\|(\boldsymbol{\sigma}-\boldsymbol{\sigma}_h)^{\mathtt{d}}\|^2_{0,T} \;+\; 2\,\|\boldsymbol{\psi}(\mathbf{t})-\boldsymbol{\psi}(\mathbf{t}_h)\|^2_{0,T}\\ &\leq 2\left\{\|(\boldsymbol{\sigma}-\boldsymbol{\sigma}_h)^{\mathtt{d}}\|^2_{0,T} \;+\; \gamma_0^2\,\|\mathbf{t}-\mathbf{t}_h\|^2_{0,T}\right\}.\end{aligned} \tag{5.20}$$

On the other hand, in order to bound the terms involving the mesh parameters h_T and h_F, we proceed as in [20] and [21] (see also [17]). The techniques applied there are based on triangle-bubble and edge-bubble functions, extension operators, and discrete trace and inverse inequalities. Hence, the estimates of the remaining eight terms defining θ^2_T (cf. (5.6)) are given as follows.

Lemma 5.5. *There exist $C_1,C_2>0$, independent of h, such that*

$$h_T^2\|\mathrm{curl}(\mathbf{t}^{\mathtt{d}}_h)\|^2_{0,T} \;\leq\; C_1\,\|\mathbf{t}-\mathbf{t}_h\|^2_{0,T}\quad\forall\; T\in\mathcal{T}_h\,,$$

and

$$h_F\|[\![\mathbf{t}^{\mathtt{d}}_h\boldsymbol{s}]\!]\|^2_{0,F} \;\leq\; C_2\,\|\mathbf{t}-\mathbf{t}_h\|^2_{0,\omega_F}\quad\forall\; F\in\mathcal{E}_h^i\,,$$

where $\omega_F:=\cup\{\,T\in\mathcal{T}_h\;:\;F\in\partial T\,\}$.

Proof. It suffices to apply the general results stated in [20, Lemmas 4.9 and 4.10] to $\boldsymbol{\rho}_h=\mathbf{t}^{\mathtt{d}}_h$ and $\boldsymbol{\rho}=\mathbf{t}=\mathbf{t}^{\mathtt{d}}$, noting that $\mathrm{curl}(\boldsymbol{\rho})=\mathrm{curl}(\nabla\mathbf{u})=\mathbf{0}$ in Ω. □

Lemma 5.6. *There exist $C_3,C_4>0$, independent of h, such that*

$$h_T^2\|\mathrm{curl}(\boldsymbol{\sigma}^{\mathtt{d}}_h-\boldsymbol{\psi}(\mathbf{t}_h)^{\mathtt{d}})\|^2_{0,T} \;\leq\; C_3\left\{\|\mathbf{t}-\mathbf{t}_h\|^2_{0,T} \;+\; \|(\boldsymbol{\sigma}-\boldsymbol{\sigma}_h)^{\mathtt{d}}\|^2_{0,T}\right\}\quad\forall\; T\in\mathcal{T}_h\,,$$

and

$$h_F\|[\![(\boldsymbol{\sigma}^{\mathtt{d}}_h-\boldsymbol{\psi}(\mathbf{t}_h)^{\mathtt{d}})\boldsymbol{s}]\!]\|^2_{0,F} \;\leq\; C_4\left\{\|\mathbf{t}-\mathbf{t}_h\|^2_{0,\omega_F} \;+\; \|(\boldsymbol{\sigma}-\boldsymbol{\sigma}_h)^{\mathtt{d}}\|^2_{0,\omega_F}\right\}\quad\forall\; F\in\mathcal{E}_h\,,$$

where, we define $[\![(\boldsymbol{\sigma}^{\mathtt{d}}_h-\boldsymbol{\psi}(\mathbf{t}_h)^{\mathtt{d}})\boldsymbol{s}]\!]:=(\boldsymbol{\sigma}^{\mathtt{d}}_h-\boldsymbol{\psi}(\mathbf{t}_h)^{\mathtt{d}})\boldsymbol{s}$ on $\mathcal{E}_h^\partial$.

Proof. As in the proof of Lemma 5.5, it suffices now to apply the general results stated in [20, Lemmas 4.9 and 4.10] to $\boldsymbol{\rho}_h=\boldsymbol{\sigma}^{\mathtt{d}}_h-\boldsymbol{\psi}(\mathbf{t}_h)^{\mathtt{d}}$ and $\boldsymbol{\rho}=\boldsymbol{\sigma}^{\mathtt{d}}-\boldsymbol{\psi}(\mathbf{t})^{\mathtt{d}}=\mathbf{0}$ in Ω, and then use the Lipschitz-continuity of $\mathbb{A}$ (cf. Lemma 3.2) restricted to T and ω_F. □

Lemma 5.7. *There exists $C_5>0$, independent of h, such that*

$$h_T^2\|\nabla\mathbf{u}_h-\mathbf{t}^{\mathtt{d}}_h\|^2_{0,T} \;\leq\; C_5\left\{\|\mathbf{u}-\mathbf{u}_h\|^2_{0,T} \;+\; h_T^2\|\mathbf{t}-\mathbf{t}_h\|^2_{0,T}\right\}\quad\forall\; T\in\mathcal{T}_h\,.$$

Proof. As in [21, Lemma 4.8], it follows from the proof of [20, Lemma 4.13]. □

Lemma 5.8. *Assume that $\mathbf{g}$ is piecewise polynomial. Then there exists $C_6>0$, independent of h, such that*

$$h_F\left\|\frac{d\mathbf{g}}{d\boldsymbol{s}}-\mathbf{t}^{\mathtt{d}}_h\boldsymbol{s}\right\|^2_{0,F} \;\leq\; C_6\,\|\mathbf{t}-\mathbf{t}_h\|^2_{0,T}\quad\forall\; F\in\mathcal{E}_h^\partial\,, \tag{5.21}$$

where T is the triangle of $\mathcal{T}_h$ having F as an edge.

Proof. It is a slight modification of the proof of [20, Lemma 4.15]. In fact, it suffices to replace $\frac{1}{2\mu}\boldsymbol{\sigma}_h$ by our $\mathbf{t}_h$ and use now that $\frac{d\mathbf{g}}{d\boldsymbol{s}} = (\nabla\mathbf{u})\boldsymbol{s} = \mathbf{t}\boldsymbol{s} = \mathbf{t}^{\mathtt{d}}\boldsymbol{s}$ on Γ. □

Lemma 5.9. *There exists $C_7 > 0$, independent of h, such that*

$$h_F\|\mathbf{g} - \mathbf{u}_h\|^2_{0,F} \;\leq\; C_7\left\{\|\mathbf{u} - \mathbf{u}_h\|^2_{0,T} \;+\; h_T^2\|\mathbf{t} - \mathbf{t}_h\|^2_{0,T}\right\} \quad \forall\, F \in \mathcal{E}_h^{\partial}\,,$$

where T is the triangle of $\mathcal{T}_h$ having F as an edge.

Proof. Similarly to the previous lemmas, it follows by replacing $\frac{1}{2\mu}\boldsymbol{\sigma}_h$ by our $\mathbf{t}_h$ in the proof of [20, Lemma 4.14], and then using that $\nabla\mathbf{u} = \mathbf{t} = \mathbf{t}^{\mathtt{d}}$ in Ω and $\mathbf{u} = \mathbf{g}$ on Γ. The estimate given by Lemma 5.7 is also employed here. □

We remark here that if $\mathbf{g}$ were not a piecewise polynomial, but a sufficiently smooth function, then higher order terms given by the errors arising from suitable polynomial approximations would appear in (5.21). This explains the eventual expression *h.o.t.* in (5.7). Consequently, the efficiency of $\boldsymbol{\theta}$ follows directly from estimates (5.18), (5.19) and (5.20), together with Lemmas 5.5 throughout 5.9, after summing up over $T \in \mathcal{T}_h$.

6 Numerical results

In this section we present four numerical examples illustrating the good performance of our augmented HDG method, confirming the reliability and efficiency of the *a posteriori* error estimator $\boldsymbol{\theta}$, and showing the behaviour of the associated adaptive algorithm. We remark that we refer to the original HDG system (2.8) since, as explained before, the equivalent reduced scheme given by (2.10) was introduced just for the sake of the analysis. In addition, in all the computations, we consider polynomial degrees $k \in \{0, 1, 2\}$. We begin by setting additional notations. In what follows, N denotes the total number of unknowns of (2.8), whereas N_{comp} stands for the number of unknowns effectively employed in the computations (involved in the resolution of the corresponding linear systems). In other words, N is the total number of degrees of freedom defining $\mathbf{t}_h$, $\boldsymbol{\sigma}_h$, $\mathbf{u}_h$, and $\boldsymbol{\lambda}_h$. On the other hand, as is natural in the HDG implementations, we can reduce N to N_{comp}, where in the case of (2.8), N_{comp} is the total number of degrees of freedom defining $\boldsymbol{\lambda}_h$, plus one constant for each $T \in \mathcal{T}_h$, which has the task of imposing the condition $\int_\Omega \mathrm{tr}\,(\boldsymbol{\sigma}) = 0$ (see [22, Section 5] for details). In turn, the individual and total errors are defined by

$$\begin{array}{rclcrclcrcl}
\mathtt{e}(\mathbf{t}) & := & \|\mathbf{t} - \mathbf{t}_h\|_{0,\Omega}\,, & & \mathtt{e}(\boldsymbol{\sigma}) & := & \|\boldsymbol{\sigma} - \boldsymbol{\sigma}_h\|_{\Sigma_h}\,, & & \mathtt{e}(\mathbf{u}) & := & \|\mathbf{u} - \mathbf{u}_h\|_{0,\Omega}\,, \\
\mathtt{e}_0(\boldsymbol{\sigma}) & := & \|\boldsymbol{\sigma} - \boldsymbol{\sigma}_h\|_{0,\Omega}\,, & & \mathtt{e}(\boldsymbol{\lambda}) & := & \|\mathbf{u} - \widehat{\mathbf{u}}_h\|_h\,, & & \mathtt{e}(p) & := & \|p - p_h\|_{0,\Omega}\,,
\end{array}$$

$$\mathtt{e}^\star(\boldsymbol{\sigma}) \;:=\; \|\boldsymbol{\sigma} - \boldsymbol{\sigma}^\star_{h,0}\|_{\mathbf{div},\Omega}\,, \quad \mathtt{e}(\mathbf{t},\boldsymbol{\sigma},\mathbf{u}) \;:=\; \left\{[\mathtt{e}(\mathbf{t})]^2 \;+\; [\mathtt{e}(\boldsymbol{\sigma})]^2 \;+\; [\mathtt{e}(\mathbf{u})]^2\right\}^{1/2},$$

where p_h is computed by the postprocessing formulae (4.10), whereas $\|\mathbf{u} - \widehat{\mathbf{u}}_h\|_h$ is defined in (4.12). The effectivity index with respect to $\boldsymbol{\theta}$ is given by

$$\mathtt{eff}(\boldsymbol{\theta}) \;:=\; \left\{[\mathtt{e}(\mathbf{t},\boldsymbol{\sigma},\mathbf{u})]^2 \;+\; [\mathtt{e}^\star(\boldsymbol{\sigma})]^2\right\}^{1/2} / \,\boldsymbol{\theta}\,,$$

and the experimental rates of convergence are defined as

$$\begin{array}{rclcrcl}
\mathtt{r}(\mathbf{t}) & := & \dfrac{\log(\mathtt{e}(\mathbf{t})/\mathtt{e}'(\mathbf{t}))}{\log(h/h')}\,, & & \mathtt{r}(\boldsymbol{\sigma}) & := & \dfrac{\log(\mathtt{e}(\boldsymbol{\sigma})/\mathtt{e}'(\boldsymbol{\sigma}))}{\log(h/h')}\,, \\
\mathtt{r}(\mathbf{u}) & := & \dfrac{\log(\mathtt{e}(\mathbf{u})/\mathtt{e}'(\mathbf{u}))}{\log(h/h')}\,, & & \mathtt{r}(\mathbf{t},\boldsymbol{\sigma},\mathbf{u}) & := & \dfrac{\log(\mathtt{e}(\mathbf{t},\boldsymbol{\sigma},\mathbf{u})/\mathtt{e}'(\mathbf{t},\boldsymbol{\sigma},\mathbf{u}))}{\log(h/h')}\,,
\end{array}$$

and similarly for $\mathtt{r}_0(\boldsymbol{\sigma})$, $\mathtt{r}(\boldsymbol{\lambda})$, $\mathtt{r}(p)$ and $\mathtt{r}^\star(\boldsymbol{\sigma})$, where $\mathtt{e}$ and $\mathtt{e}'$ denote the corresponding errors for two consecutive triangulations with mesh sizes h and h', respectively. Nevertheless, when the adaptive algorithm is applied (see details below), the expression $\log(h/h')$ appearing in the computation of the above rates is replaced by $-\frac{1}{2}\log(N/N')$, where N and N' denote the corresponding total degrees of freedom of each triangulation.

The numerical results presented below were obtained using a C^{++} code. The corresponding nonlinear algebraic systems arising from (2.8) are solved by the Newton-Raphson method with a tolerance of 10^{-6} and taking as initial iteration the solution of the associated linear Stokes problem. In all the examples less than four iterations were required to achieve the given tolerance. In turn, the linear systems were solved using the Conjugate Gradient method as the main solver. In addition, for the adaptive 3D mesh generation (cf. Example 4), we use the software TetGen developed in [30]. The examples to be considered in this section are described next. Example 1 and 2 (linear and nonlinear, respectively) are employed to illustrate the performance of the augmented HDG scheme (2.8) and to confirm the reliability and efficiency of the *a posteriori* error estimator $\boldsymbol{\theta}$. Examples 3 and 4 are utilized to show the behaviour of the associated adaptive algorithm, which applies the following procedure:

(1) Start with a coarse mesh $\mathcal{T}_h$.

(2) Solve the linear version of the discrete problem (2.8), in order to obtain an initial guess $\mathbf{x}_0$, for the Newton iterations.

(3) Solve the discrete problem (2.8) for the actual mesh $\mathcal{T}_h$, with the actual initial guess $\mathbf{x}_0$.

(4) Compute θ_T (cf. (5.6)) for each triangle $T \in \mathcal{T}_h$,

(5) Evaluate stopping criterion and decide to finish or go to next step.

(6) Use *red-green-blue* procedure (cf. [31]) to refine each $T' \in \mathcal{T}_h$ whose indicator $\theta_{T'}$ satisfies

$$\theta_{T'} \ \geq \ \frac{1}{2}\max\{\theta_T \ : \ T \in \mathcal{T}_h\} \ .$$

(7) Use the solution given by step 3 and the new mesh to interpolate a new initial guess $\widetilde{\mathbf{x}}_0$ and then replace $\mathbf{x}_0$ by $\widetilde{\mathbf{x}}_0$.

(8) Define the new mesh as actual mesh $\mathcal{T}_h$ and go to step 3.

For Example 1 we take $\mu = 1$ and for the remaining three examples we consider the nonlinear function $\mu : R^+ \to R^+$ given by the Carreau law

$$\mu(t) \ := \ \mu_0 \ + \ \mu_1(1+t^2)^{(\beta-2)/2} \quad \forall \ t \in R^+,$$

with $\mu_0 = \mu_1 = 0.5$ and $\beta = 1.5$. It is easy to check that the assumptions (2.2) and (2.3) are satisfied with

$$\gamma_0 \ = \ \mu_0 \ + \ \mu_1 \left\{ \frac{|\beta-2|}{2} + 1 \right\} \quad \text{and} \quad \alpha_0 \ = \ \mu_0 \, .$$

Hence, for the implementation of the augmented HDG scheme (2.8) we use the stabilization parameter $\kappa_1 = \frac{\alpha_0}{\gamma_0^2}$, which obviously satisfies the assumption in Lemma 3.4, and then, as in [22], we simply choose $\kappa_2 = \frac{\kappa_1}{2}$.

In Example 1 we consider $\Omega =]-1,1[^2$, and choose the data $\mathbf{f}$ and $\mathbf{g}$ so that the exact solution is given for each $\mathbf{x} := (x_1, x_2)^{\mathtt{t}} \in \Omega$ by

$$\mathbf{u}(\mathbf{x}) \ = \ \begin{pmatrix} \sin(\pi\, x_1)\, \cos(\pi\, x_2) \\ -\cos(\pi\, x_1)\, \sin(\pi\, x_2) \end{pmatrix}$$

and

$$p(\mathbf{x}) \;=\; 4\,x_2^2\,\cos(6\,x_1) \;-\; \frac{2}{9}\,\sin(6)\,.$$

It is easy to check that $\mathbf{u}$ is divergence free, and $(\mathbf{u},p)$ is regular in the whole domain Ω.

In Example 2 we consider $\Omega = (0,1)^2$, and choose the data $\mathbf{f}$ and $\mathbf{g}$ so that the exact solution is given for each $\mathbf{x} := (x_1,x_2)^{\mathtt{t}} \in \Omega$ by

$$\mathbf{u}(\mathbf{x}) \;=\; \begin{pmatrix} (1+x_1-\exp(x_1))\,(1-\cos(x_2)) \\ (\exp(x_1)-1)\,(x_2-\sin(x_2)) \end{pmatrix}$$

and

$$p(\mathbf{x}) \;=\; \frac{1}{2}\,\exp(2\pi x_1) \;+\; \frac{1}{4\pi}\,(1-\exp(2\pi))\,.$$

Note that $\mathbf{u}$ is divergence free and $(\mathbf{u},p)$ is regular in the whole domain Ω.

Next, in Example 3 we consider the L-shaped domain $\Omega = \,]-1,1[^2 \setminus [0,1]^2$, and choose $\mathbf{f}$ and $\mathbf{g}$ so that the exact solution is given for each $\mathbf{x} := (x_1,x_2)^{\mathtt{t}} \in \Omega$ by

$$\mathbf{u}(\mathbf{x}) \;=\; \mathbf{curl}\Big(\sqrt{(x_1-0.01)^2 \;+\; (x_2-0.01)^2}\Big)$$

and

$$p(\mathbf{x}) \;=\; \frac{1}{x_2 \;+\; 1.1} \;-\; \frac{1}{3}\,\ln(231)\,.$$

Note that $\mathbf{u}$ and p are singular at $(0.01,0.01)$ and along the line $x_2 = -1.1$, respectively. Hence, we should expect regions of high gradients around the origin, which is the middle corner of the L, and along the line $x_2 = -1$.

Finally, in Example 4 we consider the non-convex three dimensional domain

$$\Omega \;:=\; \left]-\tfrac{3}{4},\tfrac{3}{4}\right[\times\left]-\tfrac{3}{4},\tfrac{3}{4}\right[\times\left]-\tfrac{1}{4},\tfrac{1}{4}\right[\;\setminus\; \Big\{ \left[-\tfrac{3}{4},-\tfrac{1}{4}\right]\times\left[-\tfrac{3}{4},\tfrac{1}{4}\right]\times\left[-\tfrac{1}{4},\tfrac{1}{4}\right] \;\cup\; \left[\tfrac{1}{4},\tfrac{3}{4}\right]\times\left[-\tfrac{3}{4},\tfrac{1}{4}\right]\times\left[-\tfrac{1}{4},\tfrac{1}{4}\right] \Big\}\,,$$

and choose the data $\mathbf{f}$ and $\mathbf{g}$ so that the exact solution is given for each $\mathbf{x} := (x_1,x_2,x_3)^{\mathtt{t}} \in \Omega$ by

$$\begin{aligned}\mathbf{u}(\mathbf{x}) \;=\; \mathbf{curl}\Big(&\sqrt{(x_1+0.3)^2 \;+\; (x_2-0.2)^2 \;+\; (x_3-0.3)^2} \\ &+\; \sqrt{(x_1-0.3)^2 \;+\; (x_2-0.2)^2 \;+\; (x_3-0.3)^2}\Big)\end{aligned}$$

and

$$p(\mathbf{x}) \;=\; \frac{1}{x_2 \;+\; 0.85} \;+\; \frac{4}{5}\,\ln\left(\frac{11}{64}\right).$$

Note that Ω is a T-shaped domain and that $\mathbf{u}$ and p are singular at $(-0.3,0.2,0.3)$ and $(0.3,0.2,0.3)$, and along the plane $x_2 = -0.85$, respectively. Hence, similarly to Example 3, we should expect regions of high gradients around $(-0.25,0.25,0.25)$ and $(0.25,0.25,0.25)$, which are the middle corners of the T, and along the plane $x_2 = -0.75$.

In Tables 6.1, 6.2, 6.3, and 6.4, we summarize the convergence history of the augmented HDG scheme (2.8) as applied to Example 1 and 2, for a sequence of quasi-uniform triangulations of each domain. We notice there that the rate of convergence $O(h^{k+1})$ predicted by (4.9), (4.11) and Theorems 4.1 and 4.2 is attained by all the unknowns. In particular, as observed in the tenth column of Table 6.3, the convergence of $\mathbf{u}_h$ is a bit faster than expected, which could correspond to either a superconvergence phenomenon or a special feature of Example 2. A similar phenomenon holds for the variable $\boldsymbol{\lambda}_h$ in Table 6.4. We also remark the good behaviour of the *a posteriori* error estimator $\boldsymbol{\theta}$ in this case. In

particular, in Table 6.1, we see that the effectivity index $\mathtt{eff}(\boldsymbol{\theta})$ remains always in the neighborhood of 0.95, 0.70, and 0.55 for $k \in \{0, 1, 2\}$, respectively, which illustrates the reliability and efficiency result provided by Theorem 5.1.

Next, in Tables 6.5 to 6.12, we provide the convergence history of the quasi-uniform and adaptive schemes as applied to Examples 3 and 4. In particular, we emphasize here, as announced right before the discrete Helmholtz decomposition (5.14), that Example 4 considers a non-convex domain, which is a case not fully covered by the *a posteriori* error analysis developed in Section 5. In other words, the reliability of $\boldsymbol{\theta}$ is not guaranteed in these cases, at least theoretically. However, the numerical results shown below are far of being affected by the lack of convexity of the domain, and, on the contrary, they support the conjecture identifying that requirement as a simple technical assumption. Now, the stopping criterion in Example 3 corresponds to a maximum of 20 iterations, whereas in Example 4 it corresponds to a maximum of 9 iterations. We observe here, as expected, that the errors of the adaptive methods decrease faster than those obtained by the quasi-uniform ones. This fact is better illustrated in Figures 6.1 and 6.4, where we display the errors $\mathtt{e}(\mathbf{t}, \boldsymbol{\sigma}, \mathbf{u})$ vs. the degrees of freedom N for both refinements. In addition, the effectivity indices remain again bounded from above and below, which confirms the reliability and efficiency of $\boldsymbol{\theta}$ for the associated adaptive algorithm as well. Some intermediate meshes obtained with this procedure are displayed in Figures 6.2 and 6.5. Notice here that the adapted meshes concentrate the refinements around the origin and the line $x_2 = -1$ in Example 3, and around the points $(-0.25, 0.25, 0.25)$ and $(0.25, 0.25, 0.25)$ and the plane $x_2 = -0.75$ in Example 4, which means that the method is in fact able to recognize the regions with high gradients of the solutions. Finally, in Figures 6.3 and 6.6, we display some components of the discrete solutions for both examples.

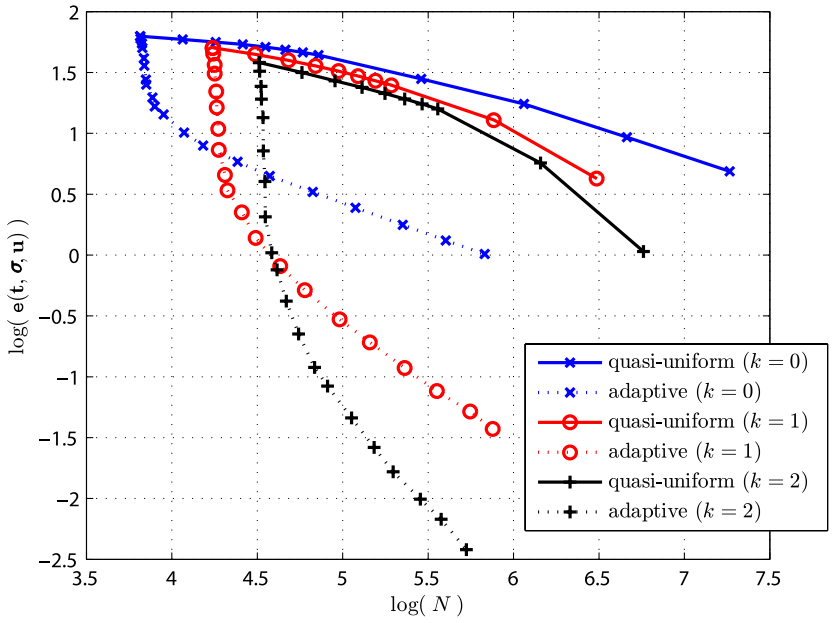

Figure 6.1: Example 3, $\mathtt{e}(\mathbf{t}, \boldsymbol{\sigma}, \mathbf{u})$ vs. N.

k	h	N	N_{comp}	$\mathtt{e}(\mathbf{t})$	$\mathtt{r}(\mathbf{t})$	$\mathtt{e}(\boldsymbol{\sigma})$	$\mathtt{r}(\boldsymbol{\sigma})$	$\mathtt{e}(\mathbf{u})$	$\mathtt{r}(\mathbf{u})$	$\mathtt{e}(\mathbf{t},\boldsymbol{\sigma},\mathbf{u})$	$\mathtt{r}(\mathbf{t},\boldsymbol{\sigma},\mathbf{u})$	$\mathtt{eff}(\boldsymbol{\theta})$
	0.1250	15424	4161	8.30e-1	−−	3.53e-0	−−	1.32e-1	−−	3.63e-0	−−	0.9624
	0.1000	24080	6481	6.67e-1	0.98	2.83e-0	1.00	1.05e-1	1.01	2.91e-0	0.99	0.9580
	0.0833	34656	9313	5.57e-1	0.99	2.36e-0	1.00	8.77e-2	1.00	2.42e-0	1.00	0.9554
	0.0714	47152	12657	4.78e-1	0.99	2.02e-0	1.00	7.51e-2	1.00	2.08e-0	1.00	0.9536
0	0.0625	61568	16513	4.19e-1	0.99	1.77e-0	1.00	6.57e-2	1.00	1.82e-0	1.00	0.9523
	0.0556	77904	20881	3.72e-1	0.99	1.57e-0	1.00	5.84e-2	1.00	1.62e-0	1.00	0.9514
	0.0417	138432	37057	2.80e-1	1.00	1.18e-0	1.00	4.38e-2	1.00	1.21e-0	1.00	0.9496
	0.0313	246016	65793	2.10e-1	1.00	8.85e-1	1.00	3.28e-2	1.00	9.10e-1	1.00	0.9484
	0.0208	553344	147841	1.40e-1	1.00	5.90e-1	1.00	2.19e-2	1.00	6.07e-1	1.00	0.9474
	0.0156	983552	262657	1.05e-1	1.00	4.43e-1	1.00	1.64e-2	1.00	4.55e-1	1.00	0.9469
	0.1250	41088	7297	4.07e-2	−−	2.12e-1	−−	7.96e-3	−−	2.16e-1	−−	0.7057
	0.1000	64160	11361	2.62e-2	1.98	1.36e-1	2.00	5.09e-3	2.00	1.39e-1	2.00	0.7033
	0.0833	92352	16321	1.82e-2	1.99	9.45e-2	2.00	3.54e-3	2.00	9.63e-2	2.00	0.7017
	0.0714	125664	22177	1.34e-2	1.99	6.94e-2	2.00	2.60e-3	2.00	7.07e-2	2.00	0.7005
1	0.0625	164096	28929	1.03e-2	1.99	5.31e-2	2.00	1.99e-3	2.00	5.42e-2	2.00	0.6997
	0.0556	207648	36577	8.13e-3	1.99	4.20e-2	2.00	1.57e-3	2.00	4.28e-2	2.00	0.6991
	0.0417	369024	64897	4.58e-3	1.99	2.36e-2	2.00	8.84e-4	2.00	2.41e-2	2.00	0.6978
	0.0313	655872	115201	2.58e-3	2.00	1.33e-2	2.00	4.97e-4	2.00	1.35e-2	2.00	0.6968
	0.0208	1475328	258817	1.15e-3	2.00	5.91e-3	2.00	2.21e-4	2.00	6.02e-3	2.00	0.6959
	0.0156	2622464	459777	6.46e-4	2.00	3.32e-3	2.00	1.24e-4	2.00	3.39e-3	2.00	0.6954
	0.1250	76992	10433	1.58e-3	−−	9.64e-3	−−	3.19e-4	−−	9.78e-3	−−	0.5638
	0.1000	120240	16241	8.08e-4	3.00	4.94e-3	3.00	1.63e-4	3.00	5.01e-3	3.00	0.5604
	0.0833	173088	23329	4.68e-4	3.00	2.86e-3	3.00	9.46e-5	3.00	2.90e-3	3.00	0.5583
	0.0714	235536	31697	2.95e-4	3.00	1.80e-3	3.00	5.96e-5	3.00	1.83e-3	3.00	0.5568
2	0.0625	307584	41345	1.98e-4	3.00	1.21e-3	3.00	3.99e-5	3.00	1.22e-3	3.00	0.5557
	0.0556	389232	52273	1.39e-4	3.00	8.47e-4	3.00	2.80e-5	3.00	8.59e-4	3.00	0.5548
	0.0417	691776	92737	5.86e-5	3.00	3.57e-4	3.00	1.18e-5	3.00	3.62e-4	3.00	0.5532
	0.0313	1229568	164609	2.47e-5	3.00	1.51e-4	3.00	4.99e-6	3.00	1.53e-4	3.00	0.5519
	0.0208	2765952	369793	7.33e-6	3.00	4.47e-5	3.00	1.48e-6	3.00	4.53e-5	3.00	0.5508
	0.0156	4916736	656897	3.10e-6	2.99	1.91e-5	2.96	6.24e-7	3.00	1.93e-5	2.96	0.5514

Table 6.1: Example 1, quasi-uniform scheme (Part 1).

k	h	N	N_{comp}	$\mathtt{e}_0(\boldsymbol{\sigma})$	$\mathtt{r}_0(\boldsymbol{\sigma})$	$\mathtt{e}(\boldsymbol{\lambda})$	$\mathtt{r}(\boldsymbol{\lambda})$	$\mathtt{e}(p)$	$\mathtt{r}(p)$	$\mathtt{e}^\star(\boldsymbol{\sigma})$	$\mathtt{r}^\star(\boldsymbol{\sigma})$
	0.1250	15424	4161	9.57e-1	−−	1.14e-1	−−	4.43e-1	−−	3.58e-0	−−
	0.1000	24080	6481	7.63e-1	1.02	9.00e-2	1.04	3.49e-1	1.07	2.87e-0	1.00
	0.0833	34656	9313	6.34e-1	1.02	7.45e-2	1.03	2.87e-1	1.06	2.39e-0	1.00
	0.0714	47152	12657	5.42e-1	1.01	6.36e-2	1.02	2.44e-1	1.05	2.05e-0	1.00
0	0.0625	61568	16513	4.74e-1	1.01	5.55e-2	1.02	2.13e-1	1.04	1.79e-0	1.00
	0.0556	77904	20881	4.21e-1	1.01	4.93e-2	1.02	1.88e-1	1.04	1.59e-0	1.00
	0.0417	138432	37057	3.15e-1	1.01	3.68e-2	1.01	1.40e-1	1.03	1.19e-0	1.00
	0.0313	246016	65793	2.36e-1	1.01	2.76e-2	1.01	1.04e-1	1.02	8.96e-1	1.00
	0.0208	553344	147841	1.57e-1	1.00	1.84e-2	1.00	6.94e-2	1.01	5.97e-1	1.00
	0.0156	983552	262657	1.18e-1	1.00	1.38e-2	1.00	5.19e-2	1.01	4.48e-1	1.00
	0.1250	41088	7297	4.77e-2	−−	1.63e-2	−−	2.18e-2	−−	2.13e-1	−−
	0.1000	64160	11361	3.06e-2	1.99	1.04e-2	1.99	1.40e-2	2.01	1.36e-1	2.00
	0.0833	92352	16321	2.13e-2	1.99	7.26e-3	1.99	9.69e-3	2.01	9.48e-2	2.00
	0.0714	125664	22177	1.57e-2	1.99	5.34e-3	1.99	7.11e-3	2.00	6.97e-2	2.00
1	0.0625	164096	28929	1.20e-2	2.00	4.09e-3	2.00	5.44e-3	2.00	5.33e-2	2.00
	0.0556	207648	36577	9.48e-3	2.00	3.23e-3	2.00	4.30e-3	2.00	4.21e-2	2.00
	0.0417	369024	64897	5.34e-3	2.00	1.82e-3	2.00	2.42e-3	2.00	2.37e-2	2.00
	0.0313	655872	115201	3.00e-3	2.00	1.02e-3	2.00	1.36e-3	2.00	1.33e-2	2.00
	0.0208	1475328	258817	1.34e-3	2.00	4.56e-4	2.00	6.03e-4	2.00	5.93e-3	2.00
	0.0156	2622464	459777	7.52e-4	2.00	2.56e-4	2.00	3.39e-4	2.00	3.33e-3	2.00
	0.1250	76992	10433	2.15e-3	−−	4.43e-4	−−	1.01e-3	−−	9.73e-3	−−
	0.1000	120240	16241	1.10e-3	3.01	2.26e-4	3.01	5.12e-4	3.03	4.98e-3	3.00
	0.0833	173088	23329	6.34e-4	3.01	1.31e-4	3.01	2.95e-4	3.02	2.88e-3	3.00
	0.0714	235536	31697	3.99e-4	3.01	8.22e-5	3.00	1.86e-4	3.02	1.82e-3	3.00
2	0.0625	307584	41345	2.67e-4	3.00	5.51e-5	3.00	1.24e-4	3.01	1.22e-3	3.00
	0.0556	389232	52273	1.87e-4	3.00	3.87e-5	3.00	8.70e-5	3.01	8.54e-4	3.00
	0.0417	691776	92737	7.90e-5	3.00	1.63e-5	3.00	3.66e-5	3.01	3.60e-4	3.00
	0.0313	1229568	164609	3.33e-5	3.00	6.88e-6	3.00	1.54e-5	3.00	1.52e-4	3.00
	0.0208	2765952	369793	9.87e-6	3.00	2.04e-6	3.00	4.57e-6	3.00	4.51e-5	3.00
	0.0156	4916736	656897	4.18e-6	2.99	8.62e-7	3.00	1.94e-6	2.98	1.90e-5	3.00

Table 6.2: Example 1, quasi-uniform scheme (Part 2).

k	h	N	N_{comp}	$\mathtt{e}(\mathbf{t})$	$\mathtt{r}(\mathbf{t})$	$\mathtt{e}(\boldsymbol{\sigma})$	$\mathtt{r}(\boldsymbol{\sigma})$	$\mathtt{e}(\mathbf{u})$	$\mathtt{r}(\mathbf{u})$	$\mathtt{e}(\mathbf{t},\boldsymbol{\sigma},\mathbf{u})$	$\mathtt{r}(\mathbf{t},\boldsymbol{\sigma},\mathbf{u})$	$\mathtt{eff}(\boldsymbol{\theta})$
	0.0625	15424	4161	8.48e-0	−−	3.15e+1	−−	1.06e-1	−−	3.26e+1	−−	1.0010
	0.0500	24080	6481	6.66e-0	1.08	2.52e+1	0.99	6.68e-2	2.07	2.61e+1	1.00	1.0019
	0.0417	34656	9313	5.46e-0	1.10	2.10e+1	0.99	4.57e-2	2.09	2.17e+1	1.00	1.0042
	0.0357	47152	12657	4.60e-0	1.11	1.81e+1	1.00	3.31e-2	2.10	1.86e+1	1.00	1.0071
0	0.0313	61568	16513	3.96e-0	1.12	1.58e+1	1.00	2.50e-2	2.10	1.63e+1	1.00	1.0103
	0.0278	77904	20881	3.47e-0	1.13	1.41e+1	1.00	1.95e-2	2.11	1.45e+1	1.00	1.0136
	0.0208	138432	37057	2.50e-0	1.14	1.05e+1	1.00	1.06e-2	2.11	1.08e+1	1.01	1.0231
	0.0156	246016	65793	1.79e-0	1.16	7.91e-0	1.00	5.81e-3	2.09	8.11e-0	1.01	1.0343
	0.0104	553344	147841	1.12e-0	1.17	5.28e-0	1.00	2.54e-3	2.04	5.39e-0	1.01	1.0513
	0.0078	983552	262657	7.98e-1	1.16	3.96e-0	1.00	1.44e-3	1.96	4.04e-0	1.01	1.0627
	0.0625	41088	7297	2.07e-1	−−	1.19e-0	−−	9.63e-4	−−	1.21e-0	−−	0.7779
	0.0500	64160	11361	1.32e-1	2.04	7.65e-1	1.99	4.96e-4	2.97	7.76e-1	1.99	0.7845
	0.0417	92352	16321	9.12e-2	2.01	5.32e-1	1.99	2.90e-4	2.95	5.40e-1	1.99	0.7877
	0.0357	125664	22177	6.70e-2	2.00	3.91e-1	1.99	1.84e-4	2.94	3.97e-1	1.99	0.7895
1	0.0313	164096	28929	5.13e-2	1.99	3.00e-1	1.99	1.24e-4	2.94	3.04e-1	1.99	0.7906
	0.0278	207648	36577	4.06e-2	1.99	2.37e-1	2.00	8.80e-5	2.93	2.41e-1	2.00	0.7913
	0.0208	369024	64897	2.29e-2	1.99	1.33e-1	2.00	3.79e-5	2.93	1.35e-1	2.00	0.7925
	0.0156	655872	115201	1.29e-2	1.99	7.51e-2	2.00	1.63e-5	2.92	7.62e-2	2.00	0.7933
	0.0104	1475328	258817	5.76e-3	1.99	3.34e-2	2.00	5.07e-6	2.89	3.39e-2	2.00	0.7940
	0.0078	2622464	459777	3.24e-3	1.99	1.88e-2	2.00	2.25e-6	2.83	1.91e-2	2.00	0.7943
	0.0625	76992	10433	4.68e-3	−−	3.29e-2	−−	1.28e-5	−−	3.32e-2	−−	0.6260
	0.0500	120240	16241	2.41e-3	2.97	1.69e-2	2.98	5.28e-6	3.96	1.71e-2	2.98	0.6244
	0.0417	173088	23329	1.40e-3	2.98	9.80e-3	2.99	2.56e-6	3.96	9.90e-3	2.99	0.6233
	0.0357	235536	31697	8.83e-4	2.98	6.18e-3	2.99	1.39e-6	3.97	6.24e-3	2.99	0.6224
2	0.0313	307584	41345	5.93e-4	2.99	4.14e-3	2.99	8.18e-7	3.97	4.18e-3	2.99	0.6218
	0.0278	389232	52273	4.17e-4	2.99	2.91e-3	3.00	5.13e-7	3.97	2.94e-3	3.00	0.6213
	0.0208	691776	92737	1.76e-4	2.99	1.23e-3	3.00	1.64e-7	3.96	1.24e-3	3.00	0.6202
	0.0156	1229568	164609	7.45e-5	2.99	5.19e-4	3.00	5.25e-8	3.95	5.24e-4	3.00	0.6194
	0.0104	2765952	369793	2.21e-5	3.00	1.54e-4	3.00	1.07e-8	3.93	1.55e-4	3.00	0.6190
	0.0078	4916736	656897	9.34e-6	3.00	6.49e-5	3.00	3.40e-9	3.98	6.55e-5	3.00	0.6196

Table 6.3: Example 2, quasi-uniform scheme (Part 1).

k	h	N	N_{comp}	$\mathtt{e}_0(\boldsymbol{\sigma})$	$\mathtt{r}_0(\boldsymbol{\sigma})$	$\mathtt{e}(\boldsymbol{\lambda})$	$\mathtt{r}(\boldsymbol{\lambda})$	$\mathtt{e}(p)$	$\mathtt{r}(p)$	$\mathtt{e}^\star(\boldsymbol{\sigma})$	$\mathtt{r}^\star(\boldsymbol{\sigma})$
	0.0625	15424	4161	8.22e-0	−−	3.00e-1	−−	3.93e-0	−−	3.19e+1	−−
	0.0500	24080	6481	6.59e-0	0.99	1.89e-1	2.07	3.14e-0	1.01	2.56e+1	0.99
	0.0417	34656	9313	5.49e-0	1.00	1.29e-1	2.09	2.61e-0	1.01	2.14e+1	0.99
	0.0357	47152	12657	4.71e-0	1.00	9.33e-2	2.10	2.24e-0	1.01	1.83e+1	1.00
0	0.0313	61568	16513	4.12e-0	1.00	7.03e-2	2.11	1.96e-0	1.01	1.60e+1	1.00
	0.0278	77904	20881	3.66e-0	1.00	5.48e-2	2.12	1.74e-0	1.01	1.43e+1	1.00
	0.0208	138432	37057	2.75e-0	1.00	2.97e-2	2.13	1.30e-0	1.01	1.07e+1	1.00
	0.0156	246016	65793	2.06e-0	1.00	1.61e-2	2.13	9.73e-1	1.01	8.03e-0	1.00
	0.0104	553344	147841	1.37e-0	1.00	6.84e-3	2.11	6.48e-1	1.00	5.36e-0	1.00
	0.0078	983552	262657	1.03e-0	1.00	3.77e-3	2.07	4.85e-1	1.00	4.02e-0	1.00
	0.0625	41088	7297	2.95e-1	−−	3.69e-3	−−	1.38e-1	−−	1.21e-0	−−
	0.0500	64160	11361	1.90e-1	1.98	1.89e-3	2.99	8.86e-2	1.99	7.75e-1	1.99
	0.0417	92352	16321	1.32e-1	1.98	1.10e-3	2.97	6.16e-2	1.99	5.39e-1	1.99
	0.0357	125664	22177	9.73e-2	1.99	6.97e-4	2.96	4.53e-2	1.99	3.97e-1	1.99
1	0.0313	164096	28929	7.46e-2	1.99	4.70e-4	2.96	3.47e-2	1.99	3.04e-1	1.99
	0.0278	207648	36577	5.90e-2	1.99	3.32e-4	2.96	2.75e-2	2.00	2.40e-1	2.00
	0.0208	369024	64897	3.33e-2	1.99	1.42e-4	2.96	1.55e-2	2.00	1.35e-1	2.00
	0.0156	655872	115201	1.87e-2	1.99	6.05e-5	2.96	8.70e-3	2.00	7.61e-2	2.00
	0.0104	1475328	258817	8.35e-3	2.00	1.83e-5	2.95	3.87e-3	2.00	3.38e-2	2.00
	0.0078	2622464	459777	4.70e-3	2.00	7.86e-6	2.93	2.18e-3	2.00	1.90e-2	2.00
	0.0625	76992	10433	7.44e-3	−−	5.44e-5	−−	3.60e-3	−−	3.33e-2	−−
	0.0500	120240	16241	3.81e-3	2.99	2.24e-5	3.98	1.84e-3	3.01	1.71e-2	2.98
	0.0417	173088	23329	2.21e-3	3.00	1.08e-5	3.99	1.06e-3	3.01	9.91e-3	2.99
	0.0357	235536	31697	1.39e-3	3.00	5.85e-6	3.99	6.68e-4	3.01	6.25e-3	2.99
2	0.0313	307584	41345	9.32e-4	3.00	3.43e-6	3.99	4.47e-4	3.01	4.19e-3	2.99
	0.0278	389232	52273	6.55e-4	3.00	2.14e-6	3.99	3.13e-4	3.01	2.94e-3	3.00
	0.0208	691776	92737	2.76e-4	3.00	6.80e-7	3.99	1.32e-4	3.01	1.24e-3	3.00
	0.0156	1229568	164609	1.17e-4	2.99	2.16e-7	3.99	5.58e-5	2.99	5.25e-4	3.00
	0.0104	2765952	369793	3.56e-5	2.93	4.28e-8	3.99	1.75e-5	2.85	1.56e-4	3.00
	0.0078	4916736	656897	1.50e-5	3.00	1.36e-8	3.98	7.42e-6	2.99	6.62e-5	2.97

Table 6.4: Example 2, quasi-uniform scheme (Part 2).

k	h	N	N_{comp}	$\mathtt{e}(\mathbf{t})$	$\mathtt{r}(\mathbf{t})$	$\mathtt{e}(\boldsymbol{\sigma})$	$\mathtt{r}(\boldsymbol{\sigma})$	$\mathtt{e}(\mathbf{u})$	$\mathtt{r}(\mathbf{u})$	$\mathtt{e}(\mathbf{t},\boldsymbol{\sigma},\mathbf{u})$	$\mathtt{r}(\mathbf{t},\boldsymbol{\sigma},\mathbf{u})$	$\mathtt{eff}(\boldsymbol{\theta})$
	0.1667	6528	1777	2.32e-0	−−	6.27e+1	−−	1.12e-1	−−	6.27e+1	−−	1.4002
	0.1250	11584	3137	2.08e-0	0.38	5.91e+1	0.20	8.63e-2	0.91	5.92e+1	0.20	1.4031
	0.1000	18080	4881	1.90e-0	0.39	5.62e+1	0.23	7.01e-2	0.93	5.62e+1	0.23	1.4046
	0.0833	26016	7009	1.77e-0	0.40	5.37e+1	0.25	5.92e-2	0.93	5.37e+1	0.25	1.4054
	0.0714	35392	9521	1.66e-0	0.40	5.11e+1	0.31	5.13e-2	0.93	5.11e+1	0.31	1.4060
0	0.0625	46208	12417	1.58e-0	0.41	4.86e+1	0.38	4.53e-2	0.92	4.86e+1	0.38	1.4064
	0.0556	58464	15697	1.50e-0	0.42	4.62e+1	0.43	4.07e-2	0.92	4.62e+1	0.43	1.4067
	0.0500	72160	19361	1.43e-0	0.43	4.39e+1	0.48	3.70e-2	0.92	4.40e+1	0.48	1.4069
	0.0250	288320	77121	9.90e-1	0.53	2.80e+1	0.65	1.90e-2	0.96	2.80e+1	0.65	1.4068
	0.0125	1152640	307841	5.08e-1	0.96	1.74e+1	0.69	9.32e-3	1.03	1.74e+1	0.69	1.4068
	0.0063	4609280	1230081	2.63e-1	0.95	9.28e-0	0.91	4.66e-3	1.00	9.29e-0	0.91	1.4064
	0.0031	18434560	4917761	1.35e-1	0.97	4.87e-0	0.93	2.33e-3	1.00	4.87e-0	0.93	1.4065
	0.1667	17376	3121	1.51e-0	−−	5.05e+1	−−	2.57e-2	−−	5.05e+1	−−	1.3935
	0.1250	30848	5505	1.33e-0	0.44	4.45e+1	0.44	1.92e-2	1.02	4.45e+1	0.44	1.3972
	0.1000	48160	8561	1.20e-0	0.46	3.97e+1	0.51	1.56e-2	0.94	3.97e+1	0.51	1.3990
	0.0833	69312	12289	1.10e-0	0.49	3.58e+1	0.56	1.30e-2	0.98	3.58e+1	0.56	1.3998
1	0.0714	94304	16689	1.01e-0	0.54	3.25e+1	0.64	1.10e-2	1.07	3.25e+1	0.64	1.4003
	0.0625	123136	21761	9.34e-1	0.61	2.95e+1	0.71	9.43e-3	1.19	2.95e+1	0.71	1.4005
	0.0556	155808	27505	8.62e-1	0.68	2.70e+1	0.76	8.08e-3	1.31	2.70e+1	0.76	1.4004
	0.0500	192320	33921	7.95e-1	0.76	2.49e+1	0.78	6.94e-3	1.44	2.49e+1	0.78	1.4001
	0.0250	768640	135041	3.46e-1	1.20	1.29e+1	0.95	1.96e-3	1.82	1.29e+1	0.95	1.3964
	0.0125	3073280	538881	1.08e-1	1.69	4.24e-0	1.60	5.09e-4	1.95	4.25e-0	1.60	1.3916
	0.1667	32544	4465	1.14e-0	−−	3.81e+1	−−	1.36e-2	−−	3.82e+1	−−	1.3820
	0.1250	57792	7873	9.77e-1	0.53	3.16e+1	0.66	1.02e-2	0.99	3.16e+1	0.66	1.3843
	0.1000	90240	12241	8.51e-1	0.62	2.70e+1	0.71	7.78e-3	1.24	2.70e+1	0.71	1.3837
	0.0833	129888	17569	7.44e-1	0.74	2.38e+1	0.69	5.89e-3	1.52	2.38e+1	0.69	1.3826
2	0.0714	176736	23857	6.50e-1	0.88	2.13e+1	0.73	4.52e-3	1.71	2.13e+1	0.73	1.3817
	0.0625	230784	31105	5.68e-1	1.00	1.92e+1	0.78	3.54e-3	1.83	1.92e+1	0.78	1.3811
	0.0556	292032	39313	4.98e-1	1.12	1.74e+1	0.82	2.83e-3	1.90	1.74e+1	0.82	1.3809
	0.0500	360480	48481	4.38e-1	1.22	1.59e+1	0.88	2.32e-3	1.91	1.59e+1	0.88	1.3810
	0.0250	1440960	192961	1.64e-1	1.42	5.71e-0	1.47	6.65e-4	1.80	5.71e-0	1.47	1.3776
	0.0125	5761920	769921	2.48e-2	2.72	1.07e-0	2.42	8.10e-5	3.04	1.07e-0	2.42	1.3646

Table 6.5: Example 3, quasi-uniform scheme (Part 1).

k	h	N	N_{comp}	$\mathtt{e}_0(\boldsymbol{\sigma})$	$\mathtt{r}_0(\boldsymbol{\sigma})$	$\mathtt{e}(\boldsymbol{\lambda})$	$\mathtt{r}(\boldsymbol{\lambda})$	$\mathtt{e}(p)$	$\mathtt{r}(p)$	$\mathtt{e}^\star(\boldsymbol{\sigma})$	$\mathtt{r}^\star(\boldsymbol{\sigma})$
	0.1667	6528	1777	1.95e-0	−−	1.51e-1	−−	8.88e-1	−−	6.27e+1	−−
	0.1250	11584	3137	1.60e-0	0.69	1.06e-1	1.23	6.78e-1	0.94	5.91e+1	0.20
	0.1000	18080	4881	1.38e-0	0.65	7.88e-2	1.32	5.60e-1	0.86	5.62e+1	0.23
	0.0833	26016	7009	1.24e-0	0.60	6.17e-2	1.35	4.90e-1	0.73	5.37e+1	0.25
	0.0714	35392	9521	1.14e-0	0.57	5.02e-2	1.33	4.45e-1	0.62	5.11e+1	0.31
0	0.0625	46208	12417	1.06e-0	0.54	4.23e-2	1.28	4.14e-1	0.54	4.86e+1	0.38
	0.0556	58464	15697	9.94e-1	0.53	3.68e-2	1.20	3.91e-1	0.49	4.62e+1	0.43
	0.0500	72160	19361	9.41e-1	0.52	3.27e-2	1.12	3.72e-1	0.47	4.40e+1	0.48
	0.0250	288320	77121	6.22e-1	0.60	1.63e-2	1.00	2.46e-1	0.60	2.80e+1	0.65
	0.0125	1152640	307841	3.40e-1	0.87	7.92e-3	1.04	1.48e-1	0.73	1.74e+1	0.69
	0.0063	4609280	1230081	1.78e-1	0.93	3.94e-3	1.01	7.90e-2	0.91	9.29e-0	0.91
	0.0031	18434560	4917761	9.12e-2	0.96	1.97e-3	1.00	4.18e-2	0.92	4.85e-0	0.94
	0.1667	17376	3121	1.03e-0	−−	3.73e-2	−−	3.88e-1	−−	5.05e+1	−−
	0.1250	30848	5505	8.87e-1	0.53	2.50e-2	1.39	3.47e-1	0.39	4.45e+1	0.44
	0.1000	48160	8561	7.87e-1	0.54	2.03e-2	0.92	3.14e-1	0.44	3.97e+1	0.51
	0.0833	69312	12289	7.07e-1	0.59	1.75e-2	0.82	2.82e-1	0.59	3.58e+1	0.56
1	0.0714	94304	16689	6.37e-1	0.67	1.53e-2	0.89	2.51e-1	0.77	3.25e+1	0.64
	0.0625	123136	21761	5.76e-1	0.75	1.33e-2	1.02	2.22e-1	0.93	2.95e+1	0.71
	0.0556	155808	27505	5.22e-1	0.84	1.16e-2	1.18	1.95e-1	1.07	2.70e+1	0.76
	0.0500	192320	33921	4.74e-1	0.92	1.00e-2	1.35	1.72e-1	1.20	2.49e+1	0.78
	0.0250	768640	135041	2.03e-1	1.22	2.90e-3	1.79	7.65e-2	1.17	1.29e+1	0.95
	0.0125	3073280	538881	6.80e-2	1.58	7.74e-4	1.90	2.83e-2	1.43	4.25e-0	1.60
	0.1667	32544	4465	7.79e-1	−−	2.14e-2	−−	3.21e-1	−−	3.82e+1	−−
	0.1250	57792	7873	6.34e-1	0.72	1.72e-2	0.75	2.49e-1	0.88	3.16e+1	0.66
	0.1000	90240	12241	5.29e-1	0.81	1.35e-2	1.09	1.94e-1	1.12	2.70e+1	0.71
	0.0833	129888	17569	4.46e-1	0.94	1.03e-2	1.49	1.51e-1	1.38	2.38e+1	0.69
2	0.0714	176736	23857	3.79e-1	1.05	7.86e-3	1.76	1.19e-1	1.54	2.13e+1	0.73
	0.0625	230784	31105	3.26e-1	1.12	6.05e-3	1.95	9.80e-2	1.45	1.92e+1	0.78
	0.0556	292032	39313	2.85e-1	1.17	4.71e-3	2.12	8.57e-2	1.14	1.74e+1	0.82
	0.0500	360480	48481	2.51e-1	1.19	3.73e-3	2.23	7.89e-2	0.79	1.59e+1	0.88
	0.0250	1440960	192961	9.61e-2	1.39	9.78e-4	1.93	3.51e-2	1.17	5.71e-0	1.47
	0.0125	5761920	769921	1.60e-2	2.58	1.32e-4	2.89	7.01e-3	2.32	1.07e-0	2.42

Table 6.6: Example 3, quasi-uniform scheme (Part 2).

k	h	N	N_{comp}	$\mathtt{e}(\mathbf{t})$	$\mathtt{r}(\mathbf{t})$	$\mathtt{e}(\boldsymbol{\sigma})$	$\mathtt{r}(\boldsymbol{\sigma})$	$\mathtt{e}(\mathbf{u})$	$\mathtt{r}(\mathbf{u})$	$\mathtt{e}(\mathbf{t},\boldsymbol{\sigma},\mathbf{u})$	$\mathtt{r}(\mathbf{t},\boldsymbol{\sigma},\mathbf{u})$	$\mathtt{eff}(\boldsymbol{\theta})$
	0.1667	6528	1777	2.32e-0	−−	6.27e+1	−−	1.12e-1	−−	6.27e+1	−−	1.4002
	0.1667	6560	1787	2.25e-0	12.24	5.98e+1	19.43	1.11e-1	2.77	5.98e+1	19.42	1.4032
	0.1667	6680	1819	2.01e-0	12.35	5.46e+1	9.96	1.03e-1	8.55	5.46e+1	9.96	1.4029
	0.1667	6712	1829	1.96e-0	10.19	5.03e+1	34.82	1.03e-1	-0.11	5.03e+1	34.79	1.4030
	0.1667	6862	1869	1.73e-0	11.43	4.14e+1	17.54	1.00e-1	2.82	4.14e+1	17.53	1.4004
	0.1667	6894	1879	1.62e-0	28.69	3.59e+1	61.79	9.99e-2	0.22	3.59e+1	61.72	1.3964
	0.1667	7044	1919	1.50e-0	7.05	2.76e+1	24.23	9.92e-2	0.65	2.77e+1	24.19	1.3876
	0.1667	7076	1929	1.40e-0	31.43	2.51e+1	42.26	9.92e-2	-0.01	2.51e+1	42.22	1.3817
	0.1667	7706	2097	1.22e-0	3.11	1.96e+1	5.77	9.39e-2	1.29	1.97e+1	5.76	1.3732
0	0.1667	7952	2167	1.20e-0	1.48	1.66e+1	10.69	9.38e-2	0.03	1.66e+1	10.64	1.3589
	0.1667	8956	2445	1.12e-0	1.12	1.42e+1	2.59	8.84e-2	1.01	1.43e+1	2.58	1.3509
	0.1667	11788	3209	8.35e-1	2.14	1.01e+1	2.50	8.05e-2	0.68	1.01e+1	2.50	1.3355
	0.1667	15242	4155	7.45e-1	0.88	7.91e-0	1.90	7.99e-2	0.05	7.94e-0	1.89	1.3082
	0.1667	24258	6571	5.66e-1	1.18	5.81e-0	1.33	7.34e-2	0.37	5.83e-0	1.33	1.3042
	0.1667	37464	10141	4.75e-1	0.81	4.44e-0	1.24	6.78e-2	0.37	4.46e-0	1.24	1.2817
	0.1667	66906	18023	3.58e-1	0.98	3.28e-0	1.04	5.51e-2	0.71	3.30e-0	1.04	1.2765
	0.1667	118938	31995	2.73e-1	0.94	2.43e-0	1.04	4.51e-2	0.69	2.45e-0	1.04	1.2697
	0.1667	224564	60225	1.98e-1	1.00	1.76e-0	1.02	3.32e-2	0.96	1.77e-0	1.02	1.2672
	0.1179	400954	107321	1.47e-1	1.02	1.31e-0	1.03	2.46e-2	1.04	1.31e-0	1.03	1.2676
	0.0833	678522	181565	1.14e-1	0.96	1.01e-0	0.96	1.92e-2	0.94	1.02e-0	0.96	1.2694
	0.1667	17376	3121	1.51e-0	−−	5.05e+1	−−	2.57e-2	−−	5.05e+1	−−	1.3935
	0.1667	17460	3139	1.38e-0	36.69	4.52e+1	46.17	2.11e-2	82.12	4.52e+1	46.17	1.3942
	0.1667	17780	3195	1.17e-0	18.64	3.65e+1	23.28	1.58e-2	32.16	3.66e+1	23.27	1.3957
	0.1667	17864	3213	9.39e-1	93.28	3.10e+1	69.70	1.31e-2	77.25	3.10e+1	69.73	1.3910
	0.1667	18264	3283	7.45e-1	20.86	2.21e+1	30.67	1.10e-2	15.87	2.21e+1	30.66	1.3910
	0.1667	18348	3301	5.13e-1	162.37	1.63e+1	131.38	1.04e-2	25.24	1.63e+1	131.41	1.3733
	0.1667	18748	3371	3.97e-1	23.78	1.08e+1	37.96	1.01e-2	2.73	1.09e+1	37.94	1.3603
	0.1667	18832	3389	3.44e-1	64.33	7.35e-0	174.39	1.01e-2	2.34	7.35e-0	174.20	1.3173
	0.1667	20512	3683	2.50e-1	7.45	4.53e-0	11.30	8.34e-3	4.36	4.54e-0	11.29	1.2751
1	0.1667	21164	3807	2.40e-1	2.80	3.39e-0	18.58	8.33e-3	0.08	3.40e-0	18.52	1.1999
	0.1667	25756	4637	1.28e-1	6.37	2.24e-0	4.20	5.42e-3	4.38	2.25e-0	4.21	1.2490
	0.1667	30972	5563	1.02e-1	2.43	1.38e-0	5.26	5.33e-3	0.19	1.38e-0	5.25	1.1836
	0.1667	43124	7749	6.13e-2	3.10	8.08e-1	3.24	3.63e-3	2.32	8.11e-1	3.24	1.1605
	0.1667	60180	10747	4.58e-2	1.75	5.11e-1	2.75	3.39e-3	0.41	5.13e-1	2.74	1.1110
	0.1667	96308	17109	2.55e-2	2.48	2.93e-1	2.37	2.13e-3	1.98	2.94e-1	2.37	1.1020
	0.1667	144196	25595	1.79e-2	1.76	1.91e-1	2.11	1.68e-3	1.18	1.92e-1	2.11	1.0779
	0.1667	230180	40695	1.10e-2	2.09	1.18e-1	2.07	1.06e-3	1.97	1.18e-1	2.07	1.0757
	0.1667	355122	62644	7.01e-3	2.07	7.60e-2	2.02	6.95e-4	1.93	7.63e-2	2.02	1.0785
	0.1667	556068	98029	4.56e-3	1.92	5.18e-2	1.70	4.37e-4	2.07	5.20e-2	1.71	1.1008
	0.1179	756780	133213	3.48e-3	1.75	3.69e-2	2.20	3.36e-4	1.70	3.71e-2	2.20	1.0715
	0.1667	32544	4465	1.14e-0	−−	3.81e+1	−−	1.36e-2	−−	3.82e+1	−−	1.3820
	0.1667	32700	4491	9.31e-1	83.69	3.23e+1	69.58	9.27e-3	160.96	3.23e+1	69.59	1.3736
	0.1667	33300	4571	7.69e-1	21.12	2.43e+1	31.23	6.12e-3	45.68	2.43e+1	31.22	1.3785
	0.1667	33456	4597	5.02e-1	181.93	1.91e+1	103.60	3.84e-3	199.63	1.91e+1	103.67	1.3664
	0.1667	34206	4697	3.55e-1	31.27	1.34e+1	31.75	2.52e-3	37.96	1.34e+1	31.75	1.3775
	0.1667	34362	4723	1.96e-1	260.23	7.17e-0	275.69	2.08e-3	84.06	7.17e-0	275.68	1.3466
	0.1667	35112	4823	1.36e-1	34.28	4.02e-0	53.71	1.93e-3	7.05	4.02e-0	53.70	1.3306
	0.1667	35268	4849	8.51e-2	210.62	2.06e-0	301.40	1.89e-3	8.17	2.06e-0	301.28	1.2150
	0.1667	38418	5269	5.12e-2	11.89	1.04e-0	15.92	1.42e-3	6.79	1.04e-0	15.91	1.1440
2	0.1667	41286	5667	3.37e-2	11.60	7.56e-1	8.92	7.14e-4	19.02	7.57e-1	8.93	1.1769
	0.1667	46734	6435	1.97e-2	8.70	4.17e-1	9.59	6.18e-4	2.32	4.18e-1	9.59	1.1348
	0.1667	55146	7567	1.41e-2	3.99	2.24e-1	7.51	5.82e-4	0.73	2.24e-1	7.50	1.0367
	0.1667	68520	9371	7.84e-3	5.42	1.19e-1	5.82	3.55e-4	4.56	1.19e-1	5.81	0.9950
	0.1667	81510	11181	5.18e-3	4.77	8.38e-2	4.06	2.56e-4	3.75	8.39e-2	4.06	1.0125
	0.1667	112740	15371	3.23e-3	2.92	4.57e-2	3.73	1.96e-4	1.66	4.58e-2	3.73	0.9695
	0.1667	152826	20747	1.90e-3	3.49	2.62e-2	3.67	1.30e-4	2.70	2.62e-2	3.67	0.9415
	0.1667	197430	26741	1.26e-3	3.19	1.65e-2	3.59	9.45e-5	2.47	1.66e-2	3.58	0.9201
	0.1667	284766	38547	7.45e-4	2.88	9.83e-3	2.84	5.76e-5	2.70	9.86e-3	2.84	0.9165
	0.1667	377358	50929	4.71e-4	3.25	6.73e-3	2.69	3.73e-5	3.10	6.75e-3	2.69	0.9631
	0.1667	530172	71403	2.75e-4	3.18	3.79e-3	3.38	2.21e-5	3.07	3.80e-3	3.38	0.9386

Table 6.7: Example 3, adaptive scheme (Part 1).

k	h	N	N_{comp}	$\mathtt{e}_0(\boldsymbol{\sigma})$	$\mathtt{r}_0(\boldsymbol{\sigma})$	$\mathtt{e}(\boldsymbol{\lambda})$	$\mathtt{r}(\boldsymbol{\lambda})$	$\mathtt{e}(p)$	$\mathtt{r}(p)$	$\mathtt{e}^\star(\boldsymbol{\sigma})$	$\mathtt{r}^\star(\boldsymbol{\sigma})$
	0.1667	6528	1777	1.95e-0	−−	1.51e-1	−−	8.88e-1	−−	6.27e+1	−−
	0.1667	6560	1787	1.96e-0	-1.11	1.49e-1	3.61	9.33e-1	-20.12	5.98e+1	19.41
	0.1667	6680	1819	1.63e-0	19.89	1.13e-1	30.42	7.05e-1	30.85	5.46e+1	9.96
	0.1667	6712	1829	1.63e-0	1.35	1.17e-1	-12.66	7.21e-1	-9.38	5.03e+1	34.81
	0.1667	6862	1869	1.47e-0	9.43	1.03e-1	11.70	6.53e-1	9.00	4.14e+1	17.54
	0.1667	6894	1879	1.41e-0	16.11	1.05e-1	-7.57	6.26e-1	18.19	3.59e+1	61.76
	0.1667	7044	1919	1.36e-0	3.45	1.02e-1	2.51	6.15e-1	1.69	2.76e+1	24.21
	0.1667	7076	1929	1.33e-0	11.24	1.02e-1	-1.83	6.07e-1	5.64	2.51e+1	42.22
	0.1667	7706	2097	1.26e-0	1.23	1.01e-1	0.33	5.83e-1	0.94	1.96e+1	5.76
0	0.1667	7952	2167	1.25e-0	0.74	1.01e-1	0.09	5.75e-1	0.85	1.66e+1	10.67
	0.1667	8956	2445	1.18e-0	0.92	9.32e-2	1.28	5.56e-1	0.58	1.42e+1	2.58
	0.1667	11788	3209	8.42e-1	2.46	7.04e-2	2.04	3.85e-1	2.67	1.01e+1	2.50
	0.1667	15242	4155	7.39e-1	1.01	6.83e-2	0.24	3.37e-1	1.04	7.92e-0	1.89
	0.1667	24258	6571	5.82e-1	1.03	6.18e-2	0.43	2.69e-1	0.97	5.82e-0	1.33
	0.1667	37464	10141	4.77e-1	0.91	5.54e-2	0.50	2.18e-1	0.97	4.44e-0	1.24
	0.1667	66906	18023	3.65e-1	0.93	4.49e-2	0.72	1.66e-1	0.93	3.29e-0	1.04
	0.1667	118938	31995	2.77e-1	0.96	3.65e-2	0.72	1.26e-1	0.96	2.44e-0	1.04
	0.1667	224564	60225	2.02e-1	1.00	2.64e-2	1.02	9.17e-2	1.01	1.76e-0	1.02
	0.1179	400954	107321	1.51e-1	1.01	1.98e-2	0.98	6.86e-2	1.00	1.31e-0	1.03
	0.0833	678522	181565	1.17e-1	0.95	1.57e-2	0.88	5.36e-2	0.94	1.02e-0	0.96
	0.1667	17376	3121	1.03e-0	−−	3.73e-2	−−	3.88e-1	−−	5.05e+1	−−
	0.1667	17460	3139	9.23e-1	46.63	3.29e-2	52.18	3.36e-1	60.65	4.52e+1	46.18
	0.1667	17780	3195	7.68e-1	20.33	2.44e-2	32.88	3.02e-1	11.57	3.66e+1	23.28
	0.1667	17864	3213	6.18e-1	92.18	2.28e-2	28.35	2.34e-1	108.31	3.10e+1	69.71
	0.1667	18264	3283	4.76e-1	23.64	1.90e-2	16.39	1.77e-1	25.37	2.21e+1	30.67
	0.1667	18348	3301	3.71e-1	107.87	1.87e-2	8.30	1.55e-1	57.42	1.63e+1	131.37
	0.1667	18748	3371	3.08e-1	17.45	1.81e-2	2.83	1.33e-1	13.91	1.09e+1	37.95
	0.1667	18832	3389	2.82e-1	38.94	1.80e-2	2.32	1.21e-1	41.75	7.35e-0	174.34
	0.1667	20512	3683	2.32e-1	4.57	1.52e-2	4.03	1.01e-1	4.40	4.54e-0	11.30
1	0.1667	21164	3807	2.27e-1	1.30	1.51e-2	0.09	9.89e-2	1.12	3.39e-0	18.56
	0.1667	25756	4637	1.34e-1	5.38	9.56e-3	4.68	6.27e-2	4.64	2.25e-0	4.20
	0.1667	30972	5563	9.71e-2	3.49	9.15e-3	0.47	4.39e-2	3.88	1.38e-0	5.26
	0.1667	43124	7749	5.97e-2	2.94	6.00e-3	2.55	2.69e-2	2.96	8.09e-1	3.24
	0.1667	60180	10747	4.42e-2	1.80	5.56e-3	0.46	1.98e-2	1.84	5.12e-1	2.75
	0.1667	96308	17109	2.43e-2	2.54	3.50e-3	1.96	1.07e-2	2.60	2.94e-1	2.37
	0.1667	144196	25595	1.76e-2	1.61	2.71e-3	1.27	7.86e-3	1.54	1.92e-1	2.11
	0.1667	230180	40695	1.07e-2	2.12	1.71e-3	1.96	4.77e-3	2.14	1.18e-1	2.07
	0.1667	355122	62644	6.81e-3	2.09	1.11e-3	1.99	3.03e-3	2.10	7.61e-2	2.02
	0.1667	556068	98029	4.50e-3	1.84	7.09e-4	2.01	2.01e-3	1.82	5.19e-2	1.70
	0.1179	756780	133213	3.37e-3	1.87	5.61e-4	1.53	1.50e-3	1.89	3.70e-2	2.20
	0.1667	32544	4465	7.79e-1	−−	2.14e-2	−−	3.21e-1	−−	3.82e+1	−−
	0.1667	32700	4491	5.95e-1	112.89	1.31e-2	205.94	2.08e-1	181.79	3.23e+1	69.59
	0.1667	33300	4571	4.68e-1	26.36	1.06e-2	22.95	1.61e-1	28.10	2.43e+1	31.23
	0.1667	33456	4597	3.22e-1	160.02	5.91e-3	250.50	1.24e-1	110.42	1.91e+1	103.60
	0.1667	34206	4697	2.17e-1	35.82	3.92e-3	36.92	8.14e-2	38.16	1.34e+1	31.75
	0.1667	34362	4723	1.30e-1	224.05	3.28e-3	79.35	5.26e-2	191.77	7.17e-0	275.68
	0.1667	35112	4823	9.03e-2	33.84	3.07e-3	5.89	3.64e-2	34.17	4.02e-0	53.71
	0.1667	35268	4849	6.83e-2	125.52	3.04e-3	5.06	3.14e-2	66.56	2.06e-0	301.34
	0.1667	38418	5269	4.79e-2	8.31	2.38e-3	5.69	2.23e-2	8.05	1.04e-0	15.91
2	0.1667	41286	5667	3.83e-2	6.24	1.38e-3	15.15	1.82e-2	5.61	7.56e-1	8.92
	0.1667	46734	6435	1.96e-2	10.79	1.10e-3	3.69	8.97e-3	11.40	4.17e-1	9.59
	0.1667	55146	7567	1.28e-2	5.18	1.04e-3	0.69	5.84e-3	5.19	2.24e-1	7.51
	0.1667	68520	9371	6.80e-3	5.80	6.31e-4	4.58	3.00e-3	6.12	1.19e-1	5.82
	0.1667	81510	11181	5.09e-3	3.34	4.54e-4	3.79	2.28e-3	3.19	8.38e-2	4.06
	0.1667	112740	15371	2.94e-3	3.39	3.56e-4	1.49	1.31e-3	3.42	4.58e-2	3.73
	0.1667	152826	20747	1.76e-3	3.35	2.33e-4	2.79	7.79e-4	3.41	2.62e-2	3.67
	0.1667	197430	26741	1.18e-3	3.15	1.70e-4	2.47	5.19e-4	3.17	1.65e-2	3.59
	0.1667	284766	38547	7.26e-4	2.65	1.04e-4	2.70	3.21e-4	2.61	9.84e-3	2.84
	0.1667	377358	50929	4.55e-4	3.32	6.77e-5	3.02	2.02e-4	3.31	6.74e-3	2.69
	0.1667	530172	71403	2.62e-4	3.24	4.03e-5	3.05	1.16e-4	3.26	3.79e-3	3.38

Table 6.8: Example 3, adaptive scheme (Part 2).

k	h	N	N_{comp}	$\mathtt{e}(\mathbf{t})$	$\mathtt{r}(\mathbf{t})$	$\mathtt{e}(\boldsymbol{\sigma})$	$\mathtt{r}(\boldsymbol{\sigma})$	$\mathtt{e}(\mathbf{u})$	$\mathtt{r}(\mathbf{u})$	$\mathtt{e}(\mathbf{t},\boldsymbol{\sigma},\mathbf{u})$	$\mathtt{r}(\mathbf{t},\boldsymbol{\sigma},\mathbf{u})$	$\mathtt{eff}(\boldsymbol{\theta})$
	0.4330	7464	1945	1.27e-0	−−	8.00e-0	−−	2.97e-1	−−	8.10e-0	−−	1.0827
	0.2165	58656	14497	7.62e-1	0.73	4.98e-0	0.68	1.50e-1	0.98	5.04e-0	0.68	1.0795
	0.1443	196776	47737	5.37e-1	0.86	3.63e-0	0.78	9.97e-2	1.01	3.68e-0	0.78	1.0847
	0.1083	465024	111745	4.14e-1	0.91	2.84e-0	0.86	7.51e-2	0.98	2.87e-0	0.86	1.0833
	0.0866	906600	216601	3.37e-1	0.92	2.33e-0	0.89	6.00e-2	1.01	2.35e-0	0.90	1.0835
0	0.0722	1564704	372385	2.83e-1	0.96	1.97e-0	0.92	4.99e-2	1.01	1.99e-0	0.92	1.0825
	0.0619	2482536	589177	2.44e-1	0.96	1.69e-0	0.97	4.28e-2	0.99	1.71e-0	0.97	1.0788
	0.0541	3703296	877057	2.14e-1	0.97	1.49e-0	0.97	3.76e-2	0.99	1.50e-0	0.97	1.0764
	0.0481	5270184	1246105	1.91e-1	0.97	1.33e-0	0.96	3.33e-2	1.01	1.34e-0	0.96	1.0759
	0.0433	7226400	1706401	1.73e-1	0.97	1.20e-0	0.98	3.00e-2	1.00	1.21e-0	0.98	1.0746
	0.0394	9615144	2268025	1.57e-1	0.99	1.09e-0	0.96	2.73e-2	1.00	1.10e-0	0.96	1.0751
	0.0361	12479616	2941057	1.44e-1	0.99	1.00e-0	0.98	2.50e-2	1.01	1.01e-0	0.98	1.0744
	0.4330	27432	5353	4.64e-1	−−	3.85e-0	−−	3.41e-2	−−	3.88e-0	−−	0.8809
	0.2165	216288	39649	1.82e-1	1.35	1.63e-0	1.24	9.96e-3	1.78	1.64e-0	1.24	0.8804
	0.1443	726408	130249	9.26e-2	1.67	8.85e-1	1.50	4.56e-3	1.93	8.89e-1	1.51	0.8962
	0.1083	1717632	304513	5.63e-2	1.73	5.51e-1	1.64	2.62e-3	1.92	5.54e-1	1.64	0.8968
1	0.0866	3349800	589801	3.75e-2	1.82	3.72e-1	1.76	1.69e-3	1.97	3.74e-1	1.76	0.9016
	0.0722	5782752	1013473	2.66e-2	1.88	2.70e-1	1.76	1.17e-3	2.00	2.72e-1	1.76	0.9089
	0.0619	9176328	1602889	2.00e-2	1.86	2.01e-1	1.93	8.68e-4	1.95	2.02e-1	1.93	0.8985
	0.0541	13690368	2385409	1.55e-2	1.90	1.55e-1	1.91	6.68e-4	1.97	1.56e-1	1.91	0.8956
	0.0481	19484712	3388393	1.23e-2	1.93	1.24e-1	1.91	5.28e-4	2.00	1.25e-1	1.91	0.8955
	0.4330	64944	10465	2.04e-1	−−	1.86e-0	−−	9.39e-3	−−	1.87e-0	−−	0.6302
	0.2165	513216	77377	5.56e-2	1.88	5.44e-1	1.77	1.82e-3	2.37	5.46e-1	1.77	0.6435
2	0.1443	1724976	254017	2.12e-2	2.37	2.26e-1	2.16	6.18e-4	2.67	2.27e-1	2.17	0.6779
	0.1083	4080384	593665	1.04e-2	2.49	1.15e-1	2.34	2.84e-4	2.70	1.16e-1	2.35	0.6728
	0.0866	7959600	1149601	5.75e-3	2.65	6.49e-2	2.57	1.52e-4	2.80	6.52e-2	2.57	0.6759
	0.0722	13742784	1975105	3.46e-3	2.78	4.05e-2	2.59	8.81e-5	2.99	4.06e-2	2.59	0.6764

Table 6.9: Example 4, quasi-uniform scheme (Part 1).

k	h	N	N_{comp}	$\mathtt{e}_0(\boldsymbol{\sigma})$	$\mathtt{r}_0(\boldsymbol{\sigma})$	$\mathtt{e}(\boldsymbol{\lambda})$	$\mathtt{r}(\boldsymbol{\lambda})$	$\mathtt{e}(p)$	$\mathtt{r}(p)$	$\mathtt{e}^\star(\boldsymbol{\sigma})$	$\mathtt{r}^\star(\boldsymbol{\sigma})$
	0.4330	7464	1945	1.07e-0	−−	2.35e-1	−−	4.28e-1	−−	8.02e-0	−−
	0.2165	58656	14497	6.34e-1	0.75	1.23e-1	0.93	2.50e-1	0.78	5.00e-0	0.68
	0.1443	196776	47737	4.43e-1	0.89	8.19e-2	1.01	1.71e-1	0.93	3.64e-0	0.78
	0.1083	465024	111745	3.38e-1	0.93	6.08e-2	1.03	1.29e-1	0.98	2.85e-0	0.86
	0.0866	906600	216601	2.73e-1	0.96	4.87e-2	0.99	1.03e-1	1.02	2.33e-0	0.90
0	0.0722	1564704	372385	2.28e-1	0.99	4.03e-2	1.04	8.54e-2	1.03	1.97e-0	0.92
	0.0619	2482536	589177	1.96e-1	0.99	3.45e-2	1.01	7.29e-2	1.03	1.70e-0	0.97
	0.0541	3703296	877057	1.72e-1	0.99	3.01e-2	1.01	6.35e-2	1.03	1.49e-0	0.97
	0.0481	5270184	1246105	1.53e-1	0.99	2.68e-2	0.99	5.62e-2	1.04	1.33e-0	0.96
	0.0433	7226400	1706401	1.38e-1	1.00	2.41e-2	1.00	5.04e-2	1.04	1.20e-0	0.98
	0.0394	9615144	2268025	1.25e-1	1.00	2.19e-2	1.01	4.57e-2	1.03	1.09e-0	0.96
	0.0361	12479616	2941057	1.15e-1	1.01	2.01e-2	1.02	4.17e-2	1.04	1.00e-0	0.98
	0.4330	27432	5353	3.63e-1	−−	5.98e-2	−−	1.33e-1	−−	3.85e-0	−−
	0.2165	216288	39649	1.32e-1	1.45	1.85e-2	1.69	4.43e-2	1.58	1.63e-0	1.24
	0.1443	726408	130249	6.75e-2	1.66	8.83e-3	1.83	2.27e-2	1.65	8.85e-1	1.50
	0.1083	1717632	304513	4.08e-2	1.75	5.14e-3	1.88	1.37e-2	1.76	5.52e-1	1.64
1	0.0866	3349800	589801	2.71e-2	1.83	3.37e-3	1.89	9.11e-3	1.82	3.73e-1	1.76
	0.0722	5782752	1013473	1.93e-2	1.87	2.36e-3	1.96	6.44e-3	1.90	2.70e-1	1.76
	0.0619	9176328	1602889	1.44e-2	1.89	1.75e-3	1.93	4.78e-3	1.93	2.01e-1	1.93
	0.0541	13690368	2385409	1.11e-2	1.92	1.35e-3	1.93	3.69e-3	1.94	1.56e-1	1.91
	0.0481	19484712	3388393	8.87e-3	1.94	1.08e-3	1.95	2.94e-3	1.94	1.24e-1	1.91
	0.4330	64944	10465	1.39e-1	−−	1.74e-2	−−	4.08e-2	−−	1.86e-0	−−
	0.2165	513216	77377	3.63e-2	1.94	3.56e-3	2.29	1.06e-2	1.95	5.44e-1	1.77
2	0.1443	1724976	254017	1.41e-2	2.33	1.28e-3	2.52	4.25e-3	2.25	2.26e-1	2.16
	0.1083	4080384	593665	6.91e-3	2.48	5.95e-4	2.67	2.10e-3	2.45	1.15e-1	2.34
	0.0866	7959600	1149601	3.84e-3	2.64	3.26e-4	2.70	1.19e-3	2.54	6.49e-2	2.57
	0.0722	13742784	1975105	2.31e-3	2.79	1.92e-4	2.91	7.10e-4	2.84	4.05e-2	2.59

Table 6.10: Example 4, quasi-uniform scheme (Part 2).

k	h	N	N_{comp}	$\mathtt{e}(\mathbf{t})$	$\mathtt{r}(\mathbf{t})$	$\mathtt{e}(\boldsymbol{\sigma})$	$\mathtt{r}(\boldsymbol{\sigma})$	$\mathtt{e}(\mathbf{u})$	$\mathtt{r}(\mathbf{u})$	$\mathtt{e}(\mathbf{t},\boldsymbol{\sigma},\mathbf{u})$	$\mathtt{r}(\mathbf{t},\boldsymbol{\sigma},\mathbf{u})$	$\mathtt{eff}(\boldsymbol{\theta})$
	0.4330	7464	1945	1.27e-0	−−	8.00e-0	−−	2.97e-1	−−	8.10e-0	−−	1.0827
	0.4330	12174	3113	1.01e-0	0.94	6.10e-0	1.11	2.37e-1	0.93	6.19e-0	1.10	1.0485
	0.4330	25077	6310	8.65e-1	0.42	4.30e-0	0.97	2.16e-1	0.25	4.40e-0	0.95	0.9371
	0.4330	74127	18307	6.10e-1	0.64	2.92e-0	0.71	1.46e-1	0.72	2.99e-0	0.71	0.9193
0	0.2795	153618	37469	4.73e-1	0.70	2.44e-0	0.49	1.10e-1	0.79	2.49e-0	0.50	0.9611
	0.2275	422067	101816	3.50e-1	0.59	1.64e-0	0.79	8.45e-2	0.52	1.68e-0	0.78	0.9044
	0.2165	699573	167837	2.86e-1	0.80	1.45e-0	0.50	6.58e-2	0.99	1.48e-0	0.51	0.9476
	0.1768	1956981	466720	2.11e-1	0.59	9.76e-1	0.76	5.12e-2	0.49	1.00e-0	0.76	0.8957
	0.1250	3822273	906633	1.64e-1	0.76	8.06e-1	0.57	3.85e-2	0.86	8.23e-1	0.58	0.9301
	0.4330	27432	5353	4.64e-1	−−	3.85e-0	−−	3.41e-2	−−	3.88e-0	−−	0.8809
	0.4330	44796	8549	2.56e-1	2.42	2.27e-0	2.15	2.04e-2	2.10	2.29e-0	2.15	0.8580
	0.4330	87576	16461	1.70e-1	1.23	1.10e-0	2.18	1.81e-2	0.35	1.11e-0	2.16	0.6720
	0.4330	186330	34163	1.05e-1	1.26	8.81e-1	0.58	1.10e-2	1.32	8.87e-1	0.59	0.8235
1	0.4330	353526	64371	6.93e-2	1.31	4.20e-1	2.31	8.59e-3	0.78	4.26e-1	2.29	0.6572
	0.2795	705015	126520	4.41e-2	1.31	3.35e-1	0.65	4.21e-3	2.07	3.38e-1	0.67	0.7822
	0.2500	1384584	247005	2.89e-2	1.25	1.70e-1	2.01	3.27e-3	0.75	1.72e-1	1.99	0.6428
	0.2296	2227491	394576	2.02e-2	1.51	1.36e-1	0.95	2.31e-3	1.45	1.37e-1	0.96	0.7173
	0.1768	4218372	742429	1.15e-2	1.76	8.02e-2	1.65	1.30e-3	1.80	8.10e-2	1.65	0.6923
	0.4330	64944	10465	2.04e-1	−−	1.86e-0	−−	9.39e-3	−−	1.87e-0	−−	0.6302
	0.4330	106140	16703	7.31e-2	4.18	8.31e-1	3.27	3.15e-3	4.44	8.34e-1	3.28	0.7124
	0.4330	195594	30339	3.91e-2	2.05	2.77e-1	3.60	2.62e-3	0.60	2.79e-1	3.58	0.4474
	0.4330	268422	41196	2.67e-2	2.42	2.47e-1	0.71	1.81e-3	2.35	2.49e-1	0.73	0.5931
2	0.4330	449226	67867	1.79e-2	1.56	1.82e-1	1.20	1.24e-3	1.47	1.82e-1	1.20	0.6436
	0.3783	900066	134396	9.40e-3	1.85	6.68e-2	2.88	6.81e-4	1.72	6.75e-2	2.86	0.4727
	0.3536	1345116	198767	5.82e-3	2.38	5.62e-2	0.86	3.84e-4	2.85	5.65e-2	0.88	0.6289
	0.3125	1638588	241631	4.68e-3	2.20	4.40e-2	2.49	3.13e-4	2.08	4.42e-2	2.48	0.6046
	0.2795	2625642	385834	2.44e-3	2.77	2.35e-2	2.65	1.60e-4	2.84	2.37e-2	2.65	0.6021

Table 6.11: Example 4, adaptive scheme (Part 1).

k	h	N	N_{comp}	$\mathtt{e}_0(\boldsymbol{\sigma})$	$\mathtt{r}_0(\boldsymbol{\sigma})$	$\mathtt{e}(\boldsymbol{\lambda})$	$\mathtt{r}(\boldsymbol{\lambda})$	$\mathtt{e}(p)$	$\mathtt{r}(p)$	$\mathtt{e}^\star(\boldsymbol{\sigma})$	$\mathtt{r}^\star(\boldsymbol{\sigma})$
	0.4330	7464	1945	1.07e-0	−−	2.35e-1	−−	4.28e-1	−−	8.02e-0	−−
	0.4330	12174	3113	9.60e-1	0.44	2.45e-1	-0.18	4.12e-1	0.16	6.13e-0	1.10
	0.4330	25077	6310	7.23e-1	0.79	2.29e-1	0.19	2.83e-1	1.04	4.31e-0	0.97
	0.4330	74127	18307	5.08e-1	0.65	1.66e-1	0.59	2.02e-1	0.63	2.92e-0	0.72
0	0.2795	153618	37469	4.16e-1	0.55	1.37e-1	0.53	1.70e-1	0.47	2.44e-0	0.49
	0.2275	422067	101816	2.93e-1	0.69	1.00e-1	0.62	1.15e-1	0.77	1.64e-0	0.79
	0.2165	699573	167837	2.38e-1	0.83	7.63e-2	1.08	9.15e-2	0.92	1.45e-0	0.50
	0.1768	1956981	466720	1.68e-1	0.68	5.98e-2	0.47	6.18e-2	0.76	9.74e-1	0.77
	0.1250	3822273	906633	1.31e-1	0.73	4.46e-2	0.88	4.82e-2	0.74	8.05e-1	0.57
	0.4330	27432	5353	3.63e-1	−−	5.98e-2	−−	1.33e-1	−−	3.85e-0	−−
	0.4330	44796	8549	2.69e-1	1.22	4.41e-2	1.24	1.17e-1	0.51	2.28e-0	2.14
	0.4330	87576	16461	1.38e-1	2.00	3.83e-2	0.43	5.04e-2	2.52	1.10e-0	2.19
	0.4330	186330	34163	9.61e-2	0.96	2.43e-2	1.21	3.84e-2	0.72	8.82e-1	0.58
1	0.4330	353526	64371	5.63e-2	1.67	1.88e-2	0.79	2.06e-2	1.95	4.20e-1	2.32
	0.2795	705015	126520	3.81e-2	1.13	9.25e-3	2.06	1.45e-2	1.02	3.36e-1	0.65
	0.2500	1384584	247005	2.30e-2	1.50	7.20e-3	0.74	8.09e-3	1.73	1.70e-1	2.01
	0.2296	2227491	394576	1.66e-2	1.36	5.11e-3	1.44	6.07e-3	1.21	1.36e-1	0.95
	0.1768	4218372	742429	1.03e-2	1.51	2.90e-3	1.77	3.70e-3	1.55	9.91e-2	0.99
	0.4330	64944	10465	1.39e-1	−−	1.74e-2	−−	4.08e-2	−−	1.86e-0	−−
	0.4330	106140	16703	7.28e-2	2.63	7.72e-3	3.32	2.97e-2	1.29	8.32e-1	3.27
	0.4330	195594	30339	3.04e-2	2.85	6.05e-3	0.80	1.03e-2	3.46	2.77e-1	3.60
	0.4330	268422	41196	2.33e-2	1.68	4.23e-3	2.26	8.88e-3	0.96	2.48e-1	0.70
2	0.4330	449226	67867	1.63e-2	1.38	2.90e-3	1.46	6.35e-3	1.30	1.82e-1	1.20
	0.3783	900066	134396	7.29e-3	2.32	1.67e-3	1.59	2.48e-3	2.70	6.69e-2	2.88
	0.3536	1345116	198767	5.10e-3	1.78	9.28e-4	2.92	1.95e-3	1.20	5.63e-2	0.86
	0.3125	1638588	241631	4.01e-3	2.43	7.54e-4	2.11	1.50e-3	2.68	4.40e-2	2.49
	0.2795	2625642	385834	2.15e-3	2.65	3.78e-4	2.93	8.08e-4	2.61	2.25e-2	2.84

Table 6.12: Example 4, adaptive scheme (Part 2).

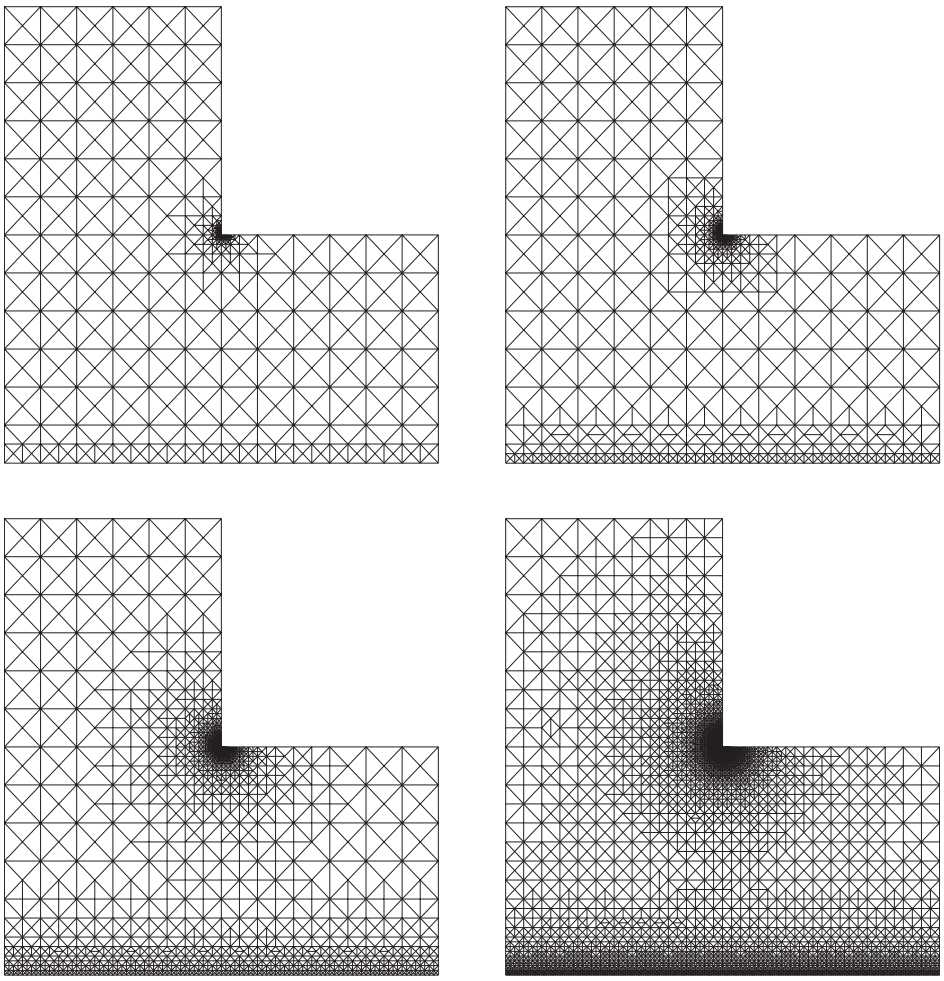

Figure 6.2: Example 3, adapted meshes for $k = 0$ with 11788, 24258, 66906, and 224564 degrees of freedom.

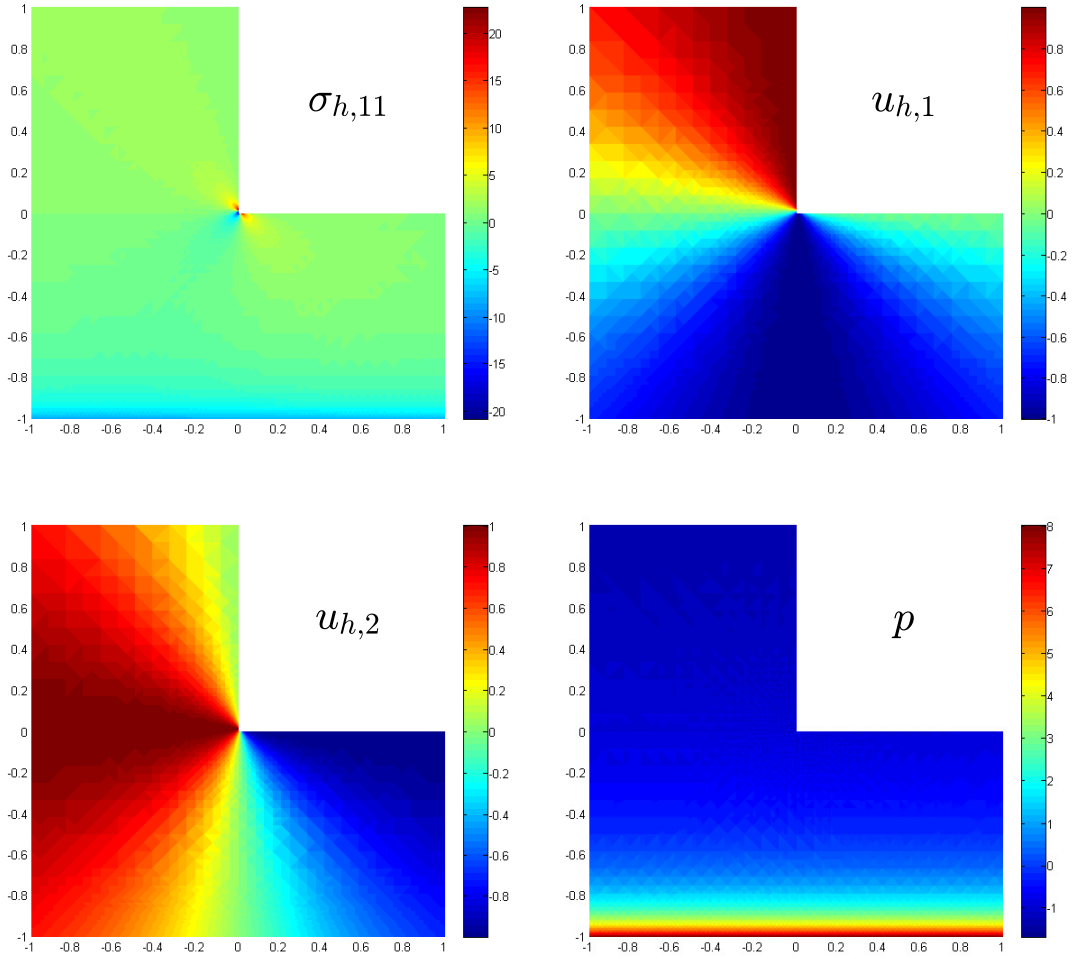

Figure 6.3: Example 3, some components of the approximate solutions ($k = 0$ and $N = 118938$) for the adaptive scheme.

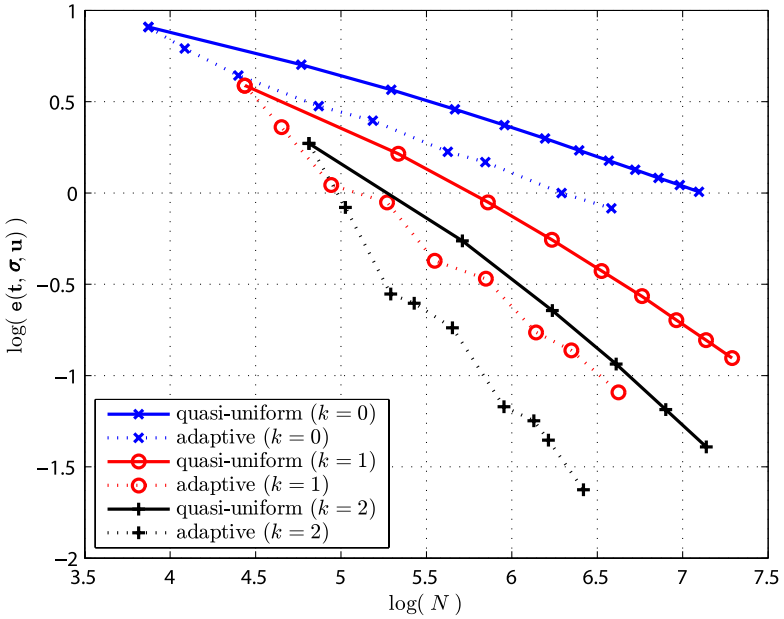

Figure 6.4: Example 4, $\mathsf{e}(\mathbf{t},\boldsymbol{\sigma},\mathbf{u})$ vs. N.

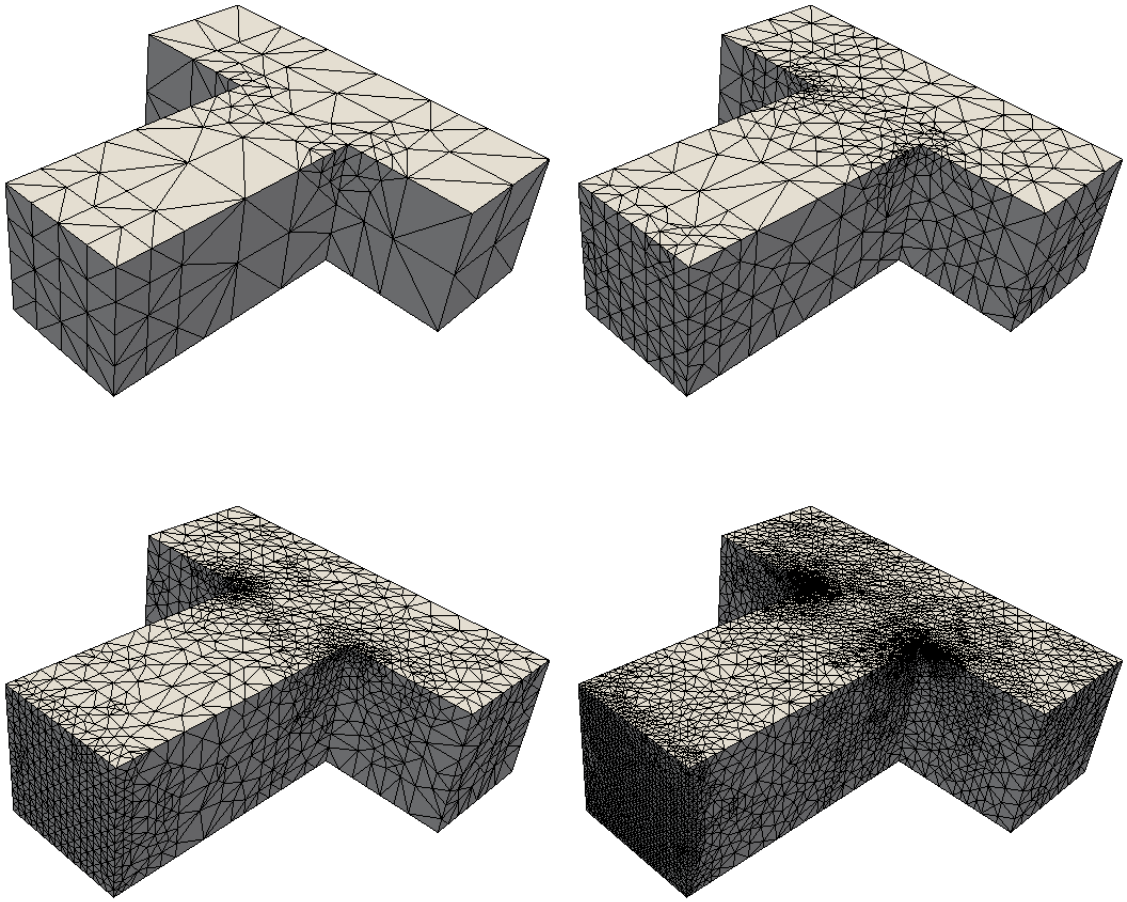

Figure 6.5: Example 4, adapted meshes for $k=0$ with 25077, 153618, 699573, and 3822273 degrees of freedom.

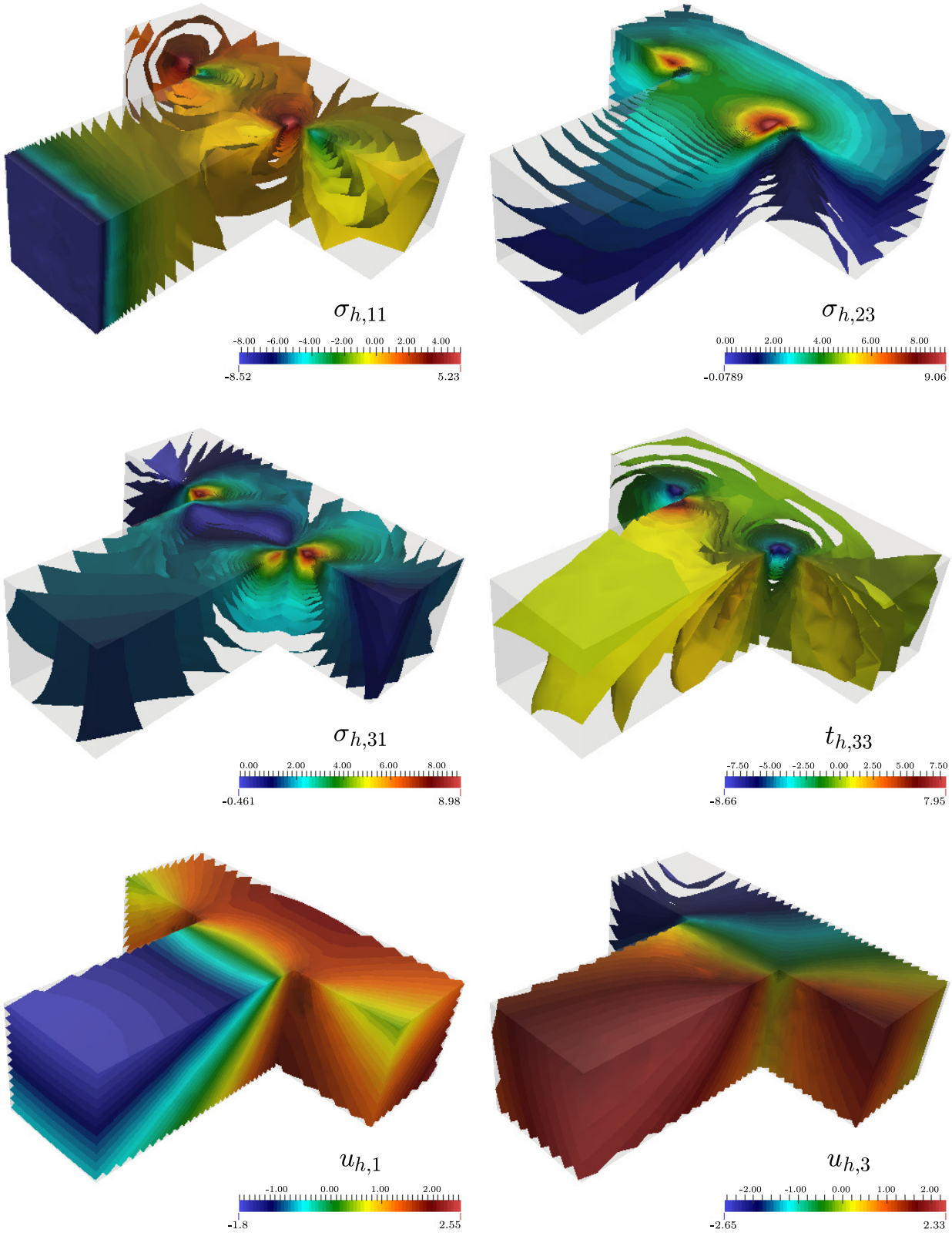

Figure 6.6: Example 4, iso-surfaces of some components of the approximate solutions ($k = 2$ and $N = 1638588$) for the adaptive scheme.

References

[1] C. Amrouche, C. Bernardi, M. Dauge, and V. Girault, *Vector potentials in three-dimensional nonsmooth domains*, Math. Methods Appl. Sci., 21 (1998), pp. 823–864.

[2] J. Baranger, K. Najib, and D. Sandri, *Numerical analysis of a three-fields model for a quasi-Newtonian flow*, Comput. Methods Appl. Mech. Engrg., 109 (1993), pp. 281–292.

[3] F. Brezzi and M. Fortin, *Mixed and Hybrid Finite Element Methods*, Springer Verlag, 1991.

[4] R. Bustinza and G. N. Gatica, *A local discontinuous Galerkin method for nonlinear diffusion problems with mixed boundary conditions*, SIAM J. Sci. Comput., 26 (2004), pp. 152–177.

[5] ——, *A mixed local discontinuous Galerkin for a class of nonlinear problems in fluid mechanics*, J. Comput. Phys., 207 (2005), pp. 427–456.

[6] R. Bustinza, G. N. Gatica, and B. Cockburn, *An a posteriori error estimate for the local discontinuous Galerkin method applied to linear and nonlinear diffusion problems*, J. Sci. Comput., 22-23 (2005), pp. 147–185.

[7] H. Chen, J. Li, and W. Qiu, *Robust a posteriori error estimates for hdg method for convection-diffusion equations*, IMA J. Numer. Anal., (2015).

[8] P. G. Ciarlet, *The Finite Element Method for Elliptic Problems*, Nort-Holland, 1978.

[9] P. Clément, *Approximation by finite element functions using local regularisation*, ESAIM Math. Model. Numer. Anal., 9 (1975), pp. 77–84.

[10] B. Cockburn, J. Gopalakrishnan, N. C. Nguyen, J. Peraire, and F. J. Sayas, *Analysis of HDG methods for Stokes flow*, Math. Comp., 80 (2011), pp. 723–760.

[11] B. Cockburn, J. Gopalakrishnan, and F. J. Sayas, *A projection-based error analysis of HDG methods*, Math. Comp., 79 (2010), pp. 1351–1367.

[12] B. Cockburn, J. Guzmán, and H. Wang, *Superconvergent discontinuous Galerkin methods for second-order elliptic problems*, Math. Comp., 78 (2009), pp. 1–24.

[13] B. Cockburn and W. Zhang, *A posteriori error estimates for HDG methods*, J. Sci. Comput., 51 (2012), pp. 582–607.

[14] ——, *A posteriori error analysis for hybridizable discontinuous Galerkin methods for second order elliptic problems*, SIAM J. Numer. Anal., 51 (2013), pp. 676–693.

[15] L. Figueroa, G. N. Gatica, and A. Márquez, *Augmented mixed finite element methods for the stationary Stokes equations*, SIAM J. Sci. Comput., 31 (2008/09), pp. 1082–1119.

[16] G. N. Gatica, *A Simple Introduction to the Mixed Finite Element Method: Theory and Applications*, SpringerBriefs in Mathematics, Springer, 2014.

[17] G. N. Gatica, L. F. Gatica, and A. Márquez, *Analysis of a pseudostress-based mixed finite element method for the Brinkman model of porous media flow*, Numer. Math., 126 (2014), pp. 635–677.

[18] G. N. Gatica, L. F. Gatica, and F. A. Sequeira, *A priori and a posteriori error analyses of a pseudostress-based mixed formulation for linear elasticity*, Preprint 2015-14, Centro de Investigación en Ingeniería Matemática (CI^2MA), Universidad de Concepción, Chile, (2015).

[19] G. N. Gatica, N. Heuer, and S. Meddahi, *On the numerical analysis of nonlinear twofold saddle point problems*, IMA J. Numer. Anal., 23 (2003), pp. 301–330.

[20] G. N. Gatica, A. Márquez, and M. A. Sánchez, *Analysis of a velocity-pressure-pseudostress formulation for the stationary Stokes equations*, Comput. Methods Appl. Mech. Engrg., 199 (2010), pp. 1064–1079.

[21] G. N. Gatica, A. Márquez, and M. A. Sánchez, *A priori and a posteriori error analyses of a velocity-pseudostress formulation for a class of quasi-Newtonian Stokes flows*, Comput. Methods Appl. Mech. Engrg., 200 (2011), pp. 1619–1636.

[22] G. N. Gatica and F. A. Sequeira, *Analysis of an augmented HDG method for a class of quasi-Newtonian Stokes flows*, J. Sci. Comput., DOI:http://dx.doi.org/10.1007/s10915-015-0008-5 (2015).

[23] V. Girault and P. A. Raviart, *Finite Element Methods for Navier-Stokes Equations. Theory and Algorithms*, Springer Series in Computational Mathematics, Vol. 5. Berlin: Springer, 1986.

[24] R. Hiptmair, *Finite elements in computational electromagnetism*, Acta Numer., 11 (2002), pp. 237–339.

[25] O. Ladyzhenskaya, *New equations for the description of the viscous incompressible fluids and solvability in the large for the boundary value problems of them. In: Boundary Value Problems of Mathematical Physics V*, Providence, RI: AMS, 1970.

[26] A. F. D. Loula and J. N. C. Guerreiro, *Finite element analysis of nonlinear creeping flows*, Comput. Methods Appl. Mech. Engrg., 99 (1990), pp. 87–109.

[27] N. C. Nguyen, J. Peraire, and B. Cockburn, *A hybridizable discontinuous Galerkin method for Stokes flow*, Comput. Methods Appl. Mech. Engrg., 199 (2010), pp. 582–597.

[28] J. E. Roberts and J. M. Thomas, *Mixed and Hybrid Methods. In Handbook of Numerical Analysis, edited by P.G. Ciarlet and J.L. Lions, vol. II, Finite Element Methods (Part 1)*, Nort-Holland, Amsterdam, 1991.

[29] D. Sandri, *Sur l'approximation numérique des écoulements quasi-Newtoniens dont la viscosité suit la loi puissance ou la loi de Carreau*, ESAIM Math. Model. Numer. Anal., 27 (1993), pp. 131–155.

[30] H. Si, *TetGen: A Quality Tetrahedral Mesh Generator and 3D Delaunay Triangulator v.1.5 User's manual*, Tech. Rep. 13, Weierstrass Institute for Applied Analysis and Stochastics, Berlin, 2013.

[31] R. Verfürth, *A Review of A Posteriori Error Estimation and Adaptive-Mesh-Refinement Techniques*, Wiley, Chichester, 1996.